DEPARTAMENTO DE MATEMÁTICA APLICADA

Instituto de Matemática Mutidisciplinar

Finite Difference Schemes for Option Pricing under Stochastic Volatility and Lévy Processes: Numerical Analysis and Computing

PhD THESIS

Author: Mohamed Mostafa Refaat El-Fakharany

Supervised by: Prof. Rafael Company
Prof. Lucas A. Jódar

Valencia, July 2015

My deep appreciation, respect and love to my mother

Acknowledgements

It is a pleasure to express my sincere thanks to my supervisors, Professor Dr. Rafael Company from the Institute for Multidisciplinary Mathematics and Professor Dr. Lucas A. Jódar from the Institute for Multidisciplinary Mathematics in Polytechnic University of Valencia for their great support throughout the work of my thesis. In light of their continuous guidance is the prime reason behind overcoming the obstacles that I faced.

For carefully reviewing the thesis, I would like to thank Professors O. Angulo Torga, H. V. Kojouharov and C. Vázquez Cendón. Also, my gratitude to the thesis committee; Professors Juan Carlos Cortés López from Polytechnic University of Valencia, Carlos Vázquez Cendón from University of A Coruña and Maria Do Rosário Grossinho from University of Lisbon.

My thanks to the staff and my colleagues in the Institute for Multidisciplinary Mathematics in Polytechnic University of Valencia for their hospitality. Finally, My gratitude to my wife and family for supporting me during these years.

Contents

List of Figures

List of Tables

Resumen

El proceso de estimación del precio de una acción, opción u otro derivado en los mercados de valores es objeto clave de estudio de las matemáticas financieras. En la literatura se pueden encontrar diversas técnicas para obtener un modelo matemático adecuado con el fin de mejorar el proceso de valoración de las opciones para períodos cortos o largos. Históricamente, la ecuación de Black-Scholes (1973) se considera un gran avance en la elaboración de modelos matemáticos para los mercados de valores. Supone un modelo matemático práctico para estimar un valor razonable para una determinada opción en el momento en que se adquiere. Sobre una serie de supuestos F. Black y M. Scholes obtuvieron una ecuación diferencial en derivadas parciales lineal con solución analítica.

Desde entonces, el comercio de valores ha crecido enormemente y varios factores se han incorporado llevando a la aparición de nuevos productos financieros de mayor complejidad. Supuestos de partida de Black-Scholes como la volatilidad constante y que el activo subyacente sigue el movimiento browniano estándar no pueden mantenerse con este desarrollo de los mercados financieros. En consecuencia, estas restricciones deben ser cuestionadas. Se han realizado numerosos esfuerzos para desarrollar modelos alternativos de activos que son capaces de captar las características leptocúrticas que se encuentran en los datos de los mercados y, posteriormente, utilizar estos modelos para calcular precios de las opciones que reflejen con exactitud la llamada sonrisa de volatilidad y asimetrías que se encuentran en los mercados. Dos estrategias se han desarrollado para capturar estos comportamientos; la primera modificación consiste en añadir saltos en el proceso del precio del activo subyacente, como originalmente fue propuesta por Merton; la segunda es permitir que la volatilidad evolucione estocásticamente, introducida por Heston. La primera idea conduce a los modelos de difusión con saltos y a los modelos de Lévy que se describen mediante una ecuación integro-diferencial en derivadas parciales (PIDE) con dos variables independientes, activo subyacente y tiempo. Con el segundo enfoque se llega a una ecuación diferencial en derivadas parciales (PDE) con dos variables espaciales, el activo subyacente y la volatilidad, además de la variable temporal.

En esta memoria se aborda la resolución numérica de una amplia clase de modelos bajo procesos de Lévy. Se desarrollan esquemas en diferencias finitas para opciones europeas y también para opciones

americanas con su problema de complementariedad lineal (LCP) asociado. Por otra parte, también se tratan modelos de valoración de opciones con volatilidad estocástica incorporando difusión con saltos. Se plantea el análisis numérico de los esquemas propuestos ya que es el camino eficiente y práctico para garantizar la convergencia y precisión de las soluciones numéricas. De hecho, sin análisis numérico, los cálculos inconsistentes pueden debilitar buenos modelos matemáticos.

Esta memoria está organizada en cuatro capítulos. El primero es una introducción con un breve repaso de los procesos estocásticos, el modelo de Black-Scholes asi como nociones preliminares de análisis numérico. En el segundo capítulo se trata la PIDE para las opciones europeas según el modelo CGMY. Se proponen dos esquemas en diferencias finitas; la primera aproximación garantiza consistencia incondicional de la solución con la PIDE mientras que la segunda proporciona estabilidad y positividad incondicionales. Con el primer enfoque, la parte diferencial se discretiza mediante un esquema explícito y para la parte integral se emplea la regla del trapecio. En la segunda aproximación, para la parte diferencial se usa el esquema tipo Patankar y la parte integral se aproxima mediante la fórmula de tipo abierto con cuatro puntos. Posteriormente se estudia en cada caso la positividad, estabilidad y consistencia. Se incluyen varios ejemplos y simulaciones.

En el capítulo tercero, se propone un tratamiento unificado para una amplia clase de modelos de opciones en procesos de Lévy tales como CGMY, Meixner e hiperbólico generalizado. Primero se eliminan los términos de reacción y convección en la PIDE mediante un apropiado cambio de variables. Posteriormente la parte diferencial de la PIDE se aproxima por un esquema explícito mientras que para la parte integral se usa la fórmula de cuadratura de Laguerre-Gauss. Se analizan las propiedades de positividad, estabilidad y consistencia. Para el caso de opciones americanas, la parte diferencial del LCP se discretiza mediante una aproximación con tres niveles temporales, usando la cuadratura de Laguerre-Gauss para la integración numérica de la parte integral. Por último se implementan métodos iterativos de proyección y relajación sucesiva y la técnica de multimalla. Se muestran diversos ejemplos incluyendo el estudio de errores y el coste computacional.

Finalmente, el capítulo 4 está dedicado al modelo de Bates. Este modelo combina los enfoques de volatilidad estocástica y de difusión con saltos lo que lleva a una PIDE con un término con derivadas cruzadas. Teniendo en cuenta que la discretización de una derivada cruzada conlleva la existencia de términos con coeficientes negativos en el esquema que deterioran la calidad de la solución numérica, se propone una transformación de variables que elimina dicha derivada cruzada en la ecuación. La PIDE transformada se resuelve numéricamente y se muestra el análisis numérico. Por otra parte se estudia el LCP para opciones americanas en el modelo de Bates.

Resum

El procés d'estimació del preu d'una acció, opció o un altre derivat en els mercats de valors és objecte clau d'estudi de les matemàtiques financeres . En la literatura es poden trobar diverses tècniques per a obtindre un model matemàtic adequat a fi de millorar el procés de valoració de les opcions per a períodes curts o llargs. Històricament, l'equació de Black-Scholes (1973) es considera un gran avanç en l'elaboració de models matemàtics per als mercats de valors. Suposa un model matemàtic pràctic per a estimar un valor raonable per a una determinada opció en el moment en que esta s'adquirix. Sobre una sèrie de suposats F. Black i M. Scholes van obtindre una equació diferencial en derivades parcials lineal amb solució analítica.

Des de llavors, el comerç de valors ha crescut enormement i diversos factors s'han incorporat portant a l'aparició de nous productes financers de major complexitat. Supòsits de partida de Black-Scholes com la volatilitat constant i que l'actiu subjacent segueix el moviment brownià estàndard no poden mantindre's amb este desenrotllament dels mercats financers. En conseqüència, estes restriccions han de ser qüestionades. S'han realitzat nombrosos esforços per a desenrotllar models alternatius d'actius que són capaços de captar les característiques leptocúrticas que es troben en les dades dels mercats i, posteriorment, utilitzar estos models per a calcular preus de les opcions que reflectisquen amb exactitud l'anomenada somriure de volatilitat i asimetries que es troben en els mercats. Dos estratègies s'han desenrotllat per a capturar estos comportaments; la primera modificació consisteix a afegir salts en el procés del preu de l'actiu subjacent, com originàriament va ser proposta per Merton; la segona és permetre que la volatilitat evolucione estocàsticament, introduïda per Heston. La primera idea conduïx als models de difusió amb salts i als models de Lévy que es descriuen per mitjà d'una equació integre-diferencial en derivades parcials (PIDE) amb dues variables independents, actiu subjacent i temps. Amb el segon enfocament s'arriba a una equació diferencial en derivades parcials (PDE) amb dues variables espacials, l'actiu subjacent i la volatilitat, a més de la variable temporal.

En esta memòria s'aborda la resolució numèrica d'una àmplia classe de models baix processos de Lévy. Es desenrotllen esquemes en diferències finites per a opcions europees i també per a opcions

americanes amb el seu problema de complementarietat lineal (LCP) associat. D'altra banda també es tracten models de valoració d'opcions amb volatilitat estocástica incorporant difusió amb salts. Es planteja l'anàlisi numèrica dels esquemes proposats ja que és el camí eficient i pràctic per a garantir la convergència i precisió de les solucions numèriques. De fet, sense anàlisi numèrica, els càlculs inconsistents poden debilitar bons models matemàtics.

Esta memòria està organitzada en quatre capítols. El primer és una introducció amb un breu repàs dels processos estocàstics, el model de Black-Scholes així com nocions preliminars d'anàlisi numèrica. En el segon capítol es tracta la PIDE per a les opcions europees segons el model CGMY. Es proposen dos esquemes en diferències finites; la primera aproximació garantix consistència incondicional de la solució amb la PIDE mentres que la segona proporciona estabilitat i positivitat incondicionals. Amb el primer enfocament, la part diferencial es discretitza per mitjà d'un esquema explícit i per a la part integral s'utilitza la regla del trapezi. En la segona aproximació, per a la part diferencial s'usa l'esquema tipus Patankar i la part integral s'aproxima per mitjà de la fórmula de tipus obert amb quatre punts. Posteriorment s'estudia en cada cas la positivitat, estabilitat i consistència. S'inclouen diversos exemples i simulacions.

En el capítol tercer, es proposa un tractament unificat per a una àmplia classe de models d'opcions en processos de Lévy com ara CGMY, Meixner i hiperbòlic generalitzat. Primer s'eliminen els termes de reacció i convecció en la PIDE per mitjà d'un apropiat canvi de variables. Posteriorment, la part diferencial de la PIDE s'aproxima per un esquema explícit, mentres que per a la part integral s'usa la fórmula de quadratura de Laguerre-Gauss. S'analitzen les propietats de positivitat, estabilitat i consistència. Per al cas d'opcions americanes, la part diferencial del PCL es discretitza per mitjà d'una aproximació amb tres nivells temporals, usant la quadratura de Laguerre-Gauss per a la integració numèrica de la part integral. Finalment, s'implementen mètodes iteratius de projecció i relaxació successiva i la tècnica de multimalla. Es mostren diversos exemples incloent l'estudi d'errors i el cost computacional.

Finalment, el capítol 4 està dedicat al model de Bates. Este model combina els enfocaments de volatilitat estocàstica i de difusió amb salts el que porta a una PIDE amb un terme amb derivades creuades. Tenint en compte que la discretización d'una derivada creuada comporta l'existència de termes amb coeficients negatius en l'esquema que deterioren la qualitat de la solució numèrica, es proposa una transformació de variables que elimina la esmentada derivada creuada en l'equació. La PIDE transformada es resol numèricament i es mostra l'anàlisi numèrica. D'altra banda s'estudia el LCP per a opcions americanes en el model de Bates.

Abstract

In the stock markets, the process of estimating a fair price for a stock, option or commodity in the next few months or a year is consider the corner stone for this trade. There are several attempts to obtain a suitable mathematical model in order to enhance the estimation process for evaluating the options for short or long periods. The Black-Scholes equation (1973) is considered a breakthrough in the mathematical modeling for the stock markets. It presented a practical mathematical model to estimate a fair value for a given option at that time. Based on Black-Scholes assumptions, they obtained a linear partial differential equation and it is solved analytically.

Since that time the stock trade has tremendously grown and several factors have been incorporated which lead to new complex financial products to appear. Black-Scholes assumptions as constant volatility and that the stock follows standard Brownian motion cannot keep up with these developments in the financial market. Consequently, these constraints need to be changed. There have been numerous efforts to develop alternative asset models that are capable of capturing the leptokurtic features found in financial market data, and subsequently to use these models to develop option prices that accurately reflect the volatility smiles and skews found in market traded options. Two strategies have been done to capture these behaviors; the first modification is to add jumps into the price process for the underlying asset, as originally was proposed by Merton; the second is to allow the volatility to evolve stochastically, introduced by Heston. The first modification leads to the so-called jump diffusion and Lévy models which are described by a partial integro-differential equation (PIDE) with two independent variables the underlying asset and time. Following the second approach, it leads to a partial differential equation (PDE) with two spatial variables; the underlying asset and the volatility apart from the time.

Here in this work, we solve numerically PIDEs for a wide class of Lévy processes using finite difference schemes for European options and also, the associated linear complementarity problem (LCP) for American option. Moreover, the models for options under stochastic volatility incorporated with jump-diffusion are considered. Numerical analysis for the proposed schemes is studied since it

is the efficient and practical way to guarantee the convergence and accuracy of numerical solutions. In fact, without numerical analysis, careless computations may waste good mathematical models.

This thesis consists of four chapters; the first chapter is an introduction containing historically review for stochastic processes, Black-Scholes equation and preliminaries on numerical analysis. Chapter two is devoted to solve the PIDE for European option under CGMY process. The PIDE for this model is solved numerically using two distinct discretization approximations; the first approximation guarantees unconditionally consistency while the second approximation provides unconditional positivity and stability. In the first approximation, the differential part is approximated using the explicit scheme and the integral part is approximated using the trapezoidal rule. In the second approximation, the differential part is approximated using the Patankar-scheme and the integral part is approximated using the four-point open type formula. After constructing the finite difference scheme for each case, the positivity, stability and consistency are studied. Also several examples and simulations are provided.

Chapter three provides a unified treatment for European and American options under a wide class of Lévy processes as CGMY, Meixner and Generalized Hyperbolic. First, the reaction and convection terms of the differential part of the PIDE are removed using appropriate mathematical transformation. After that the differential part for European case is discretized using the explicit scheme, while the integral part is approximated using Laguerre-Gauss quadrature formula. Numerical properties such as positivity, stability and consistency for this scheme are studied. For the American case, the differential part of the LCP is discretized using a three-time level approximation while the Laguerre-Gauss quadrature has been used to approximate the integral term. Next, the Projected successive over relaxation and multigrid techniques have been implemented to obtain the numerical solution. Several numerical examples are given including discussion of the errors and computational cost.

Finally in Chapter four, the PIDE for European option under Bates model is considered. Bates model combines both stochastic volatility and jump diffusion approaches resulting in a PIDE with a mixed derivative term. Since the presence of cross derivative terms involves the existence of negative coefficient terms in the numerical scheme deteriorating the quality of the numerical solution, the mixed derivative is eliminated using suitable mathematical transformation. The new PIDE is solved numerically and the numerical analysis is provided. Moreover, the LCP for American option under Bates model is studied.

List of Publications

Published Papers

1. M. Fakharany, R. Company and L. Jódar. "Unconditionally positive stable numerical solution of partial integro-differential option pricing problems", Journal of Applied Mathematics 2015(960728) (2015) 1–10.

2. M. Fakharany, R. Company and L. Jódar. "Positive finite difference schemes for a partial integro-differential option pricing model", Applied Mathematics and Computation 249 (2014) 320–332.

3. R. Company, L. Jódar and M. Fakharany. "Positive solutions of European option pricing with CGMY process models using double discretization difference schemes". Abstract and Applied Analysis 2013(517480) (2013) 1–11.

4. R. Company, L. Jódar, M. Fakharany and M.-C. Casabán. "Removing the correlation term in the option pricing Heston model: numerical analysis and computing", Abstract and Applied Analysis 2013(246724) (2013) 1–11.

Submitted Paper(s)

- M. Fakharany, R. Company and L. Jódar. "Solving partial integro-differential option pricing problems for a wide class of infinite activity Lévy processes", submitted to Journal of Computational and Applied Mathematics.

Chapter in Book(s)

- R. Company, M. Fakharany and L. Jódar, A chapter entitled "A finite difference scheme for options pricing modeled by Lévy processes" chapter 32, pp. 337-345, in book entitle "Mathematical modeling in social sciences and engineering", I.S.B.N.: 978-1-63117-339-4, Nova publishers, New York, 2014.

Presentations in Conferences

1. M. Fakharany, R. Company, L. Jódar, "A five-point stencil scheme for pricing American options under Bates model". Mathematical Modeling in Engineering & Human Behaviour 2014 Conference (September 4-6, 2014, Instituto de Matemática Multidisciplinar-UPV, València-Spain). Proceedings of the conference I.S.B.N.: 978-84-606-5746-0, pp. 50-54.

2. M. Fakharany, R. Company, L. Jódar, "Numerical Solution of Partial Integro-Differential Option Pricing Models with Cross Derivative term". European Consortium for Mathematics in Industry (ECMI 2014) Conference June 9-13 2014, Taormina-Italy. Proceedings in press.

3. R. Company, M. Fakharany, L. Jódar, "Un nuevo enfoque numérico de la componente no local de los modelos de Lévy para la valoración de opciones", XXIII Congreso de ecuaciones diferenciales y aplicaciones, XIII Congreso de matemática aplicada, Castelló, 9-13 septiembre de 2013. Anna Arnal et al. (eds.), Castelló de la Plana, Publicacions de la Universitat Jaume I (2014), ISBN: 978-84-8021-963-1, pp. 25-34.

4. M. Fakharany, R. Company, L. Jódar, "Numerical valuation infinite activity Lévy option pricing models". Mathematical Modeling in Engineering & Human Behaviour 2013 Conference (September 4-6, 2013, Instituto de Matemática Multidisciplinar-UPV, València-Spain). Proceedings of the conference I.S.B.N.: 978-84-695-9340-0, pp. 60-64.

5. M. Fakharany, R. Company, L. Jódar, "A mixed difference scheme guaranteeing positive solutions for European option pricing under a tempered stable process". International Conference on Computational and Mathematical Methods in Science and Engineering CMMSE 2013 (June 24-27,2013 Cabo de Gata, Alemria-Spain). Proceedings of the conference I.S.B.N.: 978-84-616-2723-3, pp. 584-589.

Chapter 1

Introduction

1.1 Derivatives markets and options

In the last 30 years, derivatives have become increasingly important in finance. Futures and options are actively traded on many exchanges throughout the world. Several types of forward contracts, options, swaps, and other derivatives are entered into by financial institutions, fund managers, and corporate treasurers in the market.

There are many different types of options that can be traded and these can be categorized in a number of ways. In a very broad sense, there are two main types: calls and puts. A call option gives the holder the right, but not the obligation, to buy the underlying asset by a certain date for a certain price. A put option gives the holder the right to sell the underlying asset by a certain date for a certain price. The price in the contract is known as the exercise price or strike price; the date in the contract is known as the expiration date or maturity. American options can be exercised at any time up to the expiration date. European options can be exercised only on the expiration date itself. Most of the options that are traded on exchanges are American [46].

A derivatives exchange is a market where individuals trade standardized contracts that have been defined by the exchange. Derivatives exchanges have existed for a long time. In 1848 the Chicago Board of Trade (CBOT) was founded to bring farmers and merchants together. Initially its original business was to standardize the quantities and qualities of the grains that were traded. Within a few years,

the first futures-type contract was developed. It was known as a to-arrive contract. Speculators soon became interested in the contract and found trading the contract to be an attractive alternative to trading the grain itself. A rival futures exchange, the Chicago Mercantile Exchange (CME), was established in 1919. Now futures exchanges exist all over the world. CME and CBOT have merged to form the CME Group which also includes the New York Mercantile Exchange.

The Chicago Board Options Exchange started trading call option contracts on 16 stocks in 1973. Options had traded prior to 1973, but the CBOE succeeded in creating an orderly market with well-defined contracts. Put option contracts started trading on the exchange in 1977. The CBOE now trades options on over 2,500 stocks and many different stock indices. Like futures, options have proved to be very popular contracts. Many other exchanges throughout the world now trade options. The underlying assets include foreign currencies and futures contracts as well as stocks and stock indices [46].

1.2 Stochastic processes

Stochastic processes models are collections of variables that develop randomly in time, space or space-time. This development will be described through an index $t \in T$. We may define a family of random variables $\{X_t,\ t \in T\}$, which will be a stochastic process [50].

Definition 1. *A stochastic process $\{X_t,\ t \in T\}$ is a collection of random variables X_t, indexed by a set T, taking values in a common measurable space P associated with an appropriate $\sigma-$algebra.*

T could be a set of times, when we have a temporal stochastic process; a set of spatial coordinates, when we have a spatial process; or a set of both time and spatial coordinates, when we deal with a spatio-temporal process.
An important concept is that of a stationary process, that is a process whose characterization is independent of time at which the observation of the process is initiated [50].

Definition 2. *We say that the stochastic process $\{X_t,\ t \in T\}$ is strictly stationary if for any n, $t_1, t_2, \ldots, t_n$ and τ, $(X_{t_1}, X_{t_2}, \ldots, X_{t_n})$ has the same distribution as $(X_{t_1+\tau}, X_{t_2+\tau}, \ldots, X_{t_n+\tau})$.*

1.2.1 Poisson process

Poisson processes are continuous time and discrete space process.

Definition 3. *Suppose that the stochastic process $\{X_t\}_{t\in T}$ describes the number of events of a certain type produced until time t and has the following properties [50]:*

1. *The number of events in nonoverlapping intervals are independent.*
2. *There is a constant λ such that the probabilities of the events that happen over small intervals of duration Δt are:*
   - $P(\text{number of events in } (t, t+\Delta t] = 1) = \lambda\Delta t + o(\Delta t)$.
   - $P(\text{number of events in } (t, t+\Delta t] > 1) = o(\Delta t), \quad o(\Delta t)/\Delta t \to 0$.

Consequently, $\{X_t\}$ is said to be a homogeneous Poisson process with parameter λ, characterized by the fact $X_t \sim Po(\lambda t)$.
Nonhomogeneous Poisson processes are described by the intensity function $\lambda(t)$ or the intensity function $m(t) = \int_0^t \lambda(s)ds$, so in general, it is a time dependent intensity function but it could be space or space-time dependent as well. For a nonhomogeneous Poisson process, the number of events that happen in the interval $(t, t+s]$ will have a $Po(m(t+s) - m(t))$ distribution.

1.2.2 Gaussian process

The Gaussian process is a continuous process in both time and state-space. Let $\{X_t\}$ be a stochastic process such that for any n times $\{t_1, t_2, \ldots, t_n\}$ the joint distribution of X_{t_i}, $i = 1, 2, \ldots, n$ is $n-$variate normal, hence the process is Gaussian. Moreover, for any finite set of time instants $\{t_i\}$, $i = 1, 2, \ldots$ when the random variables are mutually independent and X_t is normally distributed for every t, we call it a purely random Gaussian process.

1.2.3 Brownian motion

This continuous time and state-space process has the following properties [50]:

1. The process $\{X_t,\ t \geq 0\}$ has independent, stationary increments: for $t_1,\ t_2 \in T$ and $t_1 < t_2$, the distribution of $X_{t_2} - X_{t_1}$ is the same of $X_{t_2+h} - X_{t_1+h}$ for each

$h > 0$, and for non-overlapping intervals (t_1, t_2) and (t_3, t_4) with $t_1 < t_2 < t_3 < t_4$, the random variables $X_{t_2} - X_{t_1}$ and $X_{t_4} - X_{t_3}$ are independent.

2. For any time interval (t_1, t_2), the random variable $X_{t_2} - X_{t_1}$ has distribution $\mathcal{N}(0, \sigma^2(t_2 - t_1))$.

1.2.4 Itô process

Several physical phenomena and economic markets are modeled by means of deterministic differential equations $\dot{x} = \frac{dx}{dt} = a(x, t)$. This type of modeling neglects stochastic fluctuations and is not appropriate for stock prices. If the processes x are to include Wiener processes as special case, the derivative $\frac{dx}{dt}$ is meaningless. In order to circumvent non-differentiability, integral equations are used to define a general class of stochastic processes. The randomness is inserted as follows [79]

$$x(t) = x(0) + \int_{t_0}^{t} a(x(s), s)ds + \text{randomness}. \tag{1.1}$$

The first integral in the resulting integral equation is an ordinary integration (Riemann or Lebesgue). The final integral equation is written as a "stochastic differential equation" (SDE) and named after to Itô.

Definition 4. *An Itô stochastic differential equation [79]*

$$dX_t = a(X_t, t)dt + b(X_t, t)dW_t, \tag{1.2}$$

associated with $X_{t_0} = X_0$ is a symbolic short form of the integral equation

$$X_t = X_{t_0} + \int_{t_0}^{t} a(X_s, s)ds + \int_{t_0}^{t} b(X_s, s)dW_s, \tag{1.3}$$

where $a(X_s, s)$ is the drift term and $b(X_t, t)$ is the diffusion coefficient.

Itô's lemma

An important result in this area is known as Itô's lemma. In fact, it is the counterpart of the chain rule for deterministic functions. Consider a function G following an Itô process (1.2), then we have

$$dG = \left(\frac{\partial G}{\partial x} a + \frac{\partial G}{\partial t} + \frac{1}{2} \frac{\partial^2 G}{\partial x^2} b^2 \right) dt + \frac{\partial G}{\partial x} b dW_t. \tag{1.4}$$

1.2.5 Lévy process

Definition 5. *A stochastic process $\{X_t\}_{t\in T}$ on $(\Omega, \mathcal{F}, P)$ with values in $\mathbb{R}^n$ is called a Lévy process if the following properties hold [24]:*

1. *$X_0 = 0$,*
2. *Independent increments: for every increasing sequence of times $\{t_j\}_{j=0}^m$, the random variables X_{t_0}, $\{X_j - X_{j-1}\}_{j=1}^n$ are independent.*
3. *Stationary increments: the law of $X_{t+h} - X_t$ does not depend on t.*
4. *Stochastic continuity: $\forall \varepsilon > 0$, $\lim_{h\to 0} P(|X_{t+h} - X_t|) = 0$.*

1.3 The Black Scholes equation

The market is the place where the value of the option is determined. Say we want to calculate a fair value for a given option, we need a mathematical model of the market. Usually the mathematical models are used in order to approximate the complex reality of the financial world. The earlier two financial models named after the pioneers Black-Scholes [10], and Merton have been both successful and widely accepted. It was actually a major breakthrough in the pricing of European stock options. Based on Itô's lemma (1.4), the Black-Scholes equation is given by

$$\frac{\partial V}{\partial t} + \frac{\sigma^2}{2} S^2 \frac{\partial^2 V}{\partial S^2} + rS\frac{\partial V}{\partial S} - rV = 0, \tag{1.5}$$

where $V(S,t)$ is the option price function, σ is the volatility, r is the risk free interest and S is the underlying asset. Equation (1.5) is a partial differential equation (PDE) used for estimating the value function $V(S,t)$. This PDE is obtained based on the following assumptions:

1. The stock pays no dividends during the option's life.
2. This model is adapt to European exercise.
3. The markets are efficient. This means that there is no fees or taxes, all parties have an immediate access to any information, the interest rate for lending and borrowing money are equal, all securities and credits are available at any time. So in other words, all variables are perfectly divisible.

4. The asset price follows a geometric Brownian motion 1.2.3.

5. Interest rates remain constant.

6. Returns are lognormal distributed.

1.4 Preliminaries on numerical analysis

In this section we consider the necessary properties or conditions of a given numerical scheme (finite difference equations) that must be hold to guarantee that the solution of this finite difference equations is fairly accurate approximation to the solution of the corresponding PDE. Usually these conditions lead to two distinct but interrelated problems. The first investigates the convergence of the solution of the approximating difference equations to the solution of the PDE; the second focuses on the boundedness, the unbounded growth or controlled decay of the solution of the finite difference equations which is known as the stability problem.

1.4.1 Convergence

Here, we give a brief definition for the convergence [80]. Consider U represents the exact solution of a partial differential equation with independent variables x and t, also let u be the solution of the difference equations that approximate the partial differential equation.

Definition 6. *A difference scheme $F(u)$ approximating the partial differential equation $L(U)$ is a pointwise convergent scheme if for any x and t, as (ih, jk) converges to (x, t), u converges to U as δx and δt converge to 0.*

The difference $U - u$ is called the discretization error. Usually, the problem of convergence is a difficult one to investigate effectively since the final expression for the discretization error usually is given in terms of unknown derivatives. Consequently, there is no mathematical way to estimate bounds for them. However, there is another mathematical procedure in order to study the convergence of the difference equations approximating the linear parabolic and hyperbolic differential equations by studying the stability and consistency of the scheme which is known as Lax's equivalence theorem [73, pp. 45-48].

1.4.2 Stability

Before we discuss the stability of a difference scheme, we recall some useful norm $\|.\|$ definitions for vector and matrix [40, 80].

Vector norms

The norm of a vector $\mathbf{v}$ is a real positive number giving a measure of the size of the vector and is denoted by $\|\mathbf{v}\|$. Let $\mathbf{v}$ be a vector in $\mathbb{R}^n$ such that $\mathbf{v} = (v_1, v_2, \ldots, v_n)$, there are several forms of vector norm and the most three commonly used as follows

1. The 1-norm of $\mathbf{v}$ is the sum of the moduli of the components of $\mathbf{v}$, i.e.,

$$\|v\|_1 = \sum_{i=1}^{n} |v_i|. \tag{1.6}$$

2. The infinity norm of $\mathbf{v}$ is the maximum of the moduli of the components of $\mathbf{v}$, i.e.,

$$\|v\|_\infty = \max_i |v_i|. \tag{1.7}$$

3. The 2-norm of $\mathbf{v}$ is the square root of the sum of the squares of the moduli of the components of $\mathbf{v}$, i.e.,

$$\|v\|_2 = \sqrt{\sum_{i=1}^{n} |v_i|^2}. \tag{1.8}$$

Matrix norms

Definition 7. *Let $A = (a_{ij})$ be a matrix in $\mathbb{R}^{n\times n}$ and denote its set of eigenvalues by $\{\lambda_1, \lambda_2, \ldots, \lambda_n\}$. The spectral radius of A is given by*

$$\rho(A) = \max_i |\lambda_i|. \tag{1.9}$$

Now let $B = (b_{ij})$ be a matrix in $\mathbb{R}^{m\times n}$, the norm of the matrix B can be obtained by several forms. Here we recall the most three usable forms:

1. The maximum column sum norm is

$$\|B\|_1 = \max_{1\le j\le n} \sum_{i=1}^{m} |b_{ij}|. \tag{1.10}$$

2. The maximum row sum norm is

$$\|B\|_\infty = \max_{1\leq i\leq m} \sum_{j=1}^{n} |b_{ij}|. \tag{1.11}$$

3. The spectral norm is

$$\|B\|_2 = \sqrt{\rho(B^T B)} = \sqrt{\rho(BB^T)}. \tag{1.12}$$

For a matrix $B = (b_{ij})_{n\times m}$ in $\mathbb{R}^{m\times n}$, we denote by $\|B\|_\infty = \max_{1\leq i\leq m}\{\sum_{j=1}^{n} |b_{ij}\|\}$. Consequently if A is a block matrix with $n \times m$ block entries A_{ij}, then the infinite norm of A, see [40, Chap. 2],

$$\|A\|_\infty = \max_{1\leq i\leq m} \{\|[A_{i1}\ A_{i2} \dots A_{in}]\|_\infty\}. \tag{1.13}$$

An usual interpretation of stability reads that for a stable scheme, small errors in the initial conditions cause small errors in the solution which coincide with the definition of well-posedness of a partial differential equation. First, we define the stability for a two level difference scheme of the form

$$\mathbf{u}^{n+1} = Q\mathbf{u}^n, \quad n > 0, \tag{1.14}$$

which will generally be a difference scheme for solving a given initial-value problem [84].

Definition 8. *The difference scheme* (1.14) *is said to be stable with respect to the norm* $\|.\|$ *if there exist positive constants* h_0 *and* k_0*, and non-negative constants* K *and* β *such that*

$$\|\mathbf{u}^{n+1}\| \leq Ke^{\beta t}\|\mathbf{u}^0\|, \tag{1.15}$$

for $0 \leq t = (n+1)k$*,* $0 < h \leq h_0$ *and* $0 < k \leq k_0$*.*

- Based on the definition of the stability, it allows the solution to grow. Notice that the solution can grow with the time, but not with the number of time steps.

- Notice that the stability here is established for a homogenous difference scheme. When we discuss the stability of a nonhomogeneous difference scheme, the stability of the associated nonhomogeneous scheme must be considered.

The next definition provides several types of stability; whether the proposed finite difference scheme is conditionally or unconditionally strongly uniform stable.

Definition 9. *The difference scheme* (1.14) *is said to be unconditionally uniform stable when* (1.15) *holds without any restriction on the stepsizes of the independent variables h and k, otherwise the scheme* (1.14) *is conditionally stable.*

1.4.3 Consistency

Consistency for PDEs

In several cases, it is possible to approximate a PDE by a finite difference scheme that is stable but has a solution does not converge to the solution of the PDE as the mesh lengths approach to zero. Such a difference scheme is said to be inconsistent with the PDE. The consistency can be defined in two different ways as follows

Definition 10. *Consider a PDE $L[U(x,t)] = f(x,t)$ with a corresponding finite difference scheme $F_{i,j}(u) = f_{i,j}$. It is said that the finite difference scheme is consistent with the PDE if for any smooth function $\phi(x,t)$ [84]*

$$F_{i,j}(\phi) - L[\phi_{i,j}] \to 0, \quad as\ h,\ k \to 0. \tag{1.16}$$

- The difference $F_{i,j}(\phi) - L[\phi_{i,j}]$ is known the local truncation error at the point (ih, jk) and is denoted by $T_i^j(\phi)$

$$T_i^j(\phi) = F_{i,j}(\phi) - L[\phi_{i,j}]. \tag{1.17}$$

- In many papers, ϕ is replaced by U.

Definition 11. *Consider a PDE $L[U(x,t)] = f(x,t)$ with a corresponding finite difference scheme $F_{i,j}(u) = f_{i,j}$. Let $U_{i,j} = U(ih, jk)$ be the exact theoretical solution at point (ih, jk), then the truncation error is given by*

$$T_i^j(U) = F_{i,j}(U) - L[U_{i,j}]. \tag{1.18}$$

If $T_i^j \to 0$ as $h \to 0$, $k \to 0$, then the difference equation is said to be consistent with the PDE [80].

Note that for a homogenous PDE (1.18) takes the form $T_i^j(U) = F_{i,j}(U)$. Using Taylor expansions, it is simple to express T_i^j in terms of powers of h and k and

partial derivatives of U at (ih, jk). However, U and its derivatives are unknown, the analysis is worthwhile because it provides a suitable method for comparing the local accuracies of different difference schemes approximating the PDE.
Here in this study, the second definition has been used.

Consistency for integral equation

Here, we focus on the consistency for integral equations of Volterra type which has the following form [55]

$$f(t) = g(t) + \int_0^t K(t, s, f(s))ds, \quad 0 \leq t \leq T, \tag{1.19}$$

where $g(t)$ is a given function and $K(t, s, f(s))$ is the kernel of the integration. Consider the following discretization with stepsize h ($t_i = ih$)

$$F_n = g(t_n) + h\sum_{i=0}^{n} W_{ni}K(t_n, t_i, F_i), \quad n = r, r+1, \ldots. \tag{1.20}$$

Let f be the solution of (1.19), then the function

$$\delta(h, t_n) = f(t_n) - F_n = \int_0^{t_n} K(t_n, s, f(s))ds - h\sum_{i=0}^{n} W_{ni}K(t_n, t_i, F_i) \tag{1.21}$$

is the local consistency error for (1.19).

Definition 12. *Let $\mathcal{F}$ be a class of equations of the form* (1.19)*. If for every equation in $\mathcal{F}$*

$$\lim_{h} \max_{0 \leq n \leq N} |\delta(h, t_n)| = 0, \tag{1.22}$$

then the approximation method (1.20) *is said to be consistent with* (1.19) *for the class equation $\mathcal{F}$.*

Chapter 2

Positive solutions of European option pricing with CGMY process models using double discretization difference schemes

2.1 Introduction

The hypothesis that asset prices behave according to the geometric Brownian motion when one derives the option prices is inconsistent with market prices [15]. This drawback has been overcome using Lévy process models [7, 11, 16, 33, 52, 53, 57, 63] allowing the calibration of the model to the option market price and the reproduction of a wide variety of implied volatility skews/smiles, see [24] and [66, chap. 14, 15]. Among the Lévy process models, it is remarkable to distinguish these with finite activity, i.e., jump diffusion models [53, 63] and those where the intensity of the jumps is not a finite measure [7, 11, 16, 33, 52, 57, 63]. These models are characterized by the fact that option price is given by the solution of a PIDE involving a second order differential operator part, and a non local integral term that presents additional difficulties. In [61] wavelet methods are applied to infinite Lévy models. Monte Carlo approaches are developed by [59, 69]. Interesting analytic-numerical treatments have been introduced in [9, 36, 67]. The so called COS method for pricing European options is presented in [36]. This is based on the knowledge of the characteristic function and its relation with the coefficients of the Fourier-cosine ex-

pansion of the density function. In [67], an expansion of the characteristic function of local volatility models with Lévy jumps is developed. The authors in [9] derive an analytical formula for the price of European options for any model including local volatility and Poisson jump process by using Malliavin calculus techniques.

Many authors used the finite difference (FD) schemes for solving these PIDE problems [2, 4, 5, 17, 25, 54, 74, 75, 82, 85, 87]. Dealing with FD methods for such PIDEs, the following challenges should be addressed. For instance, how to approximate the integral term and how to localize a bounded computational domain in order to consider relevant information like large jumps. In addition, the possible singularities of the integral kernel should be carefully treated [25, 87].

The nonlocal character of the integral part involves a dense discretization matrix. In the outstanding paper [25], Cont and Voltchkova presented an explicit-implicit method (explicit into the integral part and implicit into the differential one) to obtain the numerical approximation of viscosity solutions for European and barrier options. An improvable issue of [25] is that in order to approximate the truncated integral term, they assume a particular behavior of the solution outside of the bounded numerical domain. This last drawback is experienced by most of the authors, see [2, 4, 85].

Implicit FD methods for the numerical solution of the CGMY model have been used by Wang *et al.* [87] who proposed an implicit timestepping method avoiding dense linear systems, but involving the iteration methods drawbacks of the implicit methods such as ungranted positivity. They also assume that for large enough values of S, the solution behaves like Black-Scholes.

In [5], the authors use an unconditionally ADI FD method and accelerate it using fast Fourier transform (FFT) for jump diffusion models with finite jump intensity. Tavella and Randall in [82] use an implicit time discretization and propose a stationary rapid convergent iterative method to solve the full matrix problem quoted above, but with poor numerical analysis. A generalization of their iterative method to price American options is proposed in [75].

One of the most relevant and versatile Lévy models is the one proposed by Carr, Geman, Madan and Yor, the so called CGMY model [16], that belongs to the family of KoBoL models [11]. It is considered a prototype of the general class of models with jumps and enjoys widespread applicability. The CGMY model allows diffusions and jumps of both finite and infinite activity. The CGMY Lévy density is given by

$$\nu(y) = \begin{cases} \frac{Ce^{-\mathcal{G}|y|}}{|y|^{1+Y}}, & y < 0, \\ \frac{Ce^{-\mathcal{M}|y|}}{|y|^{1+Y}}, & y > 0, \end{cases} \tag{2.1}$$

where $C > 0,\ \mathcal{G} \geq 0,\ \mathcal{M} \geq 0$, and $Y < 2$. The parameter Y allows to control the fine structure of asset return distribution. For $Y < 0$, the Lévy process is of finite activity, i.e., the measure is finite, $\int \nu(y)dy < \infty$. For $0 \leq Y \leq 1$, it is of infinity activity but finite variation, i.e., $\int_{|y|<1} y\nu(y)dy < \infty$. Finally, for $1 < Y < 2$, both the activity and variation are infinite. Note that for $Y = 0$ one gets the well known Variance Gamma process proposed by Madan and Seneta [58] as a particular case. So CGMY model is an improved and generalization of the Variance Gamma model [57].

The authors in [4] use FD methods discretizing the equation in space by the collocation method and using explicit difference backward schemes focused on the case of infinite activity and finite variation.

In [54] an efficient three time-level finite difference scheme is proposed for the infinite activity Lévy model. Second order convergence rate are shown in numerical experiments although the numerical analysis of the method is not developed.

Based on Itô calculus the corresponding PIDE for the CGMY model with $\nu(y)$ (2.1) is given by

$$\frac{\partial V}{\partial \tau} = \frac{\sigma^2}{2}S^2\frac{\partial^2 V}{\partial S^2} + (r-q)S\frac{\partial V}{\partial S} - rV$$

$$+ \int_{-\infty}^{+\infty} \nu(y)\big[V(Se^y,\tau) - V(S,\tau) - S(e^y-1)\frac{\partial V}{\partial S}\big]dy,\ S \in (0,\infty),\ \tau \in (0,T], \tag{2.2}$$

$$V(S,0) = f(S), \qquad S \in (0,\infty). \tag{2.3}$$

Here $V(S,\tau)$ is the option price depending on the underlying asset S, the time $\tau = T - t$, σ is the volatility parameter, r and q are the risk-free interest and the

continuous dividend paid by the asset respectively. The payoff function $f(S)$ for a vanilla call option is given by

$$f(S) = \max(S - E, 0), \tag{2.4}$$

where E is the strike price.

Like [17] and [74] for jump diffusion models we transform the original PIDE problem in order to remove the convection term to avoid possible numerical oscillations. With respect to the singularity of the integral kernel quoted above, the jump component in the neighborhood of log jump size zero is approximated by using a Taylor expansion, like [25] and [87].

The selection of the boundary conditions of the numerical domain, the discretization of the infinite domain of the integration and matching the discretization of both the differential and the integral part are important challenges. Some authors like [25], assume a particular behavior of the solution outside of the bounded numerical domain. In order to weaken these hypotheses we do not truncate the infinite integral and we use a nonuniform partition of the complete unbounded domain, allowing a proper matching of the discretizations of the differential and integral parts by assuming asymptotic linear behavior of the solution. This strategy involves a double discretization with two spatial stepsize parameters that will allow a better flexibility to improve the approximation in different zones of the domain.

In this chapter double discretization numerical schemes for solving (2.1)-(2.4) are proposed. On the one hand, a consistent and conditional stable and positive scheme is studied. On the other hand an unconditional stable and positive scheme is presented based on numerical methods for parabolic equations [14, 18] following the idea initiated by Patankar, the so-called Patankar trick [68].

This chapter is organized as follows. In Section 2.2, the integral part of (2.2) is approximated in a neighborhood of $y = 0$ to obtain a new PIDE integral part extended outside a neighborhood of $y = 0$. Then a variable transformation is developed in order to remove both the convection and reaction terms of the differential part. Following the idea developed in [17], the unbounded domain for the integral part is

converted into a bounded one. In Section 2.3, two distinct finite difference schemes are constructed; the first one treats explicitly the differential part and the integral part is discretized using the trapezoidal rule while, in the second scheme, the differential part is discretized based on what so called Patankar-trick and the integral part is approximated using the four-point open type discretization. Positivity and stability of the numerical solutions given by these schemes are studied in Section 2.4. Also, the consistency of them are treated in Section 2.5. In Section 2.6, some illustrative numerical examples show the advantages of the new discretization approach showing how the double discretization allows flexible improvement of the accuracy in different zones of the domain.

The exponential integrals have a major role in evaluating important class of integrals. Let s and z be continuous (real or complex) variables, the exponential integral of order s, denoted by $E_s(z)$ is given by [65]

$$E_s(z) = \int_1^\infty t^{-s} \exp(-zt) dt. \tag{2.5}$$

2.2 Transformation of the PIDE problem

We begin this section by removing the singularity of the kernel of the integral term of PIDE (2.2). Let $\varepsilon > 0$ and let us split the real line into two regions $R_1 = [-\varepsilon, \varepsilon]$ and $R_2 = (-\infty, -\varepsilon) \cup (\varepsilon, \infty)$. For the term $V(Se^y, \tau)$ in R_1, taking Taylor expansion for $z = Se^y$ about $z = S$ one gets

$$V(Se^y, \tau) = V(S, \tau) + S(e^y - 1)\frac{\partial V}{\partial S} + \frac{(S(e^y - 1))^2}{2}\frac{\partial^2 V}{\partial S^2} + \mathcal{O}(y^3), \ |y| < \varepsilon. \tag{2.6}$$

Taking into account (2.1) the integral part of (2.2) can be written as

$$I(V) = \frac{\sigma^2(\varepsilon)}{2} S^2 \frac{\partial^2 V}{\partial S^2} - \gamma(\varepsilon) S \frac{\partial V}{\partial S} - \lambda(\varepsilon) V(S, \tau) + \int_{R_2} \nu(y) V(Se^y, \tau) dy + \mathcal{O}(\varepsilon^{3-Y}), \tag{2.7}$$

where the integrals

$$\sigma^2(\varepsilon) = \int_{-\varepsilon}^{\varepsilon} \nu(y)(e^y - 1)^2 dy, \ \gamma(\varepsilon) = \int_{R_2} \nu(y)(e^y - 1) dy, \ \lambda(\varepsilon) = \int_{R_2} \nu(y) dy, \tag{2.8}$$

can be evaluated with high accuracy using the exponential integrals [65], [83, chapter 7] where the integrals appearing in (2.8) are convergent, [25]. Let us denote

$$\hat{f}(\alpha, M, \varepsilon) = M^{\alpha-1}\Gamma(1-\alpha) - \varepsilon^{1-\alpha}E_{\alpha}(\varepsilon M), \tag{2.9}$$

where Γ denotes the gamma function and E_{α} is the exponential integral (2.5). For the first integral in (2.8) one gets

$$\sigma^2(\varepsilon) = C\sum_{k=0}^{2}(-1)^k\binom{2}{k}\big[\hat{f}(1+Y, G+k, \varepsilon) + \hat{f}(1+Y, M-k, \varepsilon)\big]. \tag{2.10}$$

Notice that (2.10) holds for $Y \in (0,1)\cup(1,2)$. For the particular case where $Y = 0$ one gets,

$$\sigma^2(\varepsilon) = C\Big[\ln\frac{(G+1)^2(M-1)^2}{G(G+2)M(M-2)} - \sum_{k=0}^{2}\binom{2}{k}(-1)^k\big(E_1[\varepsilon(G+k)] + E_1[\varepsilon(M-k)]\big)\Big], \tag{2.11}$$

while for $Y = 1$, we have

$$\sigma^2(\varepsilon) = 2C\Big[\ln\frac{(G+2)(M-1)}{(G+1)(M-2)} + E_1[\varepsilon(G+2)] - E_1[\varepsilon(G+1)] - E_1[\varepsilon(M-2)] + E_1[\varepsilon(M-1)]\Big] +$$

$$CG\Big[\ln\frac{G(G+2)}{(G+1)^2} + \sum_{k=0}^{2}\binom{2}{k}(-1)^k E_1[\varepsilon(G+k)]\Big] - \frac{C}{\varepsilon}e^{-G\varepsilon}(e^{-\varepsilon}-1)^2 +$$

$$CM\Big[\ln\frac{M(M-2)}{(M-1)^2} + \sum_{k=0}^{2}\binom{2}{k}(-1)^k E_1[\varepsilon(M-k)]\Big] - \frac{C}{\varepsilon}e^{-M\varepsilon}(e^{\varepsilon}-1)^2. \tag{2.12}$$

For the remaining integrals in (2.8), we have

$$\gamma(\varepsilon) = C\varepsilon^{-Y}\sum_{k=0}^{1}\binom{1}{k}(-1)^{1-k}\Big[E_{1+Y}\big(\varepsilon(G+k)\big) + E_{1+Y}\big(\varepsilon(M-k)\big)\Big] \tag{2.13}$$

$$\lambda(\varepsilon) = C\varepsilon^{-Y}\Big(E_{1+Y}(G\varepsilon) + E_{1+Y}(M\varepsilon)\Big) \tag{2.14}$$

Hence, the problem (2.2) takes the following form

$$\frac{\partial V}{\partial \tau} = \frac{\hat{\sigma}^2}{2}S^2\frac{\partial^2 V}{\partial S^2} + (r-q-\gamma(\varepsilon))S\frac{\partial V}{\partial S} - (r+\lambda(\varepsilon))V$$

$$+\int_{R_2}\nu(y)V(Se^y,\tau)dy + \mathcal{O}(\varepsilon^{3-Y}), \tag{2.15}$$

where $\hat{\sigma}^2 = \hat{\sigma}^2(\varepsilon) = \sigma^2 + \sigma^2(\varepsilon)$.
In order to remove the convection and reaction terms from (2.15), let us introduce the following transformation of variables:

$$x = \exp[(r - q - \gamma(\varepsilon))\tau]S,\ U(x,\tau) = \exp[(r + \lambda(\varepsilon))\tau]V(S,\tau). \tag{2.16}$$

Hence the problem (2.15) is approximated by the following form

$$\begin{gathered}\frac{\partial U}{\partial \tau} = \frac{\hat{\sigma}^2}{2}x^2\frac{\partial^2 U}{\partial x^2} + J,\ x \in (0,+\infty),\ \tau \in (0,T], \\ U(x,0) = f(x),\ x \in (0,+\infty),\end{gathered} \tag{2.17}$$

where

$$\begin{gathered}J = J(x,\tau,\varepsilon) = \textstyle\int_{R_2} \nu(y)U(xe^y,\tau)dy = \\ \textstyle\int_{-\infty}^{-\varepsilon} \nu(y)U(xe^y,\tau)dy + \int_{\varepsilon}^{\infty} \nu(y)U(xe^y,\tau)dy.\end{gathered} \tag{2.18}$$

Finally in order to combine both discretizations of the differential and integral part, we use $\phi = xe^y$ to change the integrand J as follows:

$$J = J_1 + J_2 = \int_0^{xe^{-\varepsilon}} g(x,\phi)U(\phi,\tau)d\phi + \int_{xe^{\varepsilon}}^{\infty} g(x,\phi)U(\phi,\tau)d\phi, \tag{2.19}$$

where, $g(x,\phi) = \frac{\nu(\ln(\phi/x))}{\phi}$. For evaluating the integrals in all the positive real line, let us introduce a parameter $A > 0$ that separate $[0,\infty)$ into $[0,A] \cup [A,\infty)$. The point A can be chosen according to the criteria used by [25, 51, 62] to truncate the numerical domain. For instance, in [85] one takes $A = 4E$ and in [17] one takes $A = 3E$. To evaluate the integrals related to $x > A$, they are transformed to finite integrals by using the substitution $z = \frac{A}{\phi}$ consequently, obtaining integrals of the form

$$\int_{\alpha}^{\beta} g(x,\phi)U(\phi,\tau)d\phi = A\int_{\phi_0}^{\phi_1} g(x,\frac{A}{z})U(\frac{A}{z},\tau)\frac{dz}{z^2}, \tag{2.20}$$

where $\phi_0 = \frac{A}{\beta},\ \phi_1 = \frac{A}{\alpha}$. In particular if $\beta \to \infty$ then $\phi_0 = 0$. Hence, the problem (2.17) takes the form

$$\frac{\partial U}{\partial \tau} = \frac{\hat{\sigma}^2}{2}x^2\frac{\partial^2 U}{\partial x^2} + J,\ x \in (0,\infty),\ \tau \in (0,T], \tag{2.21}$$

$$U(x,0) = f(x), \qquad x \in (0,\infty). \tag{2.22}$$

2.3 Numerical Scheme Construction

We are going to construct two distinct finite difference scheme; the first scheme guarantees unconditionally consistency while the positivity and stability hold conditionally, the second scheme guarantees unconditionally positivity and stability meanwhile the consistency is restricted.

2.3.1 The numerical scheme that guarantee unconditionally consistency

In this section a difference scheme for the problem (2.21)-(2.22) is designed. For the time variable, given $\tau \in (0, T]$, let k be the time-step discretization $k = \Delta\tau = \frac{T}{L}$ and $\tau^l = lk$, $0 \leq l \leq L$, with L integer. With respect to the spatial variable x and for an arbitrary fixed $A > 0$, we divide the interval $[0, A]$ into N equal intervals with a spatial-step $h = \Delta x = \frac{A}{N}$, with $x_i = ih$, $0 \leq i \leq N$. Note that the unbounded domain $[A, \infty)$ is transformed into $(0, 1]$ by the above quoted change $z = \frac{A}{x}$. Thus a uniform distributed mesh partition of the interval $(0, 1]$ of the form $z_i = i\delta,\ \delta = \frac{1}{M},\ 0 < i \leq M$ is mapped into a non uniform mesh partition of $[A, \infty)$, $x_i = \frac{A}{z_{N+M-i}},\ N \leq i \leq N + M - 1$. Hence, we have

$$x_i = \begin{cases} ih,\ 0 \leq i \leq N, \\ \frac{A}{1-(i-N)\delta},\ N \leq i \leq N + M - 1. \end{cases} \tag{2.23}$$

Let us denote $U(x_i, \tau^l) \approx u_i^l,\ 0 \leq i \leq N + M - 1,\ 0 \leq l \leq L$,

$$\left.\begin{array}{c} \frac{\partial U}{\partial \tau}(x_i, \tau^l) \approx \frac{u_i^{l+1} - u_i^l}{k} \\ \frac{\partial^2 U}{\partial x^2}(x_i, \tau^l) \approx \Delta_i^l, \end{array}\right\} \tag{2.24}$$

where

$$\Delta_i^l \equiv \begin{cases} \frac{u_{i-1}^l - 2u_i^l + u_{i+1}^l}{h^2},\ 0 \leq i < N, \\ 2\big[\frac{u_{i-1}^l}{h_{i-1}(h_i + h_{i-1})} - \frac{u_i^l}{h_i h_{i-1}} + \frac{u_{i+1}^l}{h_i(h_{i-1} + h_i)}\big],\ N \leq i \leq N + M - 2, \end{cases} \tag{2.25}$$

and $h_i = x_{i+1} - x_i > 0$. With respect to the approximation of (2.19), note that for each x_i we need to evaluate two integrals corresponding to $[0, x_i e^{-\varepsilon}]$ and $[x_i e^{\varepsilon}, \infty)$, denoted by $J_{i,r}^l = J_r(x_i, \tau^l, \varepsilon),\ r = 1, 2$. Let $i_1(i)$ be the biggest j with $0 \leq j \leq N + M - 1$ such that $x_j \leq x_i e^{-\varepsilon}$ and let $i_2(i)$ be the first j such that $x_i e^{\varepsilon} \leq x_j$.

Then the expression (2.19) for the point (x_i, τ^l) has the following from

$$\left.\begin{array}{c} J_i^l = J_{i,1}^l + J_{i,2}^l, \\ J_{i,1}^l = \int_0^{x_{i_1}} g(x_i,\phi)U(\phi,\tau^l)d\phi + \int_{x_{i_1}}^{x_i e^{-\varepsilon}} g(x_i,\phi)U(\phi,\tau^l)d\phi \\ J_{i,2}^l = \int_{x_{i_2}}^{\infty} g(x_i,\phi)U(\phi,\tau^l)d\phi + \int_{x_i e^{\varepsilon}}^{x_{i_2}} g(x_i,\phi)U(\phi,\tau^l)d\phi. \end{array}\right\} \tag{2.26}$$

Then we apply the trapezoidal rule for the integrals over $(0, x_{i_1}]$ and $[x_{i_2,\infty})$ because of (2.20) and using the first mean value theorem for integrals [41, p. 1063], the two remaining integrals are approximated by

$$\int_{x_{i_1}}^{x_i e^{-\varepsilon}} g(x_i,\phi)U(\phi,\tau^l)d\phi \approx I_i^l = \Big(\int_{x_{i_1}}^{x_i e^{-\varepsilon}} g(x_i,\phi)d\phi\Big)u_{i_1}^l = \tilde{g}_{i,i_1}u_{i_1}^l, \tag{2.27}$$

$$\int_{x_i e^{\varepsilon}}^{x_{i_2}} g(x_i,\phi)U(\phi,\tau^l)d\phi \approx H_i^l = \Big(\int_{x_i e^{\varepsilon}}^{x_{i_2}} g(x_i,\phi)d\phi\Big)u_{i_2}^l = \tilde{g}_{i,i_2}u_{i_2}^l. \tag{2.28}$$

Let us denote

$$g_{i,j} = \frac{\nu(\ln x_j/x_i)}{x_j}. \tag{2.29}$$

Depending on the location of x_i for each i with $1 < i \le N+M-2$, we approximate J_i^l given by (2.26) in the following form

Case 1 $(x_i < Ae^{-\varepsilon})$

Note that in this case $x_{i_1} < A$ and thus $J_{i,1}^l$ is approximated by $h\sum_{j=1}^{i_1-1} g_{ij}u_j^l + (\frac{h}{2}g_{i,i_1} + \tilde{g}_{i,i_1})u_{i_1}^l$. Also one has $x_{i_2} < A$ in the domain of the integral $J_{i,2}^l$ and is approximated by $(\frac{h}{2}g_{i,i_2} + \tilde{g}_{i,i_2})u_{i_2}^l + h\sum_{j=i_2+1}^{N-1} g_{ij}u_j^n + \frac{g_{iN}}{2}(h + A\delta)u_N^l + \frac{\delta}{A}\sum_{j=N+1}^{N+M-1} g_{ij}x_j^2u_j^l$, taking into account (2.20) for $x_j > A$. Hence

$$\begin{aligned} \hat{J}_i^l = {} & h\sum_{j=1}^{i_1-1} g_{ij}u_j^l + (\frac{h}{2}g_{i,i_1} + \tilde{g}_{i,i_1})u_{i_1}^l + (\frac{h}{2}g_{i,i_2} + \tilde{g}_{i,i_2})u_{i_2}^l \\ & + h\sum_{j=i_2+1}^{N-1} g_{ij}u_j^l + \frac{g_{iN}}{2}(h + A\delta)u_N^l + \frac{\delta}{A}\sum_{j=N+1}^{N+M-1} g_{ij}x_j^2u_j^l. \end{aligned} \tag{2.30}$$

Case 2 $(Ae^{-\varepsilon} \leq x_i < Ae^{\varepsilon})$

As $x_{i_1} < A$ and $x_{i_2} \geq A$, the approximation of J_i^l becomes

$$\hat{J}_i^l = h\sum_{j=1}^{i_1-1} g_{ij}u_j^l + (\frac{h}{2}g_{i,i_1} + \tilde{g}_{i,i_1})u_{i_1}^l + (\frac{x_{i_2}^2\delta}{2A}g_{i,i_2} + \tilde{g}_{i,i_2})u_{i_2}^l + \frac{\delta}{A}\sum_{j=i_2+1}^{N+M-1} g_{ij}x_j^2u_j^l. \quad (2.31)$$

Case 3 $(x_i \geq Ae^{\varepsilon})$

Here $x_{i_2} > x_{i_1} \geq A$ and the approximation of J_i^l is given by

$$\hat{J}_i^l = h\sum_{j=1}^{N-1} g_{ij}u_j^l + \frac{g_{iN}}{2}(h + A\delta)u_N^l + \frac{\delta}{A}\sum_{j=N+1}^{i_1-1} g_{ij}x_j^2u_j^l$$

$$+ (\frac{x_{i_1}^2\delta}{2A}g_{i,i_1} + \tilde{g}_{i,i_2})u_{i_1}^l + (\frac{x_{i_2}^2\delta}{2A}g_{i,i_2} + \tilde{g}_{i,i_2})u_{i_2}^l + \frac{\delta}{A}\sum_{j=i_2+1}^{N+M-1} g_{ij}x_j^2u_j^l. \quad (2.32)$$

Assuming that $U(\phi,\tau)$ tends to zero at least linearly as ϕ tends to zero one has $g(x,\phi)u(\phi,\tau) \to 0$ by (2.1) and (2.29). On the other hand assuming linear behavior of the solution for large values of ϕ, the integrand of (2.20) $g(x,\frac{A}{z})U(\frac{A}{z},\tau)\frac{1}{z^2} \to 0$, as $z \to 0$. Thus, both the terms involving u_0^l and u_{N+M}^l do not appear in the expressions of (2.30)-(2.32). Taking into account (2.25)-(2.32) the resulting difference scheme for the PIDE problem (2.21) takes the form

$$u_i^{l+1} = u_i^l + \frac{k\hat{\sigma}^2}{2}x_i^2\Delta_i^l + k\hat{J}_i^l,\ 1 \leq i \leq N+M-2. \quad (2.33)$$

For the sake of convenience to study the stability, we now introduce the vector formulation of the scheme (2.33). Let us denote the vector in $\mathbb{R}^{N+M-1}$ as

$$U^l = [u_1^l\ u_2^l\ \ldots\ u_{N+M-1}^l]^t$$

and let $P = (p_{ij})$ be a tridiagonal matrix in $\mathbb{R}^{(N+M-1)\times(N+M-1)}$ related to the differential part, defined by

$$p_{ij} = \begin{cases} \alpha_i,\ j = i-1, \\ \beta_i,\ j = i, \\ \gamma_i,\ j = i+1, \\ 0,\ \text{otherwise}, \end{cases} \quad (2.34)$$

where

$$\left.\begin{array}{lll}
\gamma_1 = \dfrac{k}{2}\,\hat{\sigma}^2\,, & \alpha_{N+M-1} = 0\,, & \beta_{N+M-1} = 1\,, \\
\gamma_i = \alpha_i = \dfrac{k}{2h^2}\,\hat{\sigma}^2\,x_i^2, \quad 2 \le i \le N-1, & & \beta_i = 1 - \dfrac{k}{h^2}\,\hat{\sigma}^2\,x_i^2,\ 1 \le i \le N-1 \\
\alpha_N = \dfrac{k\hat{\sigma}^2\,A^2}{h\left(h + \frac{A\delta}{1-\delta}\right)}\,, & \beta_N = 1 - \dfrac{k\hat{\sigma}^2\,A(1-\delta)}{\delta h}\,, & \gamma_N = \dfrac{k\hat{\sigma}^2\,A(1-\delta)}{\delta\left(h + \frac{A\delta}{1-\delta}\right)}\,, \\
\alpha_i = \dfrac{k\hat{\sigma}^2\,x_i^2}{h_{i-1}(h_i + h_{i-1})}\,, & \beta_i = 1 - \dfrac{k\hat{\sigma}^2\,x_i^2}{h_i h_{i-1}}\,, & \gamma_i = \dfrac{k\hat{\sigma}^2\,x_i^2}{h_i(h_i + h_{i-1})}\,, \\
 & & N+1 \le i \le N+M-2\,.
\end{array}\right\} \tag{2.35}$$

Let $B = (b_{ij})$ the matrix in $\in \mathbb{R}^{(N+M-1)\times(N+M-1)}$ related to the integral part whose entries b_{ij} for each fixed i in $1 \le i \le N+M-2$, are defined by

$$b_{ij} = \begin{cases} kb_{ij}^{(1)},\ 1 \le i \le i_1(N) - 1, \\ kb_{ij}^{(2)},\ i_1(N) \le i \le i_2(N) - 1, \\ kb_{ij}^{(3)},\ i_2(N) \le i \le N+M-2, \\ 0,\ i = M+N-1, \end{cases} \tag{2.36}$$

where

$$b_{ij}^{(1)} = \begin{cases} hg_{ij},\ 1 \le j \le i_1 - 1, \\ \frac{h}{2}g_{i,j} + \tilde{g}_{i,j},\ j = i_1,\ i_2, \\ 0,\ i_1 + 1 \le j \le i_2 - 1, \\ hg_{ij},\ i_2 + 1 \le j \le N-1, \\ \frac{1}{2}(h + A\delta)g_{iN},\ j = N, \\ \frac{\delta}{A}x_j^2 g_{ij},\ N+1 \le j \le N+M-1, \end{cases} \tag{2.37}$$

$$b_{ij}^{(2)} = \begin{cases} hg_{ij},\ 1 \le j \le i_1 - 1, \\ \frac{h}{2}g_{i,j} + \tilde{g}_{i,j},\ j = i_1, \\ 0,\ i_1 + 1 \le j \le i_2 - 1, \\ \frac{x_{i_2}^2\delta}{2A}g_{i,j} + \tilde{g}_{i,j},\ j = i_2, \\ \frac{\delta}{A}x_j^2 g_{ij},\ i_2 + 1 \le j \le N+M-1, \end{cases} \tag{2.38}$$

and

$$b_{ij}^{(3)} = \begin{cases} hg_{ij},\ 1 \le j \le N-1, \\ \frac{1}{2}(h + A\delta)g_{iN},\ j = N, \\ \frac{\delta}{A}x_j^2 g_{ij},\ N+1 \le j \le i_1 - 1, \\ \frac{\delta x_j^2}{2A}g_{i,j} + \tilde{g}_{i,j},\ j = i_1,\ i_2, \\ 0,\ i_1 + 1 \le j \le i_2 - 1, \\ \frac{\delta}{A}x_j^2 g_{ij},\ i_2 + 1 \le j \le N + M - 1. \end{cases} \tag{2.39}$$

2.3.2 The numerical scheme based on Patankar-trick

Before the discretization, first we rewrite (2.19) in more compatible form

$$J(U) = \int_0^\infty \hat{g}(x,\phi)U(\phi,\tau)d\phi, \tag{2.40}$$

where the new kernel $\hat{g}(x,\phi)$ takes the form,

$$\hat{g}(x,\phi) = \begin{cases} \frac{\nu(\ln(\phi/x))}{\phi},\ 0 < \phi \le xe^{-\varepsilon}, \\ 0,\ xe^{-\varepsilon} < \phi < xe^{\varepsilon}, \\ \frac{\nu(\ln(\phi/x))}{\phi},\ \phi \ge xe^{\varepsilon}. \end{cases} \tag{2.41}$$

The discretization of the variables x and t are the same as in scheme 1. Here the second partial derivative is approximated using Patankar-trick [68]

$$\Delta_i^{l,l+1} \equiv \begin{cases} \frac{u_{i-1}^l - 2u_i^{l+1} + u_{i+1}^l}{h^2},\ 1 \le i < N, \\ 2\big[\frac{u_{i-1}^l}{h_{i-1}(h_i + h_{i-1})} - \frac{u_i^{l+1}}{h_i h_{i-1}} + \frac{u_{i+1}^l}{h_i(h_{i-1} + h_i)}\big],\ N \le i \le N + M - 2, \end{cases} \tag{2.42}$$

and $h_i = x_{i+1} - x_i > 0$. Then the difference scheme for (2.21) has the following form

$$u_i^{l+1} = u_i^l + \frac{k\hat{\sigma}^2}{2}x_i^2\Delta_i^{l,l+1} + k\hat{J}_i^l,\ 1 \le i \le N + M - 2. \tag{2.43}$$

Note that the first expression of (2.42) corresponds to spatial zone with uniform discretization, while the second expression of (2.42) is related to the nonuniform discretization. On the other hand, for the approximation of the integral part of (2.21), instead of using the trapezoidal rule like in [17, 25, 54], we use a composite four-point integration formula of open type because of the higher order approximation of this rule [28, pp. 92-93]. This higher accuracy comes out because the singularity points of the kernel are not nods of the integration mesh due to the truncation see (2.41), and the open type nature of the quadrature formula. Thus

the approximation of (2.20) (here with the modified kernel (2.41)) corresponding to the nodes $x = x_i$ and $\tau = \tau^l$ is given by

$$\hat{J}_i^l = \frac{5h}{24}\sum_{j=0}^{N/5}(11u_{5j+1}^l\hat{g}_{i,5j+1} + u_{5j+2}^l\hat{g}_{i,5j+2} + u_{5j+3}^l\hat{g}_{i,5j+3} + 11u_{5j+4}^l\hat{g}_{i,5j+4})$$

$$+\frac{5\delta}{24A}\sum_{j=N/5}^{(N+M)/5-1}(11u_{5j+1}^l\hat{g}_{i,5j+1}x_{5j+1}^2+u_{5j+2}^l\hat{g}_{i,5j+2}x_{5j+2}^2+u_{5j+3}^l\hat{g}_{i,5j+3}x_{5j+3}^2+11u_{5j+4}^l\hat{g}_{i,5j+4}x_{5j+4}^2), \tag{2.44}$$

where $\hat{g}_{i,j} = \hat{g}(x_i, x_j)$. Consequently the corresponding difference scheme for PIDE given by (2.21) takes the following form

$$\hat{\beta}_i u_i^{l+1} = \hat{\alpha}_i u_{i-1}^l + u_i^l + \hat{\gamma}_i u_{i+1}^l + k\hat{J}_i^l, \tag{2.45}$$

where

$$\hat{\alpha}_i = \begin{cases} \frac{k\hat{\sigma}^2 x_i^2}{2h^2}, \ 2 \le i \le N-1, \\ \frac{k\hat{\sigma}^2 A^2}{h(h+\frac{A\delta}{1-\delta})}, \ i = N, \\ \frac{k\hat{\sigma}^2 x_i^2}{h_{i-1}(h_i+h_{i-1})}, \ N+1 \le i \le N+M-2, \\ 0, \ i = N+M-1. \end{cases} \tag{2.46}$$

$$\hat{\beta}_i = \begin{cases} 1 + \frac{k\hat{\sigma}^2 x_i^2}{h^2}, \ 1 \le i \le N-1, \\ 1 + \frac{k\hat{\sigma}^2 A(1-\delta)}{h\delta}, \ i = N, \\ 1 + \frac{k\hat{\sigma}^2 x_i^2}{h_i h_{i-1}}, \ N+1 \le i \le N+M-2, \\ 1, \ i = N+M-1. \end{cases} \tag{2.47}$$

$$\hat{\gamma}_i = \begin{cases} \frac{k\hat{\sigma}^2 x_i^2}{2h^2}, \ 1 \le i \le N-1, \\ \frac{k\hat{\sigma}^2 A(1-\delta)}{\delta(h+\frac{A\delta}{1-\delta})}, \ i = N, \\ \frac{k\hat{\sigma}^2 x_i^2}{h_i(h_i+h_{i-1})}, \ N+1 \le i \le N+M-2. \end{cases} \tag{2.48}$$

From (2.45)-(2.48), one gets

$$u_i^{l+1} = \breve{\alpha}_i u_{i-1}^l + \breve{\beta}_i u_i^l + \breve{\gamma}_i u_{i+1}^l + \frac{k}{\hat{\beta}_i}\hat{J}_i^l, \tag{2.49}$$

where

$$\breve{\alpha}_i = \frac{\hat{\alpha}_i}{\hat{\beta}_i}, \ \breve{\beta}_i = \frac{1}{\hat{\beta}_i}, \ \breve{\gamma}_i = \frac{\hat{\gamma}_i}{\hat{\beta}_i}. \tag{2.50}$$

In order to obtain a complete difference scheme, we include the initial and boundary conditions. From (2.22), we have

$$u_i^0 = \max(x_i - E, 0) = f(x_i),\ 1 \leq i \leq N + M - 1. \tag{2.51}$$

On the other hand, for a vanilla call option the boundary condition for $i = 0$

$$u_0^l = 0,\ 0 \leq l \leq L, \tag{2.52}$$

and by assuming the linear behavior of the solution for large values of the spatial variable, we have $\frac{\partial^2 U}{\partial x^2} \to 0$ and thus $\Delta_{N+M-1}^l,\ \Delta_{N+M-1}^{l,l+1} = 0$ and the null integral term approximation $J_{N+M-1} = 0$, for all time level l. Thus from (2.49) for $i = N + M - 1$, one gets

$$u_{N+M-1}^{l+1} = u_{N+M-1}^l = u_{N+M-1}^0,\ 0 \leq l \leq L - 1. \tag{2.53}$$

Note: The scheme given by (2.33) with (2.51)-(2.53) is referred as scheme 1 and the scheme given by (2.49) with (2.51)-(2.53) is referred by scheme 2.
Finally in this section, we write the matrix representation for the scheme 2. The tridiagonal matrix $P \in \mathbb{R}^{(N+M-1)\times(N+M-1)}$ corresponds to the discretization of the differential part and takes the following form

$$P = \begin{bmatrix} \breve{\beta}_1 & \breve{\gamma}_1 & 0 & 0 & \cdots & 0 \\ \breve{\alpha}_2 & \breve{\beta}_2 & \breve{\gamma}_2 & 0 & \cdots & 0 \\ 0 & \breve{\alpha}_3 & \breve{\beta}_3 & \breve{\gamma}_3 & \cdots & 0 \\ & & \ddots & \ddots & \ddots & \\ & & & \ddots & \ddots & \ddots \\ 0 & \cdots & & \breve{\alpha}_{N+M-2} & \breve{\beta}_{N+M-2} & \breve{\gamma}_{N+M-2} \\ 0 & \cdots & & 0 & \breve{\alpha}_{N+M-1} & \breve{\beta}_{N+M-1} \end{bmatrix}. \tag{2.54}$$

Let $B = (b_{ij})$ be a matrix in $\in \mathbb{R}^{(N+M-1)\times(N+M-1)}$ related to the integral part whose entries b_{ij} for each fixed i in $1 \le i \le N+M-2$, are defined by $b_{ij} = \frac{k}{\hat{\beta}_i}\hat{b}_{ij}$, where

$$\hat{b}_{ij} = \begin{cases} 0,\ j = 5,\ 10\ 15,\ 20, \ldots,\ N+M-5, \\ \frac{55h}{24}\hat{g}_{ij},\ j = 1,\ 6,\ 11,\ \ldots,\ N-4,\ \frac{55\delta}{24A}x_j^2\hat{g}_{ij},\ j = N+1,\ N+6,\ \ldots,\ M+N-4, \\ \frac{5h}{24}\hat{g}_{ij},\ j = 2,\ 7,\ 12,\ \ldots,\ N-3,\ \frac{5\delta}{24A}x_j^2\hat{g}_{ij},\ j = N+2,\ N+7,\ \ldots,\ M+N-3, \\ \frac{5h}{24}\hat{g}_{ij},\ j = 3,\ 8,\ 13,\ \ldots,\ N-2,\ \frac{5\delta}{24A}x_j^2\hat{g}_{ij},\ j = N+3,\ N+8,\ \ldots,\ M+N-2, \\ \frac{55h}{24}\hat{g}_{ij},\ j = 4,\ 9,\ 14,\ \ldots,\ N-1,\ \frac{55\delta}{24A}x_j^2\hat{g}_{ij},\ j = N+4,\ N+9,\ \ldots,\ M+N-1. \end{cases} \tag{2.55}$$

Consequently scheme 1 and scheme 2 are written in the following vector form

$$\begin{aligned} &U^{l+1} = (P+B)U^l = (P+B)^l U^0, \quad 0 \le l \le L-1, \\ &U^0 = [f(x_1)\ f(x_2)\ldots f(x_{N+M-1})]^t. \end{aligned} \tag{2.56}$$

2.4 The properties of the numerical solution

2.4.1 Positive and stability of the numerical solution for scheme 1

The price of contracts modelled by PIDE must be nonnegative value. Our objective here is to demonstrate that the solution of the scheme (2.33) with (2.51)-(2.53) is conditionally nonnegative and stable.

First we study the positivity of the matrix P. The following lemma has been proved in [17].

lemma 1. *With previous notation, assume that stepsizes $k = \Delta\tau$, $h = \Delta x$ in $[0, A]$ and $0 < \delta \le \frac{1}{3}$, $\delta = \Delta z$ in $(0, 1]$, satisfy:*

C1. $\dfrac{k}{h^2} \le \dfrac{1}{\hat{\sigma}^2 A^2}$.

C2. $k \le \min\left\{\dfrac{\delta^2}{\hat{\sigma}^2(1-2\delta)},\ \dfrac{\delta h}{\hat{\sigma}^2 A(1-\delta)}\right\}$.

Then matrix P given by (2.34) *is nonnegative.*

Note that as the matrix B defined by (2.36)-(2.37) is always nonnegative, from Lemma 1 and (2.56) starting from nonnegative initial vector U^0, the following result is established:

Theorem 1. *With the hypotheses and notation of lemma 1, the solution* $\{u_i^l\}$ *of the scheme* (2.33), (2.51)-(2.53) *is nonnegative if the initial values* $u_i^0 \geq 0$, $1 \leq i \leq N + M - 1$.

The next result will be used below to guarantee stability.

lemma 2. *Let matrices* P *and* B *be defined by* (2.34)-(2.36), *and let* $\varepsilon > 0$, *then the following results hold:*

1. *Under conditions C1 and C2 of lemma 1,* $\|P\|_\infty = 1$.
2. $\|B\|_\infty \leq k(\lambda(\varepsilon) + 1)$, *where* $\lambda(\varepsilon)$ *is defined by* (2.14).

By [17, lemma 2], part 1 is proved. Since the norm of B is given by

$$\|B\|_\infty = \max_i \sum_{j=1}^{N+M-1} |b_{ij}| = \max_i \sum_{j=1}^{N+M-1} b_{ij},\ 1 \leq i \leq N + M - 1, \tag{2.57}$$

if $\tilde{m}$ denotes the row containing the maximum of (2.57), one gets

$$\|B\|_\infty = \sum_{j=1}^{N+M-1} b_{\tilde{m}j} = k \sum_{j=1}^{N+M-1} b_{\tilde{m}j}^{(r)},\ r = 1, 2, \text{ or } 3, \tag{2.58}$$

the elements of the summation in (2.58) are given by (2.36)-(2.37). To upper bound (2.58), we apply the change of variables $y = x_{\tilde{m}} e^{\phi}$ in (2.8), resulting

$$\lambda(\varepsilon) = \int_0^{x_{\tilde{m}} e^{-\varepsilon}} g(x_{\tilde{m}}, \phi) d\phi + \int_{x_{\tilde{m}} e^{\varepsilon}}^{\infty} g(x_{\tilde{m}}, \phi) d\phi, \tag{2.59}$$

which coincides with (2.19) when $U(\phi,\ \tau) = 1$. Hence from (2.19), (2.58) and (2.59), we conclude that $\sum_{j=1}^{N+M-1} b_{\tilde{m}j}^{(r)}$ is an approximation for $\lambda(\varepsilon)$. Thus, for small enough h and δ, one gets, [28]

$$\sum_{j=1}^{N+M-1} b_{\tilde{m}j}^{(r)} < \lambda(\varepsilon) + 1. \tag{2.60}$$

Hence

$$\|B\|_\infty < k(\lambda(\varepsilon) + 1), \tag{2.61}$$

independently of the value of the size of matrix B.
Based on the stability definitions (8) and (9) we have

Theorem 2. *With the previous notation, the numerical solution* $\left\{u_i^l\right\}$ *of the scheme* (2.33) *with* (2.51)-(2.53) *is strongly uniformly* $\|\cdot\|_\infty$ *stable if one satisfies the condition* $0 < \delta \leq \frac{1}{3}$ *together with*

$$\frac{k}{h^2} \leq \frac{1}{\hat{\sigma}^2\, A^2} \quad \textit{and} \quad k \leq \min\left\{\frac{\delta^2}{\hat{\sigma}^2(1-2\delta)},\ \frac{\delta h}{\hat{\sigma}^2\, A(1-\delta)}\right\}. \tag{2.62}$$

Proof. Note that scheme (2.33) with (2.51)-(2.53) is equivalent to the vector form scheme (2.56). Under condition (2.62), by lemma 2 one gets, after taking norms in (2.56)

$$\left\|U^{l+1}\right\|_\infty \leq (\|P\|_\infty + \|B\|_\infty)\left\|U^l\right\|_\infty \leq (1 + k(\lambda(\varepsilon)+1))\left\|U^l\right\|_\infty. \tag{2.63}$$

Hence, from (2.63), and that $0 \leq l \leq L$, $kL = \tau \leq T$,

$$\frac{\left\|U^l\right\|_\infty}{\|U^0\|_\infty} \leq (1 + k(\lambda(\varepsilon)+1))^l \leq \exp(lk(\lambda(\varepsilon)+1)) \leq \exp(T(\lambda(\varepsilon)+1)). \tag{2.64}$$

Thus the conditional strong uniform stability is established. □

2.4.2 Positive and stability of the numerical solution for scheme 2

The numerical solution $\{u_i^l\}$ of scheme (2.49) is unconditionally nonnegative because all coefficients of (2.49), the initial and boundary conditions (2.51)-(2.53) are nonnegative.

In order to study the stability of the scheme given by (2.49)-(2.53), we first calculate the norm of the matrices P and B. Since the norm of the matrix P is obtained by

$$\|P\|_\infty = \max_i \sum_{j=1}^{N+M-1} |P_{ij}| = \max_i \sum_{j=1}^{N+M-1} P_{ij}, \tag{2.65}$$

for $i = 1$, we have $\sum_{j=1}^{N+M-1} P_{1j} = \breve{\beta}_1 + \breve{\gamma}_1 < 1$, and for $2 \leq i \leq N+M-1$, $\sum_{j=1}^{N+M-1} P_{ij} = \breve{\alpha}_i + \breve{\beta}_i + \breve{\gamma}_i = 1$. Hence $\|P\|_\infty = 1$.

By calculating the infinity norm for the matrix B in the same way as we did for scheme 1, we conclude that its norm is bounded and its value is less than $k(\lambda(\varepsilon)+1)$, see (2.61). Now, we calculate the infinity norm of the vector solution at any time

level l, we have

$$\frac{\left\|U^l\right\|_\infty}{\|U^0\|_\infty} \leq \exp(T(\lambda(\varepsilon)+1)).$$

Based on the stability definitions (8) and (9), we conclude that the scheme 2 is unconditionally strongly uniform stable.

Wrap Up

1. For scheme 1 defined by (2.33) with (2.51)-(2.53), the positivity and stability for this scheme hold under two conditions $C1$ and $C2$ which are summarized in (2.62).

2. The positivity and stability for scheme 2 defined by (2.49) with (2.51)-(2.53) hold unconditionally (with no restriction on the stepsizes). This is due to Patankar's idea for changing the term u_i^l by u_i^{l+1} in the approximation of the second derivative of the function u with respect to x.

2.5 Consistency

First let us write (2.33) and (2.53) in the following form

$$F_{i,l}(u) = \frac{u_i^{l+1}-u_i^l}{k} - \frac{\hat{\sigma}^2}{2}x_i^2\Delta_i^l - \hat{J}_i^l = 0, \tag{2.66}$$

where $\hat{J}_i^l$ for scheme 1 is given by (2.30)-(2.32) and for scheme 2 is given by (2.44). Let us denote $U_i^l = U(x_i,\tau^l)$ as the value of the theoretical solution of (2.21). Based on (1.18), the local truncation error $T_i^l(U)$ at (x_i,τ^l) is given by

$$T_i^l(U) = F_{i,l}(U) - L(U_i^l), \tag{2.67}$$

where $L(U_i^l) = \mathcal{L}(U_i^l) - J(U_i^l)$ such that

$$\mathcal{L}(U_i^l) = \left[\frac{\partial U}{\partial \tau} - \frac{\hat{\sigma}^2}{2}x^2\frac{\partial^2 U}{\partial x^2}\right]_{(x_i,\tau^l)}, \; J(U_i^l) = J_i^l = J_{i,1}^l + J_{i,2}^l.$$

2.5.1 The consistency for scheme 1

Assuming that U is twice continuously partially differentiable with respect to τ and four times partially differentiable with respect to x, and using Taylor's expansion

about (x_i, τ^l), for $A > 0$ such that $x_i < Ae^{-\varepsilon}$ it follows that

$$\frac{U_i^{l+1} - U_i^l}{k} = \frac{\partial U}{\partial \tau}(x_i, \tau^l) + kE_i^l(1),\ E_i^l(1) = \frac{1}{2}\frac{\partial^2 U}{\partial \tau^2}(x_i, \zeta),\ \tau^l < \zeta < \tau^{l+1}, \quad (2.68)$$

$$|E_i^l(1)| \le \frac{1}{2}W_i^l(1) = \frac{1}{2}\max\left\{\left|\frac{\partial^2 U}{\partial \tau^2}(x_i, \zeta)\right|; \tau^l \le \zeta \le \tau^{l+1}\right\} \quad (2.69)$$

$$\Delta_i^l = \frac{\partial^2 U}{\partial x^2}(x_i, \tau^l) + h^2 E_i^l(2),\ E_i^l(2) = \frac{1}{12}\frac{\partial^4 U}{\partial x^4}(\tilde{\zeta}, \tau^l),\ x_i - h < \tilde{\zeta} < x_i + h, \quad (2.70)$$

$$|E_i^l(2)| \le \frac{1}{12}W_i^l(2) = \frac{1}{12}\max\left\{\left|\frac{\partial^4 U}{\partial x^4}(\tilde{\zeta}, \tau^l)\right|; x_i - h \le \tilde{\zeta} \le x_i + h\right\}. \quad (2.71)$$

In accordance with [55, p. 101] let us denote the local consistency error of $J_{i,1}^l$ see (2.30) by

$$C_{i,1}^l = J_{i,1}^l - T_{i,1}^l([0, x_i e^{-\varepsilon}]), \quad (2.72)$$

$$T_{i,1}^l([0, x_i e^{-\varepsilon}]) = h\sum_{j=1}^{i_1-1} g_{ij}U_j^l + \left(\frac{h}{2}g_{i,i_1} + \tilde{g}_{i,i_1}\right)U_{i_1}^l. \quad (2.73)$$

By (2.26) and (2.30), the local consistency error for $J_{i,2}^l$ is given by

$$C_{i,2}^l = J_{i,2}^l - \left(T_{i,2}^l([x_i e^{\varepsilon}, A]) + T_{i,3}^l([0,1])\right), \quad (2.74)$$

where

$$T_{i,2}^l([x_i e^{\varepsilon}, A]) = \left(\frac{h}{2}g_{i,i_2} + \tilde{g}_{i,i_2}\right)U_{i_2}^l + h\sum_{j=i_2+1}^{N-1} g_{ij}U_j^l + \frac{h}{2}g_{iN}U_N^l, \quad (2.75)$$

$$T_{i,3}^l([0,1]) = \frac{\delta}{A}\left(\frac{1}{2}g_{iN}x_N^2 U_N^l + \sum_{j=N+1}^{N+M-1} g_{ij}x_j^2 U_j^l\right). \quad (2.76)$$

From the first mean value theorem for integrals [41, p. 1063], one gets

$$\begin{aligned} &I(x_i, \varepsilon) = \textstyle\int_{x_{i_1}}^{x_i e^{-\varepsilon}} g(x_i, \phi)U(\phi, \tau^l)d\phi \\ &= \left(\textstyle\int_{x_{i_1}}^{x_i e^{-\varepsilon}} g(x_i, \phi)d\phi\right)U(c, \tau^l) = \tilde{g}_{i,i_1}U(c, \tau^l),\ x_{i_1} < c < x_i e^{-\varepsilon}, \end{aligned}$$

and since

$$U(c, \tau^l) = U(x_{i_1}, \tau^l) + (c - x_{i_1})\frac{\partial U}{\partial x}(\xi, \tau^l),\ x_{i_1} < \xi < c,$$

it follows that

$$|I(x_i, \varepsilon) - \tilde{g}_{i,i_1}U_{i_1}^l| \le \tilde{g}_{i,i_1}h\Lambda_i^l(1) \le h^2 W_i^l(3), \quad (2.77)$$

where

$$\Lambda_i^l(1) = \max\left\{\left|\frac{\partial U}{\partial x}(x,\tau^l)\right|;\ x_{i_1} \le x \le x_i e^{-\varepsilon}\right\},$$

$$W_i^l(3) = \Lambda_i^l(1)\max\{g(x_i,x); x_{i_1} \le x \le x_i e^{-\varepsilon}\}.$$

Analogously,

$$|H(x_i,\varepsilon) - \tilde{g}_{i,i_2}U_{i_2}^l| \le \tilde{g}_{i,i_1}h\Lambda_i^l(1) \le h^2 W_i^l(4), \tag{2.78}$$

$$H(x_i,\varepsilon) = \int_{x_i e^{\varepsilon}}^{x_{i_2}} g(x_i,\phi)U(\phi,\tau^l)d\phi,$$

$$W_i^l(4) = \Big(\max\left\{\left|\frac{\partial U}{\partial x}(x,\tau^l)\right|;\ x_i e^{-\varepsilon} \le x \le x_{i_2}\right\}\Big)\Big(\max\{g(x_i,x); x_i e^{-\varepsilon} \le x \le x_{i_2}\}\Big).$$

Let $W_i^l(5),\ W_i^l(6)$ and $W_i^l(7)$ be defined as

$$\left.\begin{array}{l} W_i^l(5) = \sup\{|\big(g(x_i,x)U(x,\tau^l)\big)^{(2)}|;\ 0 < x \le x_i e^{-\varepsilon}\}, \\ W_i^l(6) = \sup\{|\big(g(x_i,x)U(x,\tau^l)\big)^{(2)}|;\ x_i e^{\varepsilon} \le x \le A\}, \\ W_i^l(7) = \sup\left\{\left|(g(x_i,\frac{A}{z})U(\frac{A}{z},\tau^l)\frac{1}{z^2})^{(2)}\right|; 0 < x \le 1\right\}, \end{array}\right\} \tag{2.79}$$

where the second derivatives appearing in (2.79) are taken with respect to the variable x for $W_i^l(5)$ and $W_i^l(6)$, and with respect to the variable z for $W_i^l(7)$. From the expression of the error of the trapezoidal rule, [28, p. 54], (2.72)- (2.79), one gets

$$\left.\begin{array}{c} |C_{i,1}^l| \le h^2\big(W_i^l(3) + \frac{x_i e^{-\varepsilon}}{12}W_i^l(5)\big), \\ |C_{i,2}^l| \le h^2\big(W_i^l(4) + \frac{1}{12}(A - x_i e^{-\varepsilon})W_i^l(6) + \frac{A\delta^2}{12}W_i^l(7). \end{array}\right\} \tag{2.80}$$

Summarizing, one gets

$$T_i^l(U) = kE_i^l(1) - \frac{h^2}{2}\hat{\sigma}^2 x_i^2 E_i^l(2) + C_{i,1}^l + C_{i,2}^l,$$

and

$$|T_i^l(U)| \le h^2\left(\frac{W_i^l(2)}{24} + W_i^l(3) + W_i^l(4) + \frac{x_i e^{-\varepsilon}}{12}W_i^l(5) + \frac{1}{12}(A - x_i e^{-\varepsilon})W_i^l(6)\right)$$

$$+ \frac{A\delta^2}{12}W_i^l(7) + kW_i^l(1). \tag{2.81}$$

Thus,

$$T_i^l(U) = \mathcal{O}(h^2) + \mathcal{O}(\delta^2) + \mathcal{O}(k), \tag{2.82}$$

showing the unconditionally consistency of the scheme with PIDE.

2.5.2 The consistency for scheme 2

Assuming that U is twice continuously partially differentiable with respect to τ and four times partially differentiable with respect to x, and using Taylor's expansion about (x_i, τ^l), it follows that

$$\frac{U_i^{l+1} - U_i^l}{k} = \frac{\partial U}{\partial \tau}(x_i, \tau^l) + kE_i^l(1), \tag{2.83}$$

$$\frac{1}{h^2}(U_{i-1}^l - 2U_i^{l+1} + U_{i+1}^l) = \frac{\partial^2 U}{\partial x^2}(x_i, \tau^l) + h^2 E_i^l(2) - \frac{k}{h^2}E_i^l(3), \tag{2.84}$$

where $E_i^l(1)$ and $E_i^l(2)$ are given by (2.68) and (2.70) respectively.

$$E_i^l(3) = 2\frac{\partial U}{\partial \tau}(x_i, \zeta),\ \tau^l < \zeta < \tau^{l+1}. \tag{2.85}$$

Let us denote the maximum of the associated errors $E_i^l(1)$, $E_i^l(2)$ and $E_i^l(3)$ by $W_i^l(1)$, $W_i^l(2)$ and $\hat{W}_i^l(3)$ respectively, where $W_i^l(1)$ and $W_i^l(2)$ are given by (2.69) and (2.71),

$$|E_i^l(3)| \leq 2\hat{W}_i^l(3) = 2\max\left\{\left|\frac{\partial U}{\partial \tau}(x_i, \zeta)\right|; \tau^l \leq \zeta \leq \tau^{l+1}\right\}. \tag{2.86}$$

To study the consistency of the integral part, it is convenient to rewrite it in the following form

$$J = J(U) = J_1(U) + J_2(U), \tag{2.87}$$

where

$$J_1(U) = \int_0^A \hat{g}(x, \phi)U(\phi, \tau^l)d\phi,\ J_2(U) = A\int_0^1 \hat{g}(x, \frac{A}{z})U(\frac{A}{z}, \tau^l)d\phi.$$

In accordance with [55] let us denote the local consistency error of $J_{1,i}^l$

$$C_{1,i}^l(h, A) = \int_0^A \hat{g}(x, \phi)U(\phi, \tau^l)d\phi - \hat{J}_{1,i}^l([0, A]), \tag{2.88}$$

where

$$\hat{J}_{1,i}^l([0, A]) = \frac{5h}{24}\sum_{j=0}^{N/5}(11u_{5j+1}^l\hat{g}_{i,5j+1} + u_{5j+2}^l\hat{g}_{i,5j+2} + u_{5j+3}^l\hat{g}_{i,5j+3} + 11u_{5j+4}^l\hat{g}_{i,5j+4}). \tag{2.89}$$

By [28, pp. 92] we have

$$\left|C_{1,i}^{l}(h,A)\right| \leq \frac{95Ah^4}{144\hat{\beta}_i} \max_{0\leq x\leq A}\left\{\left|\left(U(x,\tau^l)\hat{g}(x,x_i)\right)^{(4)}\right|\right\} = \frac{95Ah^4}{144}\hat{W}_i^l(4), \tag{2.90}$$

where $\left(U(x,\tau^l)\hat{g}(x,x_i)\right)^{(4)}$ in (2.90) is the forth derivative with respect to the variable x.

Similarly, the local consistency error for the unbounded region is given by

$$C_{2,i}^{l}(\delta,A) = A\int_0^1 \hat{g}(x,\frac{A}{z})U(\frac{A}{z},\tau^l)\frac{dz}{z^2} - \hat{J}_{2,i}^{l}((0,1]), \tag{2.91}$$

where

$$\hat{J}_{2,i}^{l}((0,1]) = \frac{5\delta}{24A}\sum_{j=N/5}^{(N+M)/5-1}\left(11u_{5j+1}^{l}\hat{g}_{i,5j+1}x_{5j+1}^2 + u_{5j+2}^{l}\hat{g}_{i,5j+2}x_{5j+2}^2\right.$$

$$\left. + u_{5j+3}^{l}\hat{g}_{i,5j+3}x_{5j+3}^2 + 11u_{5j+4}^{l}\hat{g}_{i,5j+4}x_{5j+4}^2\right), \tag{2.92}$$

$$\left|C_{2,i}^{l}(\delta,A)\right| \leq \frac{95A\delta^4}{144\hat{\beta}_i}\max_{0\leq z\leq 1}\left\{\left|\left(\frac{1}{z^2}U(\frac{A}{z},\tau^l)\hat{g}(x_i,\frac{A}{z})\right)^{(4)}\right|\right\} = \frac{95A\delta^4}{144}\hat{W}_i^l(5). \tag{2.93}$$

Thus the local truncation error is given by

$$T_i^l(U) = kE_i^1 + \frac{\hat{\sigma}^2x_i^2}{2}\left(h^2E_i^l(2) - \frac{k}{h^2}E_i^l(3)\right) + C_{1,i}^{l}(h,A) + C_{2,i}^{l}(\delta,A), \tag{2.94}$$

$$|T_i^l(U)| \leq kW_i^l(1) + \frac{\hat{\sigma}^2A^2h^2}{24}W_i^l(2) + \frac{\hat{\sigma}^2A^2k}{h^2}\hat{W}_i^l(3) + \frac{95A}{144}\left(h^4\hat{W}_i^l(4) + \delta^4\hat{W}_i^l(5)\right). \tag{2.95}$$

Consequently, the order of the local truncated error is given by

$$T_i^l(U) = \mathcal{O}(k) + \mathcal{O}(h^2) + \mathcal{O}(\frac{k}{h^2}) + \mathcal{O}(\delta^4). \tag{2.96}$$

In light of (2.96), the scheme is conditionally consistent with the PIDE (2.21). Thus a consistency condition of type $k = \mathcal{O}(h^{2+\epsilon})$, $\epsilon > 0$, has been established:

Theorem 3. *The numerical scheme given by* (2.53) *is conditionally consistent with* (2.21) *such that the local truncation error is given by*

$$T_i^l(U) = \mathcal{O}(k) + \mathcal{O}(h^2) + \mathcal{O}(\frac{k}{h^2}) + \mathcal{O}(\delta^4).$$

2.6 Numerical examples

In this section, we illustrate with several examples the behavior of the option price obtained by schemes 1 and 2 using Matlab. All examples are done using CPU with Microprocessor 3.4 GHz Intel Core i7.

2.6.1 Examples for scheme 1

In light of the double discretization and the trapezoidal rule, a finite difference scheme has been established to obtain a numerical solution for the option price. This solution is conditionally nonnegative and stable.
The first example reveals the effect of Yor parameter on the option price. **Example 2.1.** Consider the vanilla call option problem (2.2)-(2.4) under CGMY process with parameters $T = 1,\ E = 80,\ A = 3E,\ \sigma = 0.2,\ r = 0.01,\ q = 0,\ C = 0.08,\ \mathcal{G} = \mathcal{M} = 25.04,\ \varepsilon = 0.05,\ N = 100,\ \delta = 0.15,\ k = 0.002$. Figure 2.1 exhibits the variation of the option price V versus the underlying asset at various values of Yor parameter. The next example illustrates the importance of positivity conditions given by lemma 1.

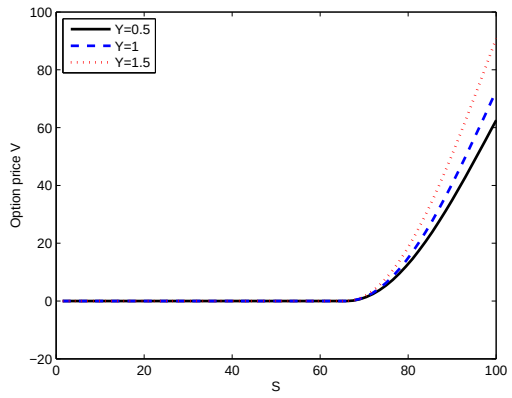

Figure 2.1: The effect of positivity conditions on V

Example 2.2. Here in this example the parameters have been selected as follows $T = 1,\ E = 80,\ A = 3E,\ \sigma = 0.2,\ r = 0.01,\ q = 0,\ C = 1,\ \mathcal{G} = 20,\ \mathcal{M} = 30,\ Y = 1.5,\ \varepsilon = 0.1,\ N = 100,\ \delta = 0.15$. Positivity conditions hold for $k = 0.002$, while for $k = 0.01$, the positivity conditions are broken and the values of the option price become unreliable as shown in Figure 2.2.

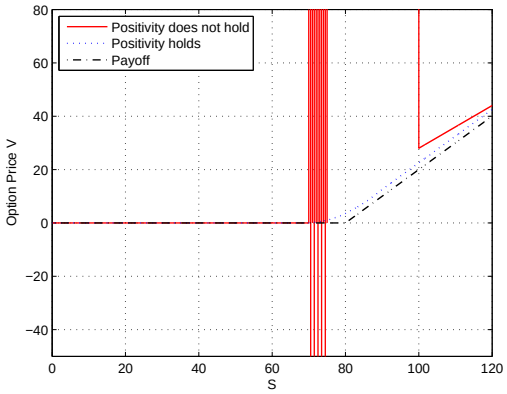

Figure 2.2: The effect of positivity conditions on V.

	$Y = 0.5$			$Y = 1.5$			$Y = 1.98$		
h	Absolute Error	Relative Error	α	Absolute Error	Relative Error	α	Absolute Error	Relative Error	α
0.8	$4.38e{-4}$	$2.2e{-5}$	–	$7.35e{-5}$	$1.48e{-6}$	–	$3.87e{-5}$	$3.87e{-7}$	–
0.4	$1.16e{-4}$	$5.85e{-6}$	1.92	$1.9e{-5}$	$3.92e{-7}$	1.952	$9.76e{-6}$	$9.76e{-8}$	1.9873
0.2	$2.95e{-5}$	$1.49e{-6}$	1.98	$4.79e{-6}$	$9.62e{-8}$	1.988	$2.46e{-6}$	$2.46e{-8}$	1.9882

Table 2.1: Errors and convergence rates.

Next example shows the variation of the absolute and relative error of the solution in light of the stability and positivity conditions hold at the strike for two cases; first, for several values of the stepsize discretization h. Second, for different values of the parameter ε.

Example 2.3. Consider the European call option for CGMY process with the following values $C = 1,\ \mathcal{G} = \mathcal{M} = 5,\ E = 100,\ T = 1, r = 0.1,\ q = 0,\ k = 0.001,\ \delta = 0.1,\ A = 3E$, for several values of Yor parameter $Y = 0.5,\ 1.5$ and 1.98. We consider the evaluation of the price option at the strike and $\tau = T$. Table 2.1 reveals the deviation between our numerical solutions and the reference values used in [36, tables 8-10] for different stepsizes h, and fixed $\varepsilon = 0.12$. Notice that the numerical solution exhibits the expected second order convergence rate α. Table 2.2 shows the deviation for several values of ε, while $h = 0.5$.

	$Y = 0.5$		$Y = 1.5$		$Y = 1.98$	
ε	Absolute Error	Relative Error	Absolute Error	Relative Error	Absolute Error	Relative Error
0.8	3.91×10^{-3}	1.97×10^{-4}	6.37×10^{-4}	1.28×10^{-5}	4.19×10^{-4}	4.19×10^{-6}
0.4	7.18×10^{-4}	3.62×10^{-5}	8.54×10^{-5}	1.72×10^{-6}	5.76×10^{-5}	5.76×10^{-7}
0.2	9.32×10^{-6}	4.7×10^{-7}	7.16×10^{-6}	1.44×10^{-7}	5.92×10^{-6}	5.92×10^{-8}

Table 2.2: Errors due to the variation of ε.

In the next two examples, we consider the Variance Gamma model as a particular case ($Y = 0$) of CGMY model for which the exact solution is known [56].

Example 2.4. Consider a call option under the Variance Gamma process with parameters $C = 1,\ \mathcal{G} = \mathcal{M} = 25,\ T = 1,\ r = 0.01,\ q = 0,\ \sigma = 0.2,\ \varepsilon = 0.12,\ E = 10,\ A = 3E,\ k = 0.01$ and $\delta = 0.15$. Figure 2.3 displays the associated error of the numerical solution for several values of the stepsize h.

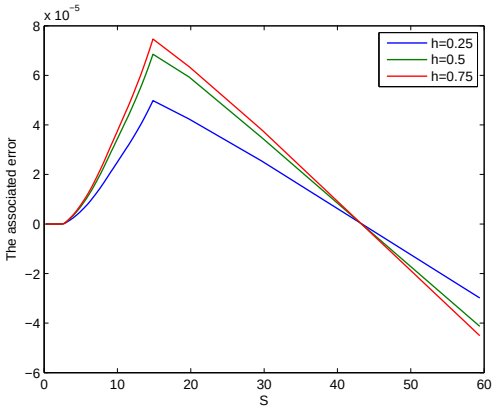

Figure 2.3: The associated error for various values of h.

The next example shows that the double discretization strategy reduces the error near the parameter A by changing the stepsize δ.

Example 2.5. Consider the previous Example 2.4 with fixed $h = 0.5$, Fig. 2.4 shows the variation of the error of the numerical solution for various values of δ. Notice that the error decreases near the right boundary A of the numerical domain by decreasing the stepsize δ, while the error near the strike E remains stationary.

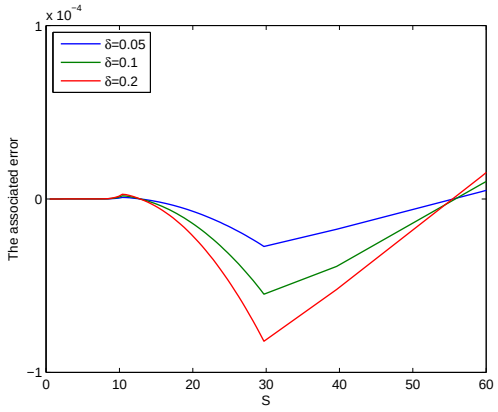

Figure 2.4: The associated error for several values of δ.

2.6.2 Examples for scheme 2

Based on the double discretization and Patankar-trick, a difference scheme has been established to obtain a numerical solution for the option price. This solution is guaranteed to be nonnegative and stable. The following example illustrates that the consistency condition $k = \mathcal{O}(h^{2+\epsilon})$ cannot be ignored.

Example 2.6. Here in this example the parameters have been selected as follows $T = 1,\ E = 10,\ A = 3E,\ \sigma = 0.25,\ r = 0.01,\ q = 0,\ C = 1,\ \mathcal{G} = 25,\ \mathcal{M} = 25,\ Y = 1.65,\ \varepsilon = 0.15,\ h = 0.25,\ \delta = 0.1$, for several values of k such that $k = h^{2.5}$, $h^{1.5}$ and h. Figure 2.5 shows that the consistency condition holds for $k = h^{2.5}$, while for the other two values, it is broken and the values of the option price become unreliable.

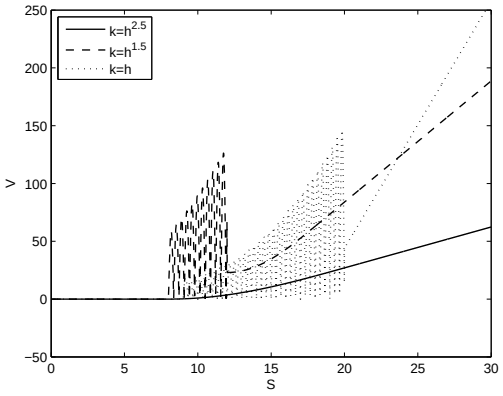

Figure 2.5: The effect of consistency condition on V.

	$\varepsilon = 0.1$			$\varepsilon = 0.15$		
h	Absolute Error	α	CPU time sec.	Absolute Error	α	CPU time sec.
1.2	6.835×10^{-4}	–	0.19	6.15×10^{-4}	–	0.19
1	4.821×10^{-4}	1.915	0.26	4.33×10^{-4}	1.925	0.26
0.8	3.138×10^{-4}	1.924	0.38	2.81×10^{-4}	1.938	0.38
0.5	1.266×10^{-4}	1.931	0.44	1.124×10^{-4}	1.95	0.44

Table 2.3: Errors and convergence rates due to the change of h for VG.

	$\varepsilon = 0.1$			$\varepsilon = 0.15$		
k	Absolute Error	β	CPU time sec.	Absolute Error	β	CPU time sec.
0.1	7.654×10^{-3}	–	0.248	5.321×10^{-3}	–	0.248
0.05	3.962×10^{-3}	0.950	0.256	2.793×10^{-3}	0.930	0.256
0.025	2.041×10^{-3}	0.957	0.263	1.429×10^{-3}	0.967	0.263
0.01	8.367×10^{-4}	0.973	0.271	5.794×10^{-4}	0.985	0.271

Table 2.4: Errors and convergence rates due to the change of k for VG.

The aim of the following examples is to exhibit the effects of different parameters such as h, k and ε on the variation of the absolute error in two cases; first, when $Y = 0$ (Variance Gamma case) and second for CGMY process when $Y = 1.5,\ 1.98$. Also the CPU time is given in seconds (sec).
In the next example we calculate the associated error with this numerical scheme for the Variance Gamma model as a particular case ($\mathbf{Y} = 0$) of CGMY model for which the exact solution is known [56].

Example 2.7. For $Y = 0$ and parameters have been selected as follows $T = 0.5$, $E = 80$, $A = 3E$, $S = 100$, $\sigma = 0.25$, $r = 0.1$, $q = 0$, $C = 1$, $\mathcal{G} = 30$, $\mathcal{M} = 20$ and $\delta = 0.1$, Table 2.3 shows the variation of the absolute error with h with fixed $k = 0.003$ and for two values of $\varepsilon = 0.1$ and 0.15. From Table 2.3, it is observed that the associated error exhibits the second order convergence rate α providing that k/h^2 is small enough in all the cases.

Table 2.4 reveals the change of the associated error for various values of time stepsize k, while $h = 0.8$ for $\varepsilon = 0.1$ and 0.15. Notice that the associated error due to the change of k satisfies the expected first order convergence rate β.

The aim of Table 2.5 is to show the sensitivity of the associated error of the option price due to the variation of ε, for $h = 0.5$ and 0.35, while $k = 0.005$.

	$h = 0.5$		$h = 0.35$	
ε	Absolute Error	CPU time (sec.)	Absolute Error	CPU time (sec.)
0.75	3.495×10^{-4}	0.45	1.473×10^{-4}	0.78
0.5	7.643×10^{-4}	0.45	4.587×10^{-4}	0.78
0.25	5.874×10^{-4}	0.45	3.198×10^{-4}	0.78
0.1	2.382×10^{-4}	0.45	1.258×10^{-4}	0.78

Table 2.5: The associated errors for several values of ε for VG.

	$\mathbf{Y} = 1.5$			$\mathbf{Y} = 1.98$		
h	Absolute Error	α	CPU time sec.	Absolute Error	α	CPU time sec.
1.5	6.1×10^{-4}	–	0.13	6.62×10^{-4}	–	0.13
1.2	3.98×10^{-4}	1.91	0.16	4.32×10^{-4}	1.913	0.16
1	2.8×10^{-4}	1.928	0.2	3.04×10^{-4}	1.927	0.2
0.8	1.8×10^{-4}	1.955	0.25	1.97×10^{-4}	1.944	0.25
0.5	7.18×10^{-5}	1.967	0.47	7.83×10^{-5}	1.962	0.47

Table 2.6: Comparison of errors and convergence rates due to the change of h for CGMY model.

Example 2.8. Here we compare in Tables 2.6 and 2.7 our results with the reference values given in [36, Tables 9, 10] related to accuracy and computational time. We consider the CGMY model for the following parameters $T = 1$, $r = 0.1$, $q = 0$, $C = 1$, $\mathcal{G} = \mathcal{M} = 5$, $E = 100$, $S = 100$, $A = 3E$, $\delta = 0.1$ and $k = 0.003$. Table 2.6 shows the variation of the associated error for several values of h when $Y = 1.5$ and 1.98, while $\varepsilon = 0.1$.

The variation of the associated error for several values of ε is presented in Table 2.7 for $Y = 1.5$ and 1.98, while $h = 1$.

The next example reveals that the double discretization strategy reduces the error near the parameter A by changing the stepsize δ.

	$\mathbf{Y} = 1.5$		$\mathbf{Y} = 1.98$	
ε	Absolute Error	CPU time (sec.)	Absolute Error	CPU time (sec.)
0.8	2.52×10^{-4}	0.2	2.63×10^{-4}	0.2
0.4	9.26×10^{-4}	0.2	7.26×10^{-4}	0.2
0.2	5.75×10^{-4}	0.2	4.39×10^{-4}	0.2
0.1	2.8×10^{-4}	0.2	3.04×10^{-4}	0.2

Table 2.7: Comparison of errors due to the variation of ε for CGMY model.

Example 2.9. Consider a call option under the Variance Gamma process with parameters $C = 1,\ \mathcal{G} = 20\ \mathcal{M} = 30,\ T = 1,\ r = 0.01,\ q = 0,\ \sigma = 0.2,\ \varepsilon = 0.12,\ E = 10,\ A = 3E,\ k = 0.005$ and $h = 0.35$, Fig. 2.6 shows the variation of the error of the numerical solution for various values of δ. Notice that the error decreases near the right boundary A of the numerical domain by decreasing the stepsize δ, while the error near the strike E remains stationary.

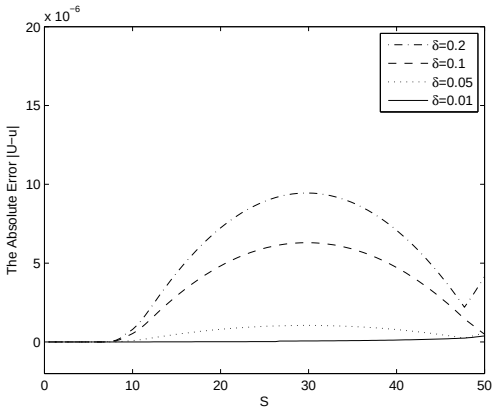

Figure 2.6: The associated error for several values of δ.

Example 2.10. Figure 2.7 describe the behavior of the Greek parameters Delta and Gamma for European call option. They exhibit the Greek parameters as functions in the underlying asset S and time t. The parameters have been chosen as follows $T = 1,\ E = 10,\ A = 3E,\ \sigma = 0.25,\ r = 0.01,\ q = 0,\ C = 1,\ \mathcal{G} = 35,\ \mathcal{M} = 35,\ Y = 1.6,\ \varepsilon = 0.15,\ h = 0.25,\ \delta = 0.1$ and $k = 0.04$.

The results of this chapter have been published in [21, 38].

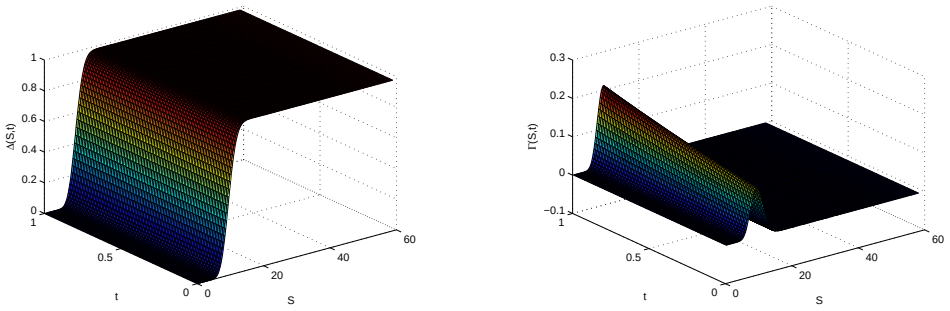

Figure 2.7: The Greeks for European call option.

Chapter 3

Solving partial integro-differential option pricing problems for a wide class of infinite activity Lévy processes

3.1 Introduction

As it has been stated in Chapter 2, since a long time ago empirical observations of the market show the evidence that the price of the underlying asset does not behave like a Brownian motion with a drift and a constant volatility. This fact motivates the emergence of alternative models to the pioneering Black-Scholes model [10]. Alternative models are stochastic volatility [44], deterministic volatility [26], jump diffusion [5, 53, 63, 85] and infinite activity Lévy models.
One of the most relevant and versatile Lévy models is the one proposed by Carr *et. al.* the so called CGMY [16], that belongs to the family of KoBoL models [11]. Apart from these models, other Lévy processes such as Meixner [60, 77], Hyperbolic and Generalized Hyperbolic (**GH**) are used to obtain better estimation for the stock returns [78]. The Meixner process was introduced in 1998, it is used when the environment is changing stochastically over the time showing a reliable valuation for some indices such as Nikkei 225 [77].

Model	The corresponding Lévy measure
KoBoL	$\nu(y) = \frac{C_- e^{-\mathcal{G}\lvert y\rvert}}{\lvert y\rvert^{1+Y}}\mathbf{1}_{y<0} + \frac{C_+ e^{-\mathcal{M}\lvert y\rvert}}{\lvert y\rvert^{1+Y}}\mathbf{1}_{y>0}$
Meixner	$\nu(y) = \frac{Ae^{-\alpha y}}{y\sinh(by)}$
GH process	$\nu(y) = \frac{e^{\beta y}}{\lvert y\rvert}\left(\int_0^\infty \frac{e^{-\sqrt{2\zeta+\alpha^2}\lvert y\rvert}}{\pi^2\zeta\left(J^2_{\lvert\lambda\rvert}(\delta\sqrt{2\zeta}) + Y^2_{\lvert\lambda\rvert}(\delta\sqrt{2\zeta})\right)}d\zeta + \max(0,\lambda)e^{-\alpha\lvert y\rvert}\right)$

Table 3.1: The forms of $\nu(y)$

The generalized hyperbolic distribution was introduced by Barndorff-Nielsen [6] and used to generate Lévy process to capture the real stock price movements of the intraday scale. It is exactly a pure discontinuous behavior of its paths what can be observed [33, 78]. Beside that the hyperbolic process is obtained as a special case from the **GH** process, it is implemented in various stock markets such as the blue chips of the German market, the DAX and also US stock market showing effective estimation for their returns [34].

However, following [78] the calibration of market option prices shows that depending on datasets, the matching between the actual price and its corresponding estimated value varies form model to another consequently, we can not say which is the perfect one. In this chapter we study the option pricing partial integro-differential equation (PIDE) unified model for several Lévy measures $\nu(y)$, given by [24, Chap. 12]

$$\frac{\partial \mathcal{C}}{\partial \tau}(S,\tau) = \frac{\sigma^2}{2}S^2\frac{\partial^2\mathcal{C}}{\partial S^2}(S,\tau) + (r-q)S\frac{\partial \mathcal{C}}{\partial S}(S,\tau) - r\mathcal{C}(S,\tau)$$

$$+\int_{-\infty}^{+\infty}\nu(y)\big[\mathcal{C}(Se^y,\tau) - \mathcal{C}(S,\tau) - S(e^y-1)\frac{\partial \mathcal{C}}{\partial S}(S,\tau)\big]dy,\ S\in(0,\infty),\ \tau\in(0,T], \tag{3.1}$$

$$\mathcal{C}(S,0) = f(S) = (S-E)^+, \qquad S\in(0,\infty), \tag{3.2}$$

$$\mathcal{C}(0,\tau) = 0;\ \lim_{S\to\infty}\mathcal{C}(S,\tau) = Se^{-q\tau} - Ee^{-r\tau}, \tag{3.3}$$

where $\mathcal{C}$ is the value of a contingent claim, S is the underlying asset and $\tau = T - t$ is the time to the maturity. The Lévy measures $\nu(y)$ are given in Table 3.1.

Note that the Hyperbolic process is obtained from the **GH** process when $\beta = 0$ and $\lambda = -1$.

To the best of our knowledge, the numerical solution and analysis of Meixner and **GH** models have not been treated. The KoBoL model and in particular the CGMY, see Table 2.1 with parameter $C_- = C_+$, has been widely studied because its versatile and includes the finite and infinite activity cases as well as the finite and infinite variation, obtained by changing the value of Yor parameter $Y < 2$. A fairly complete revision of the methods used to solve the CGMY model can be found in [21, 25, 71, 87].

In this chapter we focus on the numerical analysis of the unified model (3.1)-(3.3) for the European case, by proposing a consistent, explicit and conditionally positive and stable finite difference scheme while the integral part is approximated using Gauss-Laguerre quadrature formula. We also include the computation of the linear complementarity problem (LCP) for the American option case using both the projected successive over relaxation method (PSOR) and the multigrid method (MG). The discretization for the differential operator is done using the three-level approximation, while the integral part is discretized as the same as in the European case. So, the integral part of the PIDE operator for the American and European cases is discretized using the Gauss-Laguerre quadrature. Although the three-level method is widely used and it is argued that the approximation error is of order two, however such method has two unsuitable properties, in fact as the method needs the first time step that must be obtained using another method (usually by implicit Euler method), in practice the accuracy is reduced. Also, as it is shown in Example 3.1 for European option, the three-level method does not guarantee the positiveness.

With respect to previous relevant papers in the field, we should mention the potential advantage of our approach. Apart from the more general unified treatment of a wide class of Lévy models, we do not truncate the integral part for its approximation using Gauss-Laguerre quadrature that reduces the computational cost using a few amount of nodes to approximate the integral and improves the accuracy due to the advantages of Gauss-Laguerre quadrature. An additional positive fact of this approach is that it allows to give error information of the integral approximation as it is shown in Example 3.4.

This chapter is organized as follows. In Section 3.2, the kernel singularity of the integral part of the PIDE is replaced by adding a diffusion term following the ap-

proach developed in [25, 87] and treated in chapter 2, Section 2.1. Then the reaction and convection terms of the differential part are removed by using suitable transformation as in [21]. Finally in Section 3.2, the numerical scheme construction is included. Section 3.3 deals with the numerical analysis of the explicit proposed numerical scheme, including conditional positivity and stability in the Von Neumann sense, as well as the consistency. Section 3.4 is addressed to the study of the American option case, the LCP is solved using the PSOR and MG including the Gauss-Laguerre quadrature discretization for the integral part and the three-level for the differential part. Section 3.5 includes numerical examples to discuss and validate the results.

3.1.1 Gauss quadrature approximation

For several many cases, in order to evaluating definite integrals, the antiderivative for the integrand function cannot be found or it is extremely difficult to find. Therefore, the numerical integration is a mathematical branch that investigates how to obtain the numerical value of a definite integral using a suitable algebraic approximation. However, numerical integration is paradoxically both simple and extremely difficult. Its simplicity lies in resolving it by the simplest of methods. It is difficult in two respects: first, it may require an inordinate amount of computing time, verging in some unfavorable situations toward impossibility; second, in order to guarantee the convergence of this approximation, it can be led to some of the deepest of pure and applied analysis.
Generally, in order to obtain a suitable approximation for a definite integral, it is required to increase the number of mesh points. If this integral is a separate problem, so it will be admissible to use a large number of mesh points increasing the computational cost. Fortunately, there is an efficient method in the realm of the numerical integration that obtains an accurate approximation using few mesh points, namely the Gauss Quadrature method. In fact this method based on a famous theorem of Weierstrass, which states that any function $f(x)$ which is continuous on a closed interval $[a, b]$ can be uniformly approximated within any prescribed tolerance on that interval, by some polynomial [45].

In Gauss quadrature approximation, there are two sets of points: $\{x_i\}_{i=1}^M$ and $\{w_i\}_{i=1}^M$ such that

$$\int_a^b w(x)f(x)dx \approx \sum_{i=1}^{M} w_i f(x_i), \tag{3.4}$$

where the points $\{x_i\}_{i=1}^M$ are called the nodes and $\{w_i\}_{i=1}^M$ are called the corresponding weights. The interval $[a, b]$ can be one of the following cases:

1. A finite interval $-\infty < a < b < \infty$; then it can be mapped into $[-1, 1]$ and one of the following polynomials can be used; Legendre, Tschebyscheff, first and second kinds, Ultraspherical, Gegenbauer or Jacobi.

2. A semi infinite interval $[0, \infty)$; then the suitable utilized polynomial is Laguerre or Generalized Laguerre.

3. If the domain is the real line $\mathbb{R}$, then the integrand function is approximated using Hermite polynomial.

If the integration is approximated using $M-$points, then the used polynomial is of degree M and it is denoted by $P_M(x)$ and these points are the roots of $P_M(x)$.

3.2 Scheme construction for European options

Let us begin this section by transforming the PIDE (3.1) into a simpler one following the technique developed in Section 2.1. Since the kernel of the integral in (3.1) presents a singularity at $y = 0$, a useful technique is to split the real line, for an arbitrary small parameter $\varepsilon > 0$, into two regions $\Omega_1 = [-\varepsilon, \varepsilon]$ and $\Omega_2 = \mathbb{R}\backslash\Omega_1$, the complementary set of Ω_1 in the real line. The integral on Ω_1 is replaced by a suitable coefficient in the diffusion term of the differential part of (3.1) obtained by Taylor expansion of $V(Se^y, \tau)$ about S, see [21, 25, 71, 87]. This coefficient depending on ε is a convergent integral and takes the form

$$\breve{\sigma}^2(\varepsilon) = \int_{-\varepsilon}^{\varepsilon} \nu(y)(e^y - 1)^2 dy = \varepsilon \int_{-1}^{1} \nu(\varepsilon\phi)(e^{\varepsilon\phi} - 1)^2 d\phi. \tag{3.5}$$

The resulting approximating PIDE is given by

$$\frac{\partial \mathcal{C}}{\partial \tau} = \frac{\hat{\sigma}^2}{2} S^2 \frac{\partial^2 \mathcal{C}}{\partial S^2} + (r - q - \gamma(\varepsilon))S\frac{\partial \mathcal{C}}{\partial S} - (r + \lambda(\varepsilon))\mathcal{C}$$

$$+\int_{\Omega_2}\nu(y)\mathcal{C}(Se^y,\tau)dy, \tag{3.6}$$

where

$$\hat{\sigma}^2=\sigma^2+\breve{\sigma}^2(\varepsilon),\ \gamma(\varepsilon)=\int_{\Omega_2}\nu(y)(e^y-1)dy,\ \lambda(\varepsilon)=\int_{\Omega_2}\nu(y)dy. \tag{3.7}$$

The convergent integrals (3.5) and (3.7) are evaluated using Gauss quadrature approximation. In order to obtain an approximation for $\breve{\sigma}^2(\varepsilon)$, the Legendre-Gauss quadrature approximation is used, so the weighting function $w(\phi)=1$ such that

$$\breve{\sigma}^2(\varepsilon)\approx\varepsilon\sum_{m=1}^{M}\omega_m\nu(\varepsilon\phi_m)(e^{\varepsilon\phi_m}-1)^2, \tag{3.8}$$

where ϕ_m are the roots of the Legendre polynomial $P_M(\phi)$ of degree M and ω_m is calculated based on [1, Eq. (25.4.29) p. 887]. Here M is chosen to be an even number so that zero is not a root of P_M. The improper integrals $\lambda(\varepsilon)$ and $\gamma(\varepsilon)$ are approximated using the shifted Laguerre-Gauss quadrature [28, p. 226]. Note that under change of variables $\eta=-y-\varepsilon$ for $y<0$ and $\eta=y-\varepsilon$ for $y>0$ then $\lambda(\varepsilon)$ and $\gamma(\varepsilon)$ have the following forms

$$\lambda(\varepsilon)=\int_0^\infty\left(\nu(-\eta-\varepsilon)+\nu(\eta+\varepsilon)\right)d\eta \tag{3.9}$$

and

$$\gamma(\varepsilon)=\int_0^\infty\left[\nu(-\eta-\varepsilon)(e^{-(\eta+\varepsilon)}-1)+\nu(\eta+\varepsilon)(e^{\eta+\varepsilon}-1)\right]d\eta. \tag{3.10}$$

From (3.9), (3.10) and since the weighting function is $w(\eta)=e^{-\eta}$, then we have

$$\lambda(\varepsilon)\approx\sum_{m=1}^{M}\varpi_m F(\eta_m,\varepsilon),\ \gamma(\varepsilon)\approx\sum_{m=1}^{M}\varpi_m\mathcal{F}(\eta_m,\varepsilon), \tag{3.11}$$

where

$$F(\eta,\varepsilon)=e^{\eta}(\nu(-\eta-\varepsilon)+\nu(\eta+\varepsilon))$$
$$\mathcal{F}(\eta,\varepsilon)=e^{\eta}\left(\nu(-\eta-\varepsilon)(e^{-(\eta+\varepsilon)}-1)+\nu(\eta+\varepsilon)(e^{\eta+\varepsilon}-1)\right).$$

Here η_m are the roots of the Laguerre polynomial $L_M(\eta)$ of degree M and the weighting function ϖ_m is given in [1, Eq. (25.4.45) p. 890].
Coming back to (3.6) in order to eliminate the convection and reaction terms, using

the transformation defined by

$$x = \exp[(r - q - \gamma(\varepsilon))\tau]S,\ V(x,\tau) = \exp[(r + \lambda(\varepsilon))\tau]\mathcal{C}(S,\tau), \tag{3.12}$$

one gets

$$\frac{\partial V}{\partial \tau} = \frac{\hat{\sigma}^2}{2}x^2\frac{\partial^2 V}{\partial x^2} + \int_{\Omega_2} \nu(y)V(xe^y,\tau)dy, \quad x \in (0,\infty), \quad \tau \in (0,T], \tag{3.13}$$

with the initial and boundary conditions

$$V(x,0) = f(x) = (x - E)^+ \tag{3.14}$$

$$V(0,\tau) = 0; \quad \lim_{x\to\infty} V(x,\tau) = e^{\lambda(\varepsilon)\tau}(xe^{\gamma(\varepsilon)\tau} - E). \tag{3.15}$$

Next, for the sake of convenience in the numerical treatment we rewrite the integral part of (3.13) as follows

$$\int_{\Omega_2} \nu(y)V(xe^y,\tau)dy = \int_{-\infty}^{\infty} \hat{\nu}(y)V(xe^y,\tau)dy, \tag{3.16}$$

where

$$\hat{\nu}(y) = \begin{cases} \nu(y), & y \in \Omega_2 \\ 0, & y \in \Omega_1 \end{cases}. \tag{3.17}$$

After that, in order to match the interval of the integration with the spatial domain of the problem, we use the following substitution $\phi = xe^y$ into (3.16), obtaining

$$\int_{\Omega_2} \nu(y)V(xe^y,\tau)dy = \int_0^{\infty} \hat{\nu}(\ln(\frac{\phi}{x}))V(\phi,\tau)\frac{d\phi}{\phi}. \tag{3.18}$$

Hence the PIDE for the European option under Lévy model, takes the following form

$$\frac{\partial V}{\partial \tau} = \frac{\hat{\sigma}^2}{2}x^2\frac{\partial^2 V}{\partial x^2} + \int_0^{\infty} \hat{\nu}(\ln(\frac{\phi}{x}))V(\phi,\tau)\frac{d\phi}{\phi}. \tag{3.19}$$

Now, we are in a good situation to construct an efficient explicit numerical scheme for the transformed problem (3.19) after choosing our numerical domain $[0, x_{\max}]\times[0,T]$ for large enough value of $x_{\max}$. Based on [51] the suggested value of $x_{\max}$ is about $3E$ or $4E$.

- For the time discretization, we take $\tau^n = nk$, $n = 0, 1, \ldots, N_\tau$ where $k = \frac{T}{N_\tau}$.
- The spatial variable x is discretized by $x_j = jh$, $j = 0, 1, 2, \ldots, N_x$, $h = \frac{x_{\max}}{N_x}$.

Since the Laguerre-Gauss quadrature will be used for approximating the integral part of (3.19), then we have the sequence of roots $\{\phi_m\}_{m=1}^{M}$ of the Laguerre polynomial $L_M(\phi)$. The suitable value for M is selected such that $E < \phi_M < x_{\max}$.

By using explicit forward approximation for the time derivative of V and the central difference approximation for second spatial derivative, one gets

$$\frac{\partial V}{\partial \tau}(x_j, \tau^n) \approx \frac{V_j^{n+1} - V_j^n}{k}, \quad \frac{\partial^2 V}{\partial x^2}(x_j, \tau^n) \approx \frac{V_{j+1}^n - 2V_j^n + V_{j-1}^n}{h^2}. \tag{3.20}$$

In order to approximate the integral part of (3.19) matching the discretization of the integral and differential parts, taking into account that zeroes of Laguerre polynomial do not need to be nodes of the mesh, we use linear Lagrange interpolation polynomial. For any m, $1 \leq m \leq M$, let us denote by ℓ_m the last integer such that the mesh point $x_{\ell_m} < \phi_m$. The approximating value $V^n(\phi_m)$ is given by

$$V^n(\phi_m) = \tilde{a}_{\ell_m} V_{\ell_m}^n + \hat{a}_{\ell_m} V_{\ell_m+1}^n, \tag{3.21}$$

where the interpolation coefficients are

$$\tilde{a}_{\ell_m} = \frac{(x_{\ell_m+1} - \phi_m)}{h}; \quad \hat{a}_{\ell_m} = \frac{(\phi_m - x_{\ell_m})}{h}. \tag{3.22}$$

Note that the linear interpolation approximation (3.21) has an error of order $\mathcal{O}(h^2)$ that coincide with the associated error of the central approximation of the spatial derivative (3.20). Hence the discretization for the integral part is given by

$$I_j^n = \sum_{m=1}^{M} \hat{\nu}(\ln \frac{\phi_m}{x_j}) \frac{e^{\phi_m}}{\phi_m} \varpi_m \left(\tilde{a}_{\ell_m} V_{\ell_m}^n + \hat{a}_{\ell_m} V_{\ell_m+1}^n \right). \tag{3.23}$$

Summarizing, from (3.20)-(3.23), the discretization of (3.19) with (3.14) and (3.15) takes the form

$$V_j^{n+1} = \alpha_j (V_{j+1}^n + V_{j-1}^n) + \beta_j V_j^n + k \sum_{m=1}^{M} \hat{\nu}(\ln \frac{\phi_m}{x_j}) \frac{e^{\phi_m}}{\phi_m} \varpi_m \left(\tilde{a}_{\ell_m} V_{\ell_m}^n + \hat{a}_{\ell_m} V_{\ell_m+1}^n \right), \tag{3.24}$$

$1 \leq j \leq N_x - 1, \quad 0 \leq n \leq N_\tau - 1$, where

$$\alpha_j = \frac{k}{2h^2}\hat{\sigma}^2 x_j^2, \qquad \beta_j = 1 - 2\alpha_j, \tag{3.25}$$

satisfying

$$V_j^0 = (x_j - E)^+, \tag{3.26}$$

and

$$V_0^n = 0, \qquad V_{N_x}^n = e^{\lambda(\varepsilon)\tau^n}(x_{\max}e^{\gamma(\varepsilon)\tau^n} - E). \tag{3.27}$$

3.3 Numerical Analysis for European Options

Dealing with option prices, positive values of the numerical solution is a necessary requirement. In this section the positivity, stability as well as the consistency of the scheme (3.24)-(3.27) are studied. Note that the coefficients of scheme (3.24) are nonnegative under the condition

$$\frac{k}{h^2} \leq \frac{1}{\hat{\sigma}^2 x_{\max}^2}. \tag{3.28}$$

Thus from nonnegative initial and boundary values (3.26) and (3.27), the following result is immediate

Theorem 4. *The numerical solution* $\{V_j^n\}$ *of the scheme* (3.24)-(3.27) *is nonnegative under the condition* (3.28).

There are many approaches in the literature to study the stability for a finite difference scheme and many concepts of stability. Here we study the stability using the well known Von Neumann approach [80, 81]. Von Neumann analysis for linear parabolic PDEs with variable coefficients is treated in [30, 42][81, p. 59] and for PIDEs by [3]. Let us rewrite the numerical solution V_j^n

$$V_j^n = \xi^n e^{i\theta jh}, \tag{3.29}$$

where ξ^n is the amplitude at time level n, i is the imaginary unit and θ is the phase angle. According to [80, p. 68] the unconditional stability of scheme (3.24) is guaranteed if the amplification factor $G = \frac{\xi^{n+1}}{\xi^n}$ satisfies

$$|G| \leq 1 + Kk = 1 + \mathcal{O}(k), \tag{3.30}$$

where the positive number K is independent of h, k and θ.
When (3.30) is verified for those values of h and k satisfying a specific condition, then the stability of the scheme is said to be conditional.
By substituting into (3.24), one gets

$$G = 1 - a(k, h, \theta) + kz(j, h, \theta), \tag{3.31}$$

where

$$a(k, h, \theta) = 4\alpha_j \sin^2\left(\frac{\theta h}{2}\right), \tag{3.32}$$

$$z(j, h, \theta) = \sum_{m=1}^{M} A_{j,m} e^{i(\ell_m - j)\theta h} \left(\tilde{a}_{\ell_m} + \hat{a}_{\ell_m} e^{i\theta h}\right), \tag{3.33}$$

$$A_{j,m} = \hat{\nu}\left(\ln\frac{\phi_m}{x_j}\right) \varpi_m \frac{e^{\phi_m}}{\phi_m}. \tag{3.34}$$

Note that under the positivity condition (3.28) we have

$$\alpha_j = \frac{k}{2h^2}\hat{\sigma}^2 x_j^2 \leq \frac{1}{2}; \quad 4\alpha_j \sin^2\left(\frac{\theta h}{2}\right) \leq 2. \tag{3.35}$$

Thus

$$|1 - a(k, h, \theta)| \leq 1, \tag{3.36}$$

for h and k satisfying (3.28).
Under condition (3.28) from (3.31) and (3.36) one gets

$$\begin{aligned} |G|^2 &= (1 - a(k, h, \theta))^2 + 2k(1 - a(k, h, \theta))Re(z) + k^2|z|^2 \\ &\leq 1 + 2|z|k + |z|^2 k^2. \end{aligned} \tag{3.37}$$

Then $|G| \leq 1 + |z|k$, consequently, the stability will be guaranteed if $|z|$ is bounded. Now we are interested in obtaining a common bound for $|z|$ for all the infinite activity Lévy models considered in Table 2.1.
From (3.22), $\tilde{a}_{\ell_m} + \hat{a}_{\ell_m} = 1$, and from (3.33) one gets

$$|z| \leq \sum_{m=1}^{M} A_{j,m}(\tilde{a}_{\ell_m} + \hat{a}_{\ell_m}) = \sum_{m=1}^{M} A_{j,m}. \tag{3.38}$$

Note that from (3.9) and (3.34), $\sum_{m=1}^{M} A_m^j$ is the Gauss-Laguerre quadrature approximation for $\lambda(\varepsilon)$, then for an arbitrarily small $\rho > 0$ and large enough value of M

one gets

$$\sum_{m=1}^{M} A_{j,m} \leq \rho + \int_{\varepsilon}^{\infty} (\nu(-y) + \nu(y))dy. \tag{3.39}$$

It is easy to check from Table 1 that for all Lévy measures,

$$\nu(-y) + \nu(y) < \mathfrak{G}(y), \quad y \in (\varepsilon, \infty), \tag{3.40}$$

where

$$\mathfrak{G}(y) = 2\hat{C}\frac{e^{-\hat{M}y}}{y^{1+\hat{Y}}}, \tag{3.41}$$

and

$$\hat{C} = \begin{cases} \max(C_-, C_+), & \text{KoBoL} \\ \frac{2}{b}A, & \text{Meixner} \\ 2\max(|\lambda|, \tilde{C}_M), & \text{Generalized Hyperbolic,} \end{cases} \tag{3.42}$$

such that

$$\tilde{C}_M = \sum_{m=1}^{M} \frac{\varpi_m e^{\phi_m}}{\pi^2 \phi_m (J^2_{|\lambda|}(\delta\sqrt{(2\phi_m)}) + Y^2_{|\lambda|}(\delta\sqrt{(2\phi_m)}))},$$

$$\hat{M} = \begin{cases} \min(\mathcal{G}, \mathcal{M}), & \text{KoBoL} \\ a, & \text{Meixner} \\ \alpha - |\beta|, & \text{Generalized Hyperbolic} \end{cases} \tag{3.43}$$

$$\hat{Y} = \begin{cases} Y, & \text{KoBoL} \\ 1, & \text{Meixner} \\ 0, & \text{Generalized Hyperbolic} \end{cases}. \tag{3.44}$$

From (3.40) and (3.41), it follows that

$$\int_{\varepsilon}^{\infty} (\nu(-y) + \nu(y))dy < \int_{\varepsilon}^{\infty} \mathfrak{G}(y)dy = 2\hat{C}\varepsilon^{-\hat{Y}} E_{1+\hat{Y}}(\varepsilon\hat{M}), \tag{3.45}$$

where $E_s(\eta)$ is the exponential integral defined by (2.5).
Hence from (3.38), we have

$$|z| \leq \sum_{m=1}^{M} A^j_m \leq 2\hat{C}\varepsilon^{-\hat{Y}} E_{1+\hat{Y}}(\varepsilon\hat{M}). \tag{3.46}$$

Summarizing the following result has been established.

Theorem 5. *With previous notation, under the positivity condition* (3.28)*, the numerical scheme* (3.24) *for* (3.19) *is conditionally stable.*

Once the stability has been established, in order to guarantee the convergence of the numerical scheme for the linear PIDE problem it is sufficient to prove the consistency of the numerical scheme with the PIDE. According to its definition [55, 80], a numerical scheme is consistent with a PIDE problem if the exact theoretical solution of the PIDE approximates well the difference scheme as the stepsizes discretization tend to zero.
Let us denote $v_j^n = V(x_j, \tau^n)$ as the value of the exact solution of (3.19). The local truncated error $T_j^n(V)$ at (x_j, τ^n) is defined by

$$T_j^n(V) = \left(\frac{v_j^{n+1} - v_j^n}{k} - \frac{\hat{\sigma}^2}{2}\frac{x_j^2}{h^2}(v_{j-1}^n - 2v_j^n + v_{j+1}^n) - \frac{\partial V}{\partial \tau}(x_j, \tau^n) + \frac{\hat{\sigma}^2}{2}x^2\frac{\partial^2 V}{\partial x^2}(x_j, \tau^n) \right)$$

$$- \left(\sum_{m=1}^{M} A_{j,m} \left(\tilde{a}_{\ell_m} v_{\ell_m}^n + \hat{a}_{\ell_m} v_{\ell_m+1}^n \right) - \int_0^\infty \hat{\nu}(\ln\frac{\phi}{x}) V(\phi, \tau)\frac{d\phi}{\phi} \right) \tag{3.47}$$

$$= L(V_j^n) - I(V_j^n), \tag{3.48}$$

where $L(V_j^n)$ and $I(V_j^n)$ denote the truncation errors for the differential and integral parts respectively. In order to prove the consistency, we must show that

$$T_j^n(V) \to 0, \text{ as } h \to 0, \ k \to 0. \tag{3.49}$$

Assuming that V is twice continuously partially differentiable with respect to τ and four times partially differentiable with respect to x, and using Taylor's expansion about (x_j, τ^n), it is easy to obtain

$$L(V_j^n) = \mathcal{O}(h^2) + \mathcal{O}(k), \tag{3.50}$$

see [21] and Section 2.5.1 in Chapter 2 for a detailed development of this expression. The local truncation error for the integral part is given by

$$|I(V_j^n)| = \left| \int_0^\infty \hat{\nu}(\ln(\frac{\phi}{x_j}))V(\phi, \tau^n)\frac{d\phi}{\phi} - \sum_{m=1}^{M} \hat{\nu}(\ln\frac{\phi_m}{x_j})\varpi_m \frac{e^{\phi_m}}{\phi_m} V(\phi_m, \tau^n) \right| \tag{3.51}$$

$$= ((M!)^2)\hat{f}[\phi_1, \phi_1, \phi_2, \phi_2, \ldots, \phi_M, \phi_M, \hat{\xi}], \tag{3.52}$$

where $\hat{f}[\phi_1, \phi_1, \phi_2, \phi_2, \ldots, \phi_M, \phi_M, \hat{\xi}]$ denotes the divided difference for

$$\hat{f}(\phi) = \hat{\nu}(\ln(\frac{\phi}{x_j}))\frac{e^{\phi}}{\phi}V(\phi, \tau^n), \hat{\xi} > 0, \tag{3.53}$$

see [45, p. 397 Eq. (8.7.12)]. For smooth enough integrands the error takes the form

$$|I(V_j^n)| = \frac{(M!)^2}{2M!}\hat{f}^{(2M)}(\hat{\xi}). \tag{3.54}$$

Summarizing the scheme (3.24) is consistent with the PIDE (3.19) and the truncation error behaves

$$T_j^n = \mathcal{O}(h^2) + \mathcal{O}(k) + \epsilon(M), \tag{3.55}$$

where M is the number of the roots of Laguerre polynomial of degree M used in the numerical integration.

3.4 American options under Lévy models

The most used method for pricing an American option is the formulation of a LCP and then solving it using a numerical method, see [47, 48, 87]. Following this approach the LCP for American option under the Lévy measures in Table 3.1 and the transformation (3.12) takes the form

$$\mathcal{L}[V] \geq 0, \quad V \geq f(x), \quad \mathcal{L}[V](V - f(x)) = 0, \tag{3.56}$$

where

$$\mathcal{L}[V] = \frac{\partial V}{\partial \tau} - \mathcal{D}[V] - I(V), \tag{3.57}$$

and $f(x)$ is the payoff given by (3.14). The operators $\mathcal{D}[V]$ and $I(V)$ are given by

$$\mathcal{D}[V] = \frac{\hat{\sigma}^2}{2}x^2\frac{\partial^2 V}{\partial x^2}, \quad I(V) = \int_{\Omega_2} \nu(y)V(xe^y, \tau)dy. \tag{3.58}$$

Let us obtain the semi-discrete formulation of the problem (3.56). Using spatial central difference approximation for the second derivative and Laguerre Gauss quadra-

ture for the integral part, one gets

$$\mathcal{D}[V] + I(V) \approx \hat{\alpha}_j(V_{j-1} - 2V_j + V_{j+1}) + \sum_{m=1}^{M} A_{j,m}\left(\tilde{a}_{\ell_m} V_{\ell_m} + \hat{a}_{\ell_m} V_{\ell_m+1}\right), \quad (3.59)$$

where $\hat{\alpha}_j = \frac{\hat{\sigma}^2 x_j^2}{2h^2}$; $\tilde{a}_{\ell_m}$, $\hat{a}_{\ell_m}$ and $A_{j,m}$ are given in (3.22) and (3.34) respectively. Let $\mathcal{A} \in \mathbb{R}^{(Nx-1)\times(Nx-1)}$ be the matrix representation of (3.59)

$$\mathcal{A} = -\hat{\mathcal{D}} - \mathcal{P}, \quad (3.60)$$

where the entries $d_{j\ell}$ of the tridiagonal matrix $\hat{\mathcal{D}}$ are given by

$$d_{j\ell} = \begin{cases} -2\hat{\alpha}_j, & \ell = j, \\ \hat{\alpha}_j, & \ell = j-1, j+1. \end{cases} \quad (3.61)$$

Let us introduce the sets

$$\hat{L}_1 = \{\ell_m\}_{m=1}^{M}, \quad \hat{L}_2 = \{\ell_m + 1\}_{m=1}^{M}, \quad \tilde{m} : \ell_m \to m. \quad (3.62)$$

The matrix $\mathcal{P}$ for the integral part is represented as

$$\mathcal{P} = \tilde{\mathcal{P}} + \hat{\mathcal{P}}, \quad (3.63)$$

where

$$\tilde{p}_{j\ell} = \begin{cases} A_{j,\tilde{m}(\ell)}\tilde{a}_\ell, & \ell \in \hat{L}_1, \\ 0, & \text{otherwise}, \end{cases}, \quad \hat{p}_{j\ell} = \begin{cases} A_{j,\tilde{m}(\ell)}\hat{a}_\ell, & \ell \in \hat{L}_2, \\ 0, & \text{otherwise}. \end{cases} \quad (3.64)$$

With the above notations the LCP (3.56) has the following semi-discrete form

$$\frac{\partial \mathbf{V}}{\partial \tau} + \mathcal{A}\mathbf{V} \geq \mathbf{b}(\tau); \quad \mathbf{V} \geq \mathbf{f}; \quad \left(\frac{\partial \mathbf{V}}{\partial \tau} + \mathcal{A}\mathbf{V} - \mathbf{b}(\tau)\right)^T (\mathbf{V} - \mathbf{f}) = 0, \quad (3.65)$$

where $\mathbf{V} = \mathbf{V}(\tau)$ is the vector solution satisfying $\mathbf{V}(0) = \mathbf{f}$ and $\mathbf{b} = \mathbf{b}(\tau)$ is the vector including the boundary conditions

$$\mathbf{V} = [V_1\ V_2 \ldots V_{N_x-1}], \quad \mathbf{b} = [V_0\ 0\ 0 \ldots 0\ V_{N_x}(\tau)]. \quad (3.66)$$

Explicit time discretization is not suitable for LCP problems because of the computational cost. Also, the Crank-Nicolson approximation is convenient when the initial data and its derivative are continuous. As this is not our case we choose the three time levels which also known as the backward difference formula (BDF2) with accuracy of second order like Crank-Nicolson and better stability properties [48]. Hence the corresponding LCP for (3.65) after time discretization is denoted by

$$LCP(\tilde{\mathcal{A}}, \mathbf{V}^{n+1}, \tilde{\mathbf{V}}^n, \mathbf{f}), \tag{3.67}$$

and given by

$$\tilde{\mathcal{A}}\mathbf{V}^{n+1} - \tilde{\mathbf{V}}^n \geq 0; \quad \mathbf{V}^{n+1} \geq \mathbf{f}; \quad (\tilde{\mathcal{A}}\mathbf{V}^{n+1} - \tilde{\mathbf{V}}^n)^T(\mathbf{V}^{n+1} - \mathbf{f}), \tag{3.68}$$

where

$$\tilde{\mathcal{A}} = \begin{cases} I + k\mathcal{A}, & n = 0, \\ I + \frac{2k}{3}\mathcal{A}, & n \geq 1, \end{cases} \tag{3.69}$$

and

$$\tilde{\mathbf{V}}^n = \begin{cases} \mathbf{V}^0 + k\mathbf{b}^0, & n = 0, \\ \frac{4}{3}\mathbf{V}^n - \frac{1}{3}\mathbf{V}^{n-1} + \frac{2k}{3}\mathbf{b}^{n+1}, & n \geq 1. \end{cases} \tag{3.70}$$

Note that the first level for the solution vector is obtained using the implicit Euler approximation. Also, the matrix $\tilde{\mathcal{A}}$ is of M-Matrix type.
The pioneering method PSOR introduced by Cryer [27] is commonly used to solve LCPs. The crux of this method is to execute successive over relaxed modifications for the solution vector components associated with a projection when any component be less than the payoff. The relaxation parameter $\omega \in (0, 2)$ plays a relevant role accelerating the rate of convergence and the optimal value for ω can be calculated by the expression [80]

$$\omega_{op} = \frac{2}{1 + \sqrt{1 - \rho^2(\mathbf{G})}}, \tag{3.71}$$

where $\mathbf{G} = \mathbf{D}^{-1}(\tilde{\mathcal{A}} - \mathbf{D})$ is the Jacobi iteration matrix, $\mathbf{D}$ is the diagonal of $\tilde{\mathcal{A}}$ and $\rho(\mathbf{G})$ is the spectral radius of $\mathbf{G}$.

When solving a LCP using PSOR, one has to address two challenges; firstly the selection of the initial guess, secondly its accuracy declines as the grid becomes finer

[49]. The multigrid iterative method **MG** has been shown as a reliable alternative to overcome the quoted difficulties [13, 43, 88]. The operator that transforms the problem from the coarser to the finer grid is called the linear interpolation (prolongation) operator and symbolized by I_{2h}^{h}, while the map for the inverse transformation is called the full weighting restriction operator and denoted by I_{h}^{2h}. Here, the matrix $\tilde{\mathcal{A}}^{h}$ denotes the matrix $\tilde{\mathcal{A}}$ on the finer grid and $\tilde{\mathcal{A}}^{2h}$ is the corresponding matrix on the coarse grid and obtained by [13]

$$\tilde{\mathcal{A}}^{2h} = I_{h}^{2h}\tilde{\mathcal{A}}^{h}I_{2h}^{h}. \tag{3.72}$$

Remark

The three time-level can be used for European option but it does not guarantee the positivity of the solution, see Example 1. The corresponding scheme is given by

$$(I + \frac{2k}{3}\mathcal{A})\mathbf{V}^{n+1} = \frac{4}{3}\mathbf{V}^{n} - \frac{1}{3}\mathbf{V}^{n-1} + \frac{2k}{3}\mathbf{b}^{n+1}, \quad n \geq 1, \tag{3.73}$$

and the first level solution is obtained by

$$(I + k\mathcal{A})\mathbf{V}^{1} = \mathbf{V}^{0} + k\mathbf{b}^{0}. \tag{3.74}$$

3.5 Numerical Examples

In this section five numerical examples are included to validate, compare and discuss the proposed results. From Example 3.1 to Example 3.4 are related to European option case; Example 3.1 deals with the positivity, Example 3.4 discuss the consistency and Examples 3.2 and 3.3 report about accuracy and computational cost. Finally Example 3.5 deals with the American option case.
Throughout the examples related to European options, we will refer as scheme 1 to explicit scheme (3.24)-(3.27) and scheme 2 as the three-level scheme (3.73)-(3.74).
The objective of the first example is to exhibit the importance of the positivity condition (3.28) for the three studied Lévy models.

Example 3.1. Here, we have an European option with $E = 30$, $T = 0.5$, $r = 0.08$, $q = 0$, $\sigma = 0.2$, $x_{\min} = 0$, $x_{\max} = 90$, $M = 15$, $\varepsilon = 0.5$ and $N_x = 128$. The parameters for Lévy models are given in Table 3.2. Figures 3.1-3.4 display the behavior of

Model	Parameters
CGMY	$C = 0.5$, $\mathcal{G} = 15$, $\mathcal{M} = 25$ and $Y = 1.2945$.
Meixner	$A = 0.5$, $a = -2.5$ and $b = 8$.
GH	$\alpha = 4$, $\beta = -3.2$, $\delta = 0.4775$ and $\lambda = 2$

Table 3.2: The parameters for Lévy models used in Example 3.1.

the option price $\mathcal{C}$ evaluated by the proposed explicit scheme (3.24)-(3.27) when the positivity condition (3.28) holds for $N_\tau = 25e3$ and when it is broken for $N_\tau = 1e3$ represented by the solid and dot curves respectively under several Lévy processes. In spite of the computational performance of the three level method, from the qualitative point of view, it disregards some important issues as the positivity. With the same parameters, $N_x = 800$ and several values of N_τ Table 3.3 shows negative values of the option price under CGMY process valuated with (3.73)-(3.74).

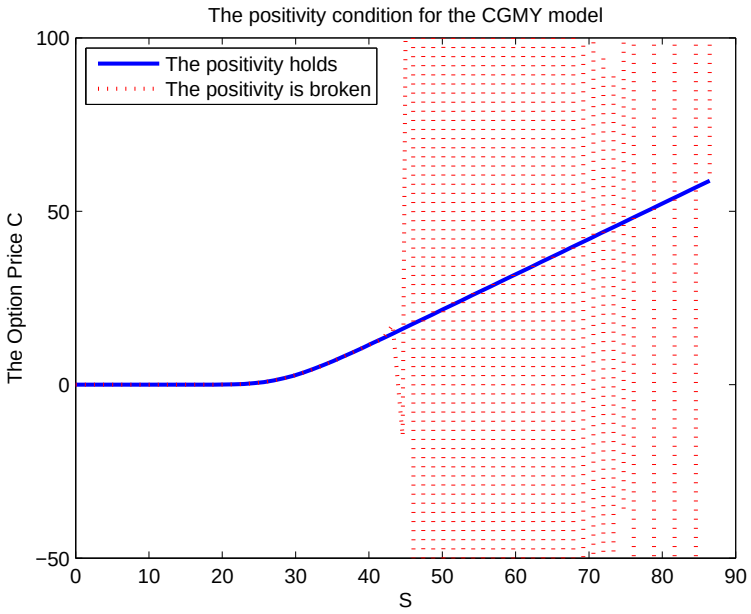

Figure 3.1: About positivity condition of the explicit scheme under CGMY process.

The aim of the next example is to show the variation of the error for the Variance Gamma **VG** model as the stepsizes h and k change. The **VG** is obtained from the CGMY model when $Y = 0$, the reference option values for $S = \{20, 30, 40, 50\}$ are obtained using the closed form solution given in [56].

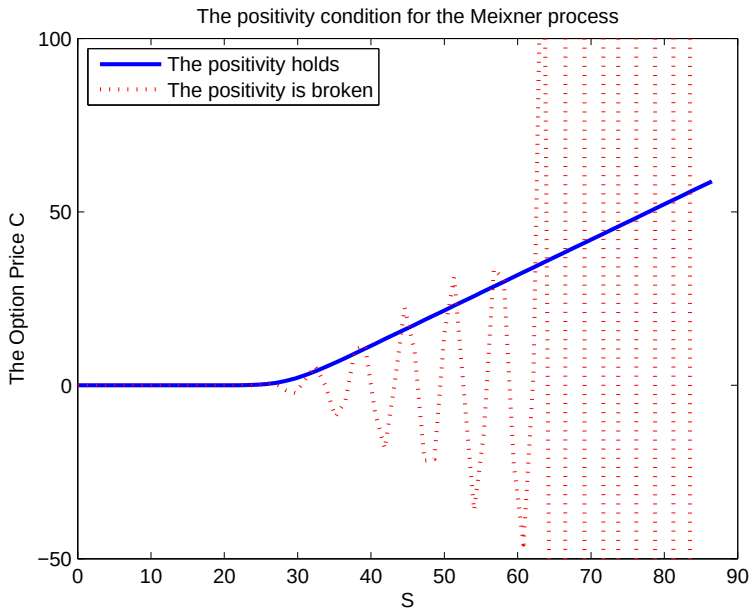

Figure 3.2: The positivity condition of the explicit scheme under Meixner process.

N_τ	S		
	8	10	12
20	-1.58e-2	-1.17e-2	-5.64e-3
40	-8.33e-3	-6.12e-3	-2.78e-3
80	-3.61e-3	-2.82e-3	-1.16e-3
160	-1.62e-3	-1.37e-3	-4.63e-4

Table 3.3: Computed negative values with the three-level method.

Example 3.2. Consider an European option under the **VG** process with parameters $E = 30$, $T = 0.5$, $r = 0.1$, $q = 0$, $\sigma = 0.25$, $C_- = C_+ = 11.718$, $\mathcal{G} = 15$ and $\mathcal{M} = 25$, $x_{\min} = 0$, $x_{\max} = 90$, $M = 15$, $\varepsilon = 0.35$. Table 3.4. reveals the variation of the absolute error (**AE**) as h changes as well as the spatial numerical convergence rate α and the CPU time while $N_\tau = 4.5e3$ for the explicit scheme 1 (3.24) and $N_\tau = 256$ for the three-level scheme 2 (3.73)-(3.74). The change of the error due to the variation of N_τ, its convergence rate β and the elapsed time are shown in Table 3.5 while $N_x = 128$.

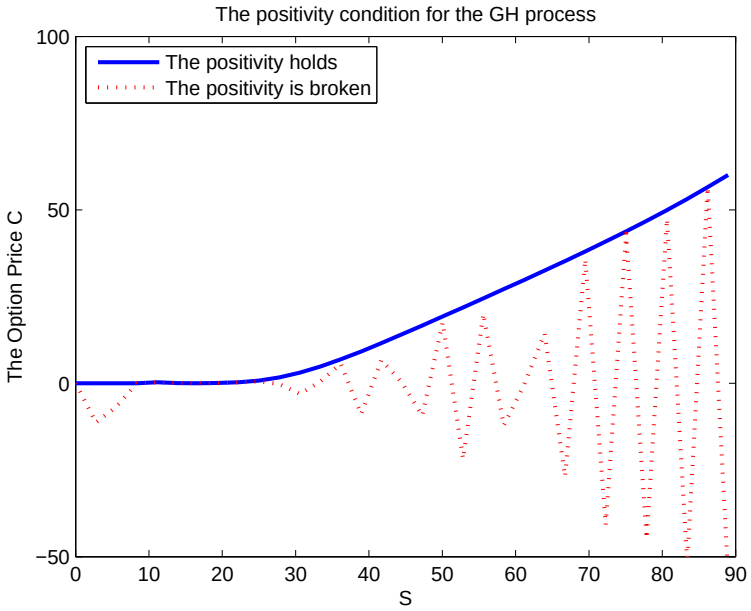

Figure 3.3: The effect of positivity condition on the option price under GH process.

	S	20		30		40		50		CPU
	N_x	**AE**	α	**AE**	α	**AE**	α	**AE**	α	in sec
Scheme 1	32	8.909e-4	–	1.926e-3	–	3.742e-3	–	4.386e-3	–	1.84
	64	2.409e-4	1.89	5.335e-4	1.85	1.022e-3	1.87	1.181e-3	1.89	4.63
	128	6.363e-5	1.92	1.413e-4	1.92	2.710e-4	1.91	3.053e-4	1.95	10.85
	256	1.552e-5	2.04	3.698e-5	1.93	6.952e-5	1.96	7.603e-5	2.01	18.99
Scheme 2	32	1.091e-3	–	1.477e-3	–	1.713e-3	–	4.873e-4	–	0.64
	64	2.861e-4	1.93	3.956e-4	1.89	4.238e-4	2.01	1.297e-4	1.91	1.31
	128	7.386e-5	1.95	1.043e-4	1.95	1.090e-4	1.96	3.340e-5	1.93	3.60
	256	1.783e-5	2.05	2.470e-5	2.08	2.550e-5	2.09	8.067e-6	2.07	8.29

Table 3.4: Errors and convergence rates for the VG model for several values of N_x.

The third example shows the variation of the root mean square relative error (**RMSRE**) as the size of grid points (N_x, N_τ) changes where

$$\textbf{RMSRE} = \sqrt{\frac{1}{5}\sum_{i=1}^{5}\left(\frac{\hat{\mathcal{C}}(S_i,T)-\mathcal{C}(S_i,T)}{\hat{\mathcal{C}}(S_i,T)}\right)^2}, \tag{3.75}$$

such that $\hat{\mathcal{C}}$ represents the reference value of the European option at $S = \{20, 30, 40, 50, 60\}$ calculated for a grid $(2048, 524288)$ and the option values are given in Table 3.6.

Example 3.3. Here an European option is priced under the three Lévy process classes with parameters $T = 0.5$, $E = 30$, $r = 0.1$, $q = 0$, $\sigma = 0.25$, $\varepsilon = 0.35$,

	S	20		30		40		50		CPU
	N_τ	**AE**	β	**AE**	β	**AE**	β	**AE**	β	in sec
Scheme 1	1.2e3	2.161e-4	–	4.790e-4	–	9.243e-4	–	1.151e-3	–	4.06
	2.4e3	1.154e-4	0.91	2.552e-4	0.89	4.883e-4	0.92	6.049e-4	0.93	7.28
	4.8e3	5.883e-5	0.97	1.304e-4	0.94	2.519e-4	0.95	3.072e-4	0.98	12.65
	9.6e3	2.916e-5	1.02	6.462e-5	0.96	1.288e-4	0.97	1.489e-5	1.04	20.37
Scheme 2	32	9.751e-4	–	1.661e-3	–	1.455e-3	–	4.807e-4	–	0.83
	64	5.046e-4	0.95	8.395e-4	0.98	7.325e-4	0.99	2.467e-4	0.96	1.46
	128	2.144e-4	1.23	3.215e-4	1.38	3.048e-4	1.26	9.843e-5	1.32	2.78
	256	7.386e-5	1.54	1.043e-4	1.62	1.090e-4	1.48	3.340e-5	1.53	3.60

Table 3.5: Errors and convergence rates for the VG model for various values of N_τ.

Model	S				
	20	30	40	50	60
CGMY	0.37224	4.82891	13.7801	24.05797	34.54281
Meixner	0.23802	2.11077	12.51470	23.74673	33.78861
GH	0.29120	2.46570	11.84807	22.08239	32.32227

Table 3.6: The reference European option values under Lévy processes.

$M = 15$, $x_{\min} = 0$, $x_{\max} = 90$ and the other parameters for Lévy models are listed in Table 3.7. The variation of the **RMSRE**, the ratio and the computational time with several grids for schemes 1 and 2 are given in Table 3.8.

Example 3.4. This example related to stability of scheme 1 is performed to plot the amplification factor G given by (3.31) for European options under Lévy models with the parameters given in Example 3.3 for $N_x = 256$ and $N_\tau = 6e3$ as shown in Fig 3.4 for $\theta \in [0, 2\pi]$. Also, the dependence of the local truncated error of the integral part given by (3.52) on the degree of Laguerre polynomial M is reported for several values of $\hat{\xi}$ in Table 3.9.

Example 3.5. Here, we deal with the LCP for American option under CGMY, Meixner and **GH** processes with parameters as in Example 3.3 while $q = 0.05$ solved

Model	Parameters
CGMY	$C = 0.5$, $G = 25$, $M = 25$ and $Y = 1.2$.
Meixner	$A = 0.3462$, $a = -3.7566$ and $b = 7.8994$.
GH	$\alpha = 3.8$, $\beta = -2.5$, $\delta = 0.2375$ and $\lambda = 2.755$

Table 3.7: The parameters for Lévy models used in Example 3.3.

	Model	CGMY			Meixner			**GH**		
	(N_x, N_τ)	**RMSRE**	Ratio	CPU (sec)	**RMSRE**	Ratio	CPU (sec)	**RMSRE**	Ratio	CPU (sec)
Scheme 1	(32,350)	3.633e-3	–	0.78	5.839e-4	–	0.57	7.013e-3	–	0.74
	(64,500)	1.392e-3	2.61	1.93	3.702e-4	1.58	1.43	1.964e-3	3.57	1.92
	(128,2.5e3)	2.545e-4	5.47	18.70	8.481e-5	4.36	13.64	4.699e-4	4.18	14.65
	(256,6e3)	8.079e-5	3.15	89.47	3.215e-5	2.64	65.10	1.227e-4	3.83	55.38
Scheme 2	(32,32)	2.116e-3	–	0.81	8.940e-4	–	0.47	6.910e-4	–	0.92
	(64,64)	8.932e-4	2.37	1.63	7.019e-4	1.27	0.86	6.008e-4	1.15	1.72
	(128,128)	2.617e-4	3.41	3.55	1.991e-4	3.52	2.38	1.727e-4	3.48	3.76
	(256,256)	5.536e-5	4.73	8.79	3.487e-5	5.71	3.87	6.718e-5	2.57	5.81

Table 3.8: Comparison of Scheme errors and CPU times for European option

		Errors		
M	$\hat{\xi}$	CGMY	Meixner	**GH** process
10	12.66	9.911e-5	1.026e-4	1.861e-6
	30.94	1.904e-4	5.752e-6	1.472e-5
	42.18	2.949e-5	3.733e-6	9.991e-6
20	12.66	1.391e-8	-5.649e-8	6.647e-9
	30.94	2.044e-11	7.172e-10	2.1726e-10
	42.18	-1.347e-11	-4.592e-10	-1.4934e-12
30	12.66	4.743e-15	-1.029e-14	1.168e-14
	30.94	-2.468e-17	1.163e-14	1.996e-18
	42.18	-1.819e-17	8.673e-15	1.475e-18

Table 3.9: The Truncated error for the integral part

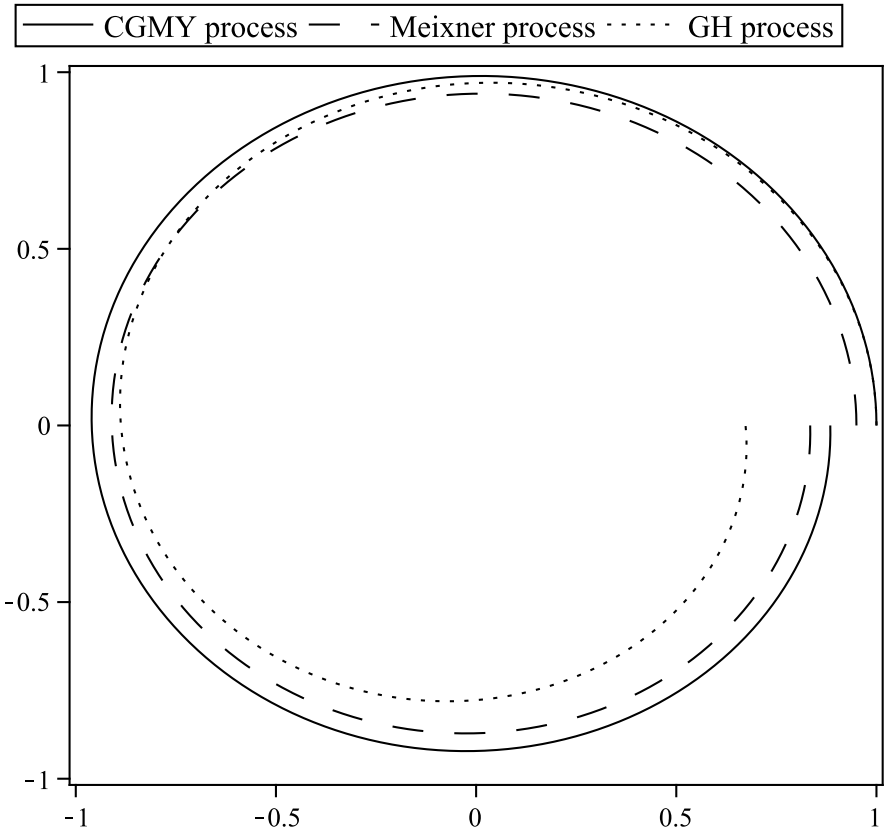

Figure 3.4: The amplification factor G under stability condition.

numerically using the scheme (3.67)-(3.70). Associated **RMSRE** is given in Table 3.10. The PSOR and MG are implemented to obtain numerical approximations, the comparison based on the accuracy and elapsed time are presented in Table 3.10. The reference values obtained for a grid $(2048, 524288)$ are listed in Table 3.11.

The results of this chapter has been submitted to Journal of Computational and Applied Mathematics.

	Model	CGMY			Meixner			**GH**		
	(N_x, N_τ)	**RMSRE**	Ratio	CPU (sec)	**RMSRE**	Ratio	CPU (sec)	**RMSRE**	Ratio	CPU (sec)
PSOR	(32,32)	2.362e-2	–	0.35	1.685e-2	–	0.19	3.548e-2	–	0.23
	(64,64)	6.775e-3	3.49	1.44	7.492e-3	4.91	0.95	9.832e-3	3.74	1.02
	(128,128)	1.403e-3	4.83	4.36	2.099e-3	3.57	3.84	1.860e-3	5.28	4.15
	(256,256)	3.727e-4	3.76	9.45	7.374e-4	2.85	8.74	8.112e-4	2.59	9.38
MG	(32,32)	1.527e-2	–	0.32	1.248e-2	–	0.19	2.394e-2	–	0.22
	(64,64)	4.421e-3	3.45	1.12	4.395e-3	2.83	0.72	9.643e-3	2.49	0.95
	(128,128)	8.0987e-4	5.46	2.13	8.052e-4	4.97	1.23	2.175e-3	4.43	2.96
	(256,256)	2.1532e-4	3.76	3.28	2.729e-4	3.24	2.93	6.173e-4	3.52	3.86

Table 3.10: The **RMSRE** for American option under Lévy processes

Model	S				
	20	30	40	50	60
CGMY	0.84963	6.74776	12.17171	22.94875	32.75316
Meixner	0.56471	4.35491	11.54473	21.24781	31.83748
GH	0.53621	5.17148	11.01960	20.75684	31.64827

Table 3.11: The reference American option values.

Chapter 4

Positive finite difference schemes for partial integro-differential option pricing Bates model

4.1 Introduction

The Bates model is considered one of the effective mathematical models that has ability to describe the behavior of real markets of options usually of complex types for instance, currency options. In Bates model, the Heston stochastic volatility model [44] and the Merton jump-diffusion model [63] are combined to describe the behavior of the underlying asset S and its variance ν [8]. These two variables are governed by the coupled stochastic differential equations:

$$dS(t) = (r - q - \lambda\xi)S(t)dt + \sqrt{\nu(t)}S(t)dW_1 + (\eta - 1)S(t)dZ(t),$$

$$d\nu(t) = \kappa(\theta - \nu(t))dt + \sigma\sqrt{\nu(t)}dW_2,$$

$$dW_1 dW_2 = \rho dt,$$

where W_1 and W_2 are standard Brownian motions, Z is the Poisson process. The parameter r is the risk free interest rate, q is the continuous dividend yield, λ is the jump intensity, κ is the mean reversion rate, θ is the long-run variance, σ is the volatility of the variance ν, ρ is the Wiener correlation parameter, η is the jump amplitude of the jump diffusion process and ξ is the expected relative jump size

($\xi = E[\eta - 1]$). By using Itô's lemma (1.4), and standard arbitrage arguments, one gets the partial integro-differential equation (PIDE) for the unknown option price $U(S, \nu, \tau)$ [8, 19]

$$\frac{\partial U}{\partial \tau} = \frac{1}{2}\nu S^2 \frac{\partial^2 U}{\partial S^2} + \rho\sigma\nu S \frac{\partial^2 U}{\partial S \partial \nu} + \frac{1}{2}\sigma^2 \nu \frac{\partial^2 U}{\partial \nu^2} + (r - q - \lambda\xi) S \frac{\partial U}{\partial S} + \kappa(\theta - \nu)\frac{\partial U}{\partial \nu} - (r + \lambda)U + \lambda \int_0^\infty U(S\eta, \nu, \tau) f(\eta) d\eta, \tag{4.1}$$

and the density function $f(\eta)$ is given by

$$f(\eta) = \frac{1}{\sqrt{2\pi}\hat{\sigma}\eta} \exp[-\frac{(\ln \eta - \mu)^2}{2\hat{\sigma}^2}], \tag{4.2}$$

where μ is the mean of the jump and $\hat{\sigma}$ is the standard deviation. For the European call option we consider the initial condition

$$U(S, \nu, 0) = g_1(S, \nu) = \max\{S - E, 0\}, \tag{4.3}$$

where E is the strike price. We assume the boundary conditions applied to the Heston model, see [29], but modified for $\nu = 0$ due to the additional integral term appearing in Bates model. For the boundaries $S = 0$ and $S \to \infty$ one gets

$$U(0, \nu, \tau) = 0, \tag{4.4}$$

$$\lim_{S \to \infty} \frac{\partial U}{\partial S}(S, \nu, \tau) = 1.$$

Note that this last condition means a linear behavior of the option price for large values of S with slope 1 when no dividend payments are considered, $q = 0$. Based on that fact, we replace it by the following condition, see [89, Chap. 3, p. 54]

$$U(S, \nu, \tau) = e^{-q\tau} S. \tag{4.5}$$

For $\nu \to \infty$ and $\nu = 0$, the corresponding boundary conditions are imposed as follows

$$\lim_{\nu \to \infty} U(S, \nu, \tau) = S, \tag{4.6}$$

$$\frac{\partial U}{\partial \tau}(S, 0, \tau) = (r - q - \lambda\xi) S \frac{\partial U}{\partial S}(S, 0, \tau) - (r + \lambda) U(S, 0, \tau) + \kappa\theta \frac{\partial U}{\partial \nu}(S, 0, \tau)$$

$$+\frac{\lambda}{\sqrt{2\pi}\hat{\sigma}}\int_0^{\infty} U(\varphi,0,\tau)\exp[-\frac{(\ln\varphi-\ln S-\hat{\mu})^2}{2\hat{\sigma}^2}]\frac{d\varphi}{\varphi}, \tag{4.7}$$

where $\varphi = S\eta$.

Some authors used an alternative boundary condition see [20, 30]. Chiarella *et. al.* [19] used the method of lines to solve the American call option problem for Bates model by discretizing with respect to time and variance variables obtaining a system of first order ordinary differential equations with two unknowns the price and its derivative with respect to asset variable. Then the system is solved using Riccati transformation, see [64]. Final discretization achieves a seven points stencil scheme treated using a linear complementarity problems (LCP). More recently [76] studies also the American call option problem under the Bates model using a full discretization for the spatial variable driving to a seven point finite difference stencil and the quadrature term is discretized using the quadrature rule based on piecewise linear interpolation. The authors use Rannacher scheme [72] for the time-stepping and the resulting LCP problem is solved using an iterative method.

The model (4.2)-(4.7) has two challenges from the numerical analysis point of view. Firstly, the presence of a mixed spatial derivative term involves the existence of negative coefficient terms into the numerical scheme deteriorating the quality of the numerical solution such as spurious oscillation and slow convergence, see the introduction of [90]. Secondly, the discretization of the improper integral part should be adequate with the bounded numerical domain and the incorporation of the initial and boundary conditions.
Dealing with prices, guaranty of the positivity of the solution is essential. In this chapter we construct an explicit difference scheme that guarantees positive solutions. We transform the PIDE (4.2) into a new PIDE without mixed spatial derivative before the discretization, following the idea of [22], and avoiding the above quoted drawbacks. Furthermore, this strategy has additional computational advantage of the reduction of the stencil scheme points, from nine [30, 32] or seven [19, 76] to just five.

The discrete treatment of the integral part is performed taking into account the chosen boundary numerical domain together with the boundary conditions and using a composite four points integration formula of open type because of the higher order

approximation of this rule [28, pp. 92-93].
The organization of this chapter is as follows. In Section 4.2 we transform the original problem into a new one without cross derivative term. We also construct the difference scheme including its matrix form that will be used in Section 4.3 to study positivity and stability. Section 4.4 is addressed to the study of consistency of the scheme. In Section 4.5, we consider the Bates model for American option using our finite difference scheme including the comparison with results of other authors. Numerical examples illustrating the results for Bates European and American option model are included in Section 4.6.

4.2 Problem Transformation and Scheme Construction

4.2.1 The transformation of the problem

We begin this section by eliminating the mixed spatial derivative term of (4.2), inspired by the reduction of second order linear partial differential equation in two independent variables to canonical form, see [39, Chap. 3] and [22] for details. Let us consider the following transformation

$$x = \tilde{\rho}\sigma \ln S;\ y = \rho\sigma \ln S - \nu;\ w(x, y, \tau) = e^{(r+\lambda)\tau} U(S, \nu, \tau), \tag{4.8}$$

where $\tilde{\rho} = \sqrt{1-\rho^2}$, $0 < |\rho| < 1$, obtaining the following transformed equation

$$\frac{\partial w}{\partial \tau} = \frac{\tilde{\rho}^2 \nu \sigma^2}{2}\Big(\frac{\partial^2 w}{\partial x^2} + \frac{\partial^2 w}{\partial y^2}\Big) + \hat{\delta}\frac{\partial w}{\partial x} + \tilde{\delta}\frac{\partial w}{\partial y} + I(w), \tag{4.9}$$

with

$$I(w) = \lambda \int_0^\infty w(x + \sigma\tilde{\rho} \ln \eta,\ y + \rho\sigma \ln \eta, \tau) f(\eta) d\eta, \tag{4.10}$$

where

$$\hat{\delta} = \sigma\tilde{\rho}(\hat{\xi} - \frac{\nu}{2}),\ \tilde{\delta} = \sigma\rho(\hat{\xi} - \frac{\nu}{2}) - \kappa(\theta - \nu) \text{ and } \hat{\xi} = r - q - \lambda\xi. \tag{4.11}$$

For the sake of convenience in the matching of the further discretization of the differential and integral parts of (4.9), we consider now the substitution

$$\phi = x + \sigma\tilde{\rho} \ln \eta. \tag{4.12}$$

Hence from (4.3) and (4.10) one gets

$$I(w) = \frac{\lambda}{\sqrt{2\pi}\hat{\sigma}\tilde{\rho}\sigma}\int_{-\infty}^{\infty} w(\phi, y + m(\phi - x), \tau)\exp\left[\frac{-1}{\hat{\sigma}^2}\left(\frac{\phi - x}{\sigma\tilde{\rho}} - \mu\right)^2\right]d\phi, \quad (4.13)$$

where $m = \frac{\rho}{\tilde{\rho}}$. Note that from (4.8), we have

$$y = mx - \nu. \quad (4.14)$$

The initial and boundary conditions (4.3)-(4.7) are transformed into the corresponding conditions using (4.8) and (4.12).

$$w(x, y, 0) = \max\{e^{\frac{x}{\sigma\tilde{\rho}}} - E, 0\}, \quad (4.15)$$

$$\lim_{x\to-\infty} w(x, y, \tau) = 0, \quad (4.16)$$

$$w(x, y, \tau) \approx \exp\left[\frac{x}{\sigma\tilde{\rho}} + (r - q + \lambda)\tau\right],\ x \to \infty, \quad (4.17)$$

$$w(x, y, \tau) \approx \exp\left[\frac{x}{\sigma\tilde{\rho}} + (r + \lambda)\tau\right],\ mx - y \to \infty, \quad (4.18)$$

$$\frac{\partial w}{\partial \tau} \approx \sigma\tilde{\rho}\hat{\xi}\frac{\partial w}{\partial x} + (\sigma\rho\hat{\xi} - \kappa\theta)\frac{\partial w}{\partial y}$$

$$+ \frac{\lambda}{\sqrt{2\pi}\hat{\sigma}\tilde{\rho}\sigma}\int_{-\infty}^{\infty} w(\phi, m\phi - \nu, \tau)\exp\left[\frac{-1}{\hat{\sigma}^2}\left(\frac{\phi - x}{\sigma\tilde{\rho}} - \mu\right)^2\right]d\phi,\ \nu \to 0. \quad (4.19)$$

From [35, 51] a suitable bound for the underlying asset variable S is available and generally accepted. In an analogous way, considering an admissible range of the variance ν, we can identify a convenient-bounded numerical domain $\mathcal{R} = [S_1, S_2] \times [\nu_1, \nu_2]$ in the $S - \nu$ plane. Under the transformation (4.8) as it is shown in [22] the rectangle $\mathcal{R}$ is transformed into the rhomboid $ABCD$ as shown in Fig 4.1 where the sides are given by

$$\begin{aligned}
\overline{AB} &= \{(x, y) \in \mathbb{R}^2 |\ a \le x \le b,\ y = mx - \nu_2\},\\
\overline{BC} &= \{(x, y) \in \mathbb{R}^2 |\ x = b,\ y = mb - \nu,\ \nu_1 \le \nu \le \nu_2\},\\
\overline{CD} &= \{(x, y) \in \mathbb{R}^2 |\ a \le x \le b,\ y = mx - \nu_1\},\\
\overline{DA} &= \{(x, y) \in \mathbb{R}^2 |\ x = a,\ y = ma - \nu,\ \nu_1 \le \nu \le \nu_2\},
\end{aligned} \quad (4.20)$$

where

$$a = \sigma\tilde{\rho}\ln S_1, \quad b = \sigma\tilde{\rho}\ln S_2. \quad (4.21)$$

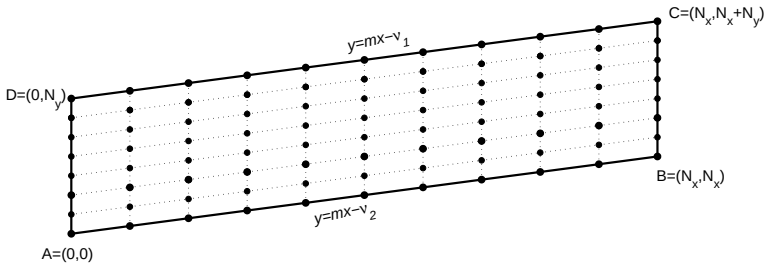

Figure 4.1: Rhomboid numerical domain $ABCD$

4.2.2 The numerical scheme

In light of the transformation (4.8) and the boundary given by (4.20), we use a discretization of the numerical domain where the space stepsizes $h = \Delta x$ and $h_y = \Delta y = |m|h$ are related by the slope $m = \frac{\rho}{\tilde{\rho}}$. Here we subdivide space-time axes into uniform spaced points using

$$\begin{aligned} x_i = a + ih,\ 0 \le i \le N_x, \qquad y_j = y_0 + j|m|h,\ i \le j \le N_y + i, \\ \nu_{i,j} = mx_i - y_j, \qquad \tau^n = nk,\ 0 \le n \le N_\tau, \end{aligned} \tag{4.22}$$

where $h = \frac{b-a}{N_x}$, $y_0 = ma - \nu_2$, $N_y = \frac{\nu_2 - \nu_1}{|m|h}$ and $k = \frac{T}{N_\tau}$. Note that any mesh point in the computational spatial domain has the form

$$(x_i, y_j) = (a + ih, mx_i - \nu_2 + (j - i)|m|h).$$

The discretization for the boundary points is given by

$$\begin{aligned} P(\overline{AB}) &= \{(x_i, y_i)|\ 0 \le i \le N_x\}, \\ P(\overline{BC}) &= \{(x_{N_x}, y_j)|\ N_x \le j \le N_x + N_y\}, \\ P(\overline{CD}) &= \{(x_i, y_{i+N_y})|\ 0 \le i \le N_x\}, \\ P(\overline{DA}) &= \{(x_0, y_j)|\ 0 \le j \le N_y\}. \end{aligned} \tag{4.23}$$

By denoting the approximate value of w at a representative mesh point $P(x_i, y_j, \tau^n)$ by $W^n_{i,j}$, we implement the center difference approximation for spatial partial deriva-

tives such that

$$\frac{\partial w}{\partial x} \approx \frac{W_{i+1,j}^n - W_{i-1,j}^n}{2h};\ \frac{\partial w}{\partial y} \approx \frac{W_{i,j+1}^n - W_{i,j-1}^n}{2|m|h}, \tag{4.24}$$

$$\frac{\partial^2 w}{\partial x^2} \approx \frac{W_{i+1,j}^n - 2W_{i,j}^n + W_{i-1,j}^n}{h^2};\ \frac{\partial^2 w}{\partial y^2} \approx \frac{W_{i,j+1}^n - 2W_{i,j}^n + W_{i,j-1}^n}{m^2h^2}, \tag{4.25}$$

and $\frac{\partial w}{\partial \tau}$ is discretized using the explicit forward approximation

$$\frac{\partial w}{\partial \tau} \approx \frac{W_{i,j}^{n+1} - W_{i,j}^n}{k}. \tag{4.26}$$

There are various kinds of approximations for the integration. The approximation is said to be of closed type if the integrand function is evaluated at the end points of the interval and it is of open type when these end points are omitted. The four point open type approximation derives its accuracy via extrapolating the integrand function based on four interior points and excluding the end points of each subinterval [28, pp. 92-93]. Furthermore, for functions whose derivatives have singularities at the end points, open type formulas are more efficient than the corresponding closed formulas. Based on this fact, the four points open type formula was used for CGMY model in Chapter 2 and now we use it again for Bates model. First, the improper integral $I(w)$ (4.13) is truncated into $[a, b]$, then the composite four points integration formula of open type has been implemented using the same step size for the variable x as in the differential part. Hence the corresponding finite difference equation for (4.9) is given by

$$W_{i,j}^{n+1} = \beta_{i,j} W_{i,j}^n + \hat{\alpha}_{i,j} W_{i+1,j}^n + \breve{\alpha}_{i,j} W_{i-1,j}^n + \alpha_{i,j} W_{i,j-1}^n + \gamma_{i,j} W_{i,j+1}^n + \hat{\lambda} J_{i,j}^n, \tag{4.27}$$

$$1 \le i \le N_x - 1,\ i+1 \le j \le N_y + i - 1,\ 0 \le n \le N_\tau - 1,$$

where

$$\begin{aligned}
\beta_{i,j} &= 1 - \tfrac{k\sigma^2}{h^2 m^2}\nu_{i,j} = (1 - \tfrac{k}{h^2}\tilde{a}_{ij}),\\
\hat{\alpha}_{i,j} &= \tfrac{k\sigma\tilde{\rho}}{2h}\left[\tfrac{(2\tilde{\rho}\sigma - h)}{2h}\nu_{i,j} + \hat{\xi}\right] = \tfrac{k}{h}(\tfrac{\rho^2}{2h}\tilde{a}_{ij} + \tilde{b}_{ij})\\
\breve{\alpha}_{i,j} &= \tfrac{k\sigma\tilde{\rho}}{2h}\left[\tfrac{(2\tilde{\rho}\sigma + h)}{2h}\nu_{i,j} - \hat{\xi}\right] = \tfrac{k}{h}(\tfrac{\rho^2}{2h}\tilde{a}_{ij} - \tilde{b}_{ij}),\\
\alpha_{i,j} &= \tfrac{k}{2|m|h}\left[\left(\tfrac{\sigma^2\tilde{\rho}^2}{|m|h} + \tfrac{\sigma\rho}{2} - \kappa\right)\nu_{i,j} - \sigma\rho\hat{\xi} + \kappa\theta\right] = \tfrac{k}{h}(\tfrac{\tilde{\rho}^2}{2h}\tilde{a}_{ij} - \tfrac{m}{|m|}\tilde{b}_{ij} + \tilde{c}_{ij}),\\
\gamma_{i,j} &= \tfrac{k}{2|m|h}\left[\left(\tfrac{\sigma^2\tilde{\rho}^2}{|m|h} - \tfrac{\sigma\rho}{2} + \kappa\right)\nu_{i,j} + \sigma\rho\hat{\xi} - \kappa\theta\right] = \tfrac{k}{h}(\tfrac{\tilde{\rho}^2}{2h}\tilde{a}_{ij} + \tfrac{m}{|m|}\tilde{b}_{ij} - \tilde{c}_{ij}),
\end{aligned} \tag{4.28}$$

$$\hat{\lambda} = \frac{5kh\lambda}{24\sqrt{2\pi}\hat{\sigma}\tilde{\rho}\sigma}, \tag{4.29}$$

and the integral part is given by

$$J_{i,j}^n = \sum_{\ell=0}^{N_x/5-1} \left(11 g_{i,5\ell+1} W_{5\ell+1,5\ell+1+j-i}^n + g_{i,5\ell+2} W_{5\ell+2,5\ell+2+j-i}^n \right.$$

$$\left. + g_{i,5\ell+3} W_{5\ell+3,5\ell+3+j-i}^n + 11 g_{i,5\ell+4} W_{5\ell+4,5\ell+4+j-i}^n \right), \tag{4.30}$$

assuming that N_x has been previously chosen as a multiple of 5. The weight function $g_{i,\ell}$ is given by

$$g_{i,\ell} \equiv g(x_i, \phi_\ell) = \exp\left[\frac{-1}{2\hat{\sigma}^2}\left(\frac{\phi_\ell - x_i}{\sigma\tilde{\rho}} - \mu\right)^2\right], \ 0 \le \ell \le N_x. \tag{4.31}$$

The initial condition (4.15) is discretized into

$$W_{i,j}^0 = \max\{\exp(\frac{x_i}{\sigma\tilde{\rho}}) - E, 0\}, \ 0 \le i \le N_x, \ i \le j \le N_y + i, \tag{4.32}$$

and the two Dirichlet conditions (4.16) along $\overline{AD}$ and (4.17) along $\overline{AB}$ take the forms

$$W_{0,j}^n = 0, \ 0 \le j \le N_y - 1, \ 1 \le n \le N_\tau, \tag{4.33}$$

$$W_{i,i}^n = \exp\left[\frac{x_i}{\sigma\tilde{\rho}} + (r+\lambda)\tau^n\right], \ 1 \le i \le N_x, \ 1 \le n \le N_\tau, \tag{4.34}$$

respectively. For the boundary condition along $\overline{BC}$, x is constant $x = b$ and from (4.17) one gets

$$W_{N_x,j}^n = \exp\left[\frac{b}{\sigma\tilde{\rho}} + (r+\lambda-q)\tau^n\right], \ N_x + 1 \le j \le N_x + N_y, \ 1 \le n \le N_\tau, \tag{4.35}$$

note that the boundary condition (4.19) along the oblique segment $\overline{CD}$ involves $\frac{\partial w}{\partial x}$ and $\frac{\partial w}{\partial y}$. By the way the spatial directional derivative of w for fixed τ along the direction $\overline{CD}$ with unitary vector $\hat{\mathbf{u}} = (\tilde{\rho}, \rho, 0)$ is given by

$$D_{\hat{\mathbf{u}}} w = \nabla w \cdot \hat{\mathbf{u}} = \tilde{\rho}\frac{\partial w}{\partial x} + \rho\frac{\partial w}{\partial y}.$$

The centered finite difference approximation for the directional derivative along CD at the mesh point $(x_i, y_{N_y+i}, \tau^n) \in P(\overline{CD})$ is given by

$$D_{\hat{\mathbf{u}}} w \approx \frac{\tilde{\rho}}{2h}(W^n_{i+1,N_y+i+1} - W^n_{i-1,N_y+i-1}), \tag{4.36}$$

and the backward difference approximation has been used for the term $\kappa\theta\frac{\partial w}{\partial y}$,

$$\kappa\theta\frac{\partial w}{\partial y} \approx \frac{\kappa\theta}{|m|h}(W^n_{i,N_y+i} - W^n_{i,N_y+i-1}), \tag{4.37}$$

while the integral part of (4.19) is approximated using four points open type formula. For the sake of positivity of the coefficients of the scheme, we take the following special approximation of the term $\frac{\partial w}{\partial \tau}$

$$\frac{\partial w}{\partial \tau} \approx \frac{1}{k}\left(W^{n+1}_{i,N_y+i} - \frac{1}{3}\left(W^n_{i-1,N_y+i-1} + W^n_{i,N_y+i} + W^n_{i+1,N_y+i+1}\right)\right). \tag{4.38}$$

From (4.36)-(4.38) the boundary condition (4.19) is approximated by

$$W^{n+1}_{i,N_y+i} = \hat{a}_1 W^n_{i-1,N_y+i-1} + \hat{a}_2 W^n_{i,N_y+i-1} + \hat{a}_3 W^n_{i,N_y+i} + \hat{a}_4 W^n_{i+1,N_y+i+1} + \hat{\lambda} J^n_{i,N_y+i}, \tag{4.39}$$

for $1 \le i \le N_x - 1$ and $0 \le n \le N_\tau - 1$, where

$$\hat{a}_1 = \frac{1}{3} - \frac{k\sigma\tilde{\rho}\hat{\xi}}{2h},\ \hat{a}_2 = \frac{k\kappa\theta}{|m|h},\ \hat{a}_3 = \frac{1}{3} - \hat{a}_2,\ \hat{a}_4 = \frac{1}{3} + \frac{k\sigma\tilde{\rho}\hat{\xi}}{2h}, \tag{4.40}$$

and J^n_{i,N_y+i} is obtained from (4.30) taking $j = N_y + i$.
In order to study the stability of the numerical scheme (4.27)-(4.40), let us write the numerical solution $W^n_{i,j}$ in a matrix form. Following the strategy of [84], let us define the vector $\mathbf{W}^n \in \mathbb{R}^{(N_x+1)(N_y+1)}$ such that

$$\mathbf{W}^n = \begin{bmatrix} \mathcal{W}^n_0 & \mathcal{W}^n_1 & \dots & \mathcal{W}^n_{N_x} \end{bmatrix}^T, \tag{4.41}$$

where $\mathcal{W}^n_i$ are vectors in $\mathbb{R}^{(N_y+1)}$

$$\mathcal{W}^n_i = \begin{bmatrix} W^n_{i,i} & W^n_{i,i+1} & \dots & W^n_{i,i+N_y} \end{bmatrix}.$$

Hence numerical scheme (4.30)-(4.40) can be written in a matrix form as

$$\mathbf{W}^{n+1} = (\mathcal{D} + \mathcal{P})\mathbf{W}^n,\ 0 \le n \le N_\tau - 1, \tag{4.42}$$

where $\mathcal{D}$ and $\mathcal{P}$ are square matrices of size $(N_x+1)(N_y+1)\times(N_x+1)(N_y+1)$ representing the discretization of the differential and integral parts of the scheme (4.30)-(4.40) respectively. The block matrix $\mathcal{D}$ can be written in the explicit form

$$\mathcal{D}=\begin{bmatrix} I & \Theta & \Theta & \Theta & \dots & \dots & \Theta \\ \breve{C}(1) & B(1) & \hat{C}(1) & \Theta & \dots & \dots & \Theta \\ \Theta & \breve{C}(2) & B(2) & \hat{C}(2) & \Theta & \dots & \Theta \\ \vdots & \Theta & \ddots & \ddots & \ddots & \vdots & \vdots \\ \vdots & \vdots & \dots & \dots & \breve{C}(N_x-1) & B(N_x-1) & \hat{C}(N_x-1) \\ \Theta & \Theta & \dots & \dots & \dots & \Theta & e^{(r-q+\lambda)k}I \end{bmatrix}, \tag{4.43}$$

where I and Θ are the identity and zero matrices in $\mathbb{R}^{(N_y+1)\times(N_y+1)}$. The block entries $\breve{C}(\ell),\ B(\ell)$ and $\hat{C}(\ell)$ are matrices $\in\mathbb{R}^{(N_y+1)\times(N_y+1)}$ such that

$$\breve{c}_{ij}(\ell)=\begin{cases} \breve{\alpha}_{\ell,\ell+i-1}, & i=2,\dots,N_y,\ j=i+1, \\ \hat{a}_1, & i=j=N_y+1, \\ 0, & \text{otherwise.} \end{cases} \tag{4.44}$$

$$b_{ij}(\ell)=\begin{cases} e^{(\lambda+r)k}, & i=j=1, \\ \alpha_{\ell,\ell+i-1}, & j=i-1,\ i=2,\dots,N_y, \\ \beta_{\ell,\ell+i-1}, & j=i,\ i=2,\dots,N_y, \\ \gamma_{\ell,\ell+i-1}, & j=i+1,\ i=2,\dots,N_y, \\ \hat{a}_2, & i=N_y+1,\ j=N_y, \\ \hat{a}_3, & i=j=N_y+1, \\ 0, & \text{otherwise.} \end{cases} \tag{4.45}$$

$$\hat{c}_{ij}(\ell)=\begin{cases} \hat{\alpha}_{\ell,\ell+i-1}, & i=2,\dots,N_y,\ j=i-1, \\ \hat{a}_4, & i=j=N_y+1, \\ 0, & \text{otherwise.} \end{cases} \tag{4.46}$$

With respect to the matrix $\mathcal{P}$, we denote its block entries by $\mathcal{P}_{\ell s}$ such that

$$\mathcal{P}_{\ell s}=\begin{cases} \Theta, & \ell=1 \text{ and } N_x+1, \text{ for } s=1,\dots,N_x+1, \\ P^{(s)}(\ell-1), & \ell=2,\dots,N_x,\ s=1,\dots,N_x+1, \end{cases} \tag{4.47}$$

where $P^{(s)}(\ell-1)$ are matrices in $\mathbb{R}^{(N_y+1)\times(N_y+1)}$ their elements are denoted by $P^s_{ij}(\ell-1)$. Note that from the periodic weight structure $(\{0,11,1,1,11,0,\dots\})$ of four points

open type formula (4.30), one gets

$$P^{(s)}(\ell-1)=\Theta,\ s=1,6,\ldots,N_x+1, \tag{4.48}$$

for $s=2,7,\ldots,N_x-3$ and $s=5,10,\ldots,N_x$, we have

$$P_{ij}^{(s)}(\ell-1)=\begin{cases} 11\hat{\lambda}g_{\ell-1,s-1}, & i=2,3,\ldots,N_y,N_y+1,\ i=j \\ 0, & \text{otherwise.}\end{cases} \tag{4.49}$$

Finally for $s=3,8,\ldots,N_x-2$ and $s=4,9,\ldots,N_x-1$,

$$P_{ij}^{(s)}(\ell-1)=\begin{cases} \hat{\lambda}g_{\ell-1,s-1}, & i=2,3,\ldots,N_y,N_y+1,\ i=j \\ 0, & \text{otherwise.}\end{cases} \tag{4.50}$$

Thus the matrix representation of the scheme (4.30)-(4.40) has been detailed in (4.42)-(4.50).

4.3 Numerical properties of the scheme

4.3.1 Positivity of the solution

We start this section by providing suitable conditions on the step sizes that guarantee the positivity of the numerical solution $\{W_{i,j}^n\}$ of scheme (4.27)-(4.40). First let us present the following lemma

lemma 3. *Let $f(z)=\frac{z}{|\alpha z+\beta|},\ z\in I=[z_1,z_2]$ and $\alpha\beta\neq 0$ then the minimum of $f(z)$ in $0<z_1\leq z\leq z_2$ is achieved in one of the extremum of I, i.e.,*

$$\min_{z\in I} f(z)=\min\left\{\frac{z_i}{|\alpha z_i+\beta|},\ i=1,2\right\}. \tag{4.51}$$

Proof. If $\alpha z+\beta\neq 0$ for all $z_1<z<z_2$, then $f(z)$ is a monotonic function, consequently (4.51) holds. Otherwise there exists a value $z_0=\frac{-\beta}{\alpha}$ such that $f(z)$ is increasing in $[z_1,z_0[$ and decreasing in $]z_0,z_2]$ and then (4.51) also holds true. □

Note that as $\nu_{i,j}$ defined in (4.22) satisfy $0<\nu_1\leq\nu_{i,j}\leq\nu_2$, the coefficient $\beta_{i,j}$ of (4.28) is nonnegative under the following condition

$$\frac{k}{h^2}<\frac{m^2}{\sigma^2\nu_2}. \tag{4.52}$$

Note also from (4.28) that coefficients $\hat{\alpha}_{i,j}$ and $\breve{\alpha}_{i,j}$ are simultaneously nonnegative provided that

$$|\tilde{b}_{ij}| \leq \frac{\rho^2}{2h}\tilde{a}_{ij}. \tag{4.53}$$

If $\tilde{b}_{ij} = 0$, then (4.53) holds for any value of the step size h. Otherwise (4.53) can be written in the following form

$$h \leq \frac{2\sigma\tilde{\rho}\nu_{i,j}}{|2\hat{\xi} - \nu_{i,j}|}, \tag{4.54}$$

and from lemma 1 for $z = \nu_{i,j}$, $\alpha = -1$ and $\beta = 2\hat{\xi}$, $z_i = \nu_i,\ i = 1, 2$, one gets that (4.54) is verified under condition

$$h \leq h_1 = \min\left\{ \frac{2\sigma\tilde{\rho}\nu_i}{|2\hat{\xi} - \nu_i|},\ i = 1, 2 \right\}. \tag{4.55}$$

Similarly, one guarantees the simultaneous positivity of the coefficients $\alpha_{i,j}$ and $\gamma_{i,j}$ under the condition

$$h \leq \frac{\tilde{\rho}^2\sigma^2\nu_{i,j}}{2m^2\left|\frac{|m|}{m}\tilde{b}_{ij} - \tilde{c}_{ij}\right|}. \tag{4.56}$$

From (4.28), we have

$$\frac{|m|}{m}\tilde{b}_{ij} - \tilde{c}_{ij} = \left(\frac{\kappa}{2|m|} - \frac{\sigma\rho}{4|m|}\right)\nu_{i,j} + \frac{\sigma\rho}{2|m|}\hat{\xi} - \frac{\kappa\theta}{2|m|} = \alpha\nu_{i,j} + \beta, \tag{4.57}$$

and from lemma 3, (4.56) holds true under the condition

$$h \leq h_2 = \min\left\{ \frac{\sigma^2\tilde{\rho}^2\nu_i}{2m^2|\alpha\nu_i + \beta|},\ i = 1, 2 \right\}, \tag{4.58}$$

where α and β are defined in (4.57). Then by incorporating the conditions (4.55) and (4.58) one gets

$$h \leq \min\{h_1, h_2\}. \tag{4.59}$$

To guarantee the positivity of the numerical solution on boundary of the domain, it is sufficient to put condition on the coefficients $\hat{a}_i$ of (4.39) defined in (4.40) in terms of h and k. This condition is

$$k \leq \min\left\{ \frac{2h}{3\sigma\tilde{\rho}|\hat{\xi}|},\ \frac{|m|h}{3\kappa\theta} \right\}. \tag{4.60}$$

The entries of matrix $\mathcal{P}$ are nonnegative since the coefficients of the integral part of the scheme given by (4.27) are nonnegative. On the other hand under conditions (4.52), (4.55), (4.58) and (4.60), the entries of matrix $\mathcal{D}$ are also nonnegative and then the following theorem is established.

Theorem 6. *With previous notation, if stepsizes h and k satisfy*

C1. $$h \leq \min\left\{ \frac{2\sigma\tilde{\rho}\nu_i}{|2\hat{\xi}-\nu_i|},\ \frac{\sigma^2\tilde{\rho}^2\nu_i}{2m^2|\alpha\nu_i+\beta|},\ i=1,2 \right\}$$

C2. $$k \leq \min\left\{ \frac{m^2h^2}{\sigma^2\nu_2},\ \frac{2h}{3\sigma\tilde{\rho}|\hat{\xi}|},\ \frac{|m|h}{3\kappa\theta} \right\},$$

then the numerical solution $\{W_{i,j}^n\}$ of the scheme (4.27)-(4.40) *is nonnegative.*

4.3.2 Stability of the scheme

Based on the stability definitions 8 and 9, we begin here by providing bounds for the infinite norm of $\mathcal{D}$ and $\mathcal{P}$. From (4.28) and (4.40), under the positivity conditions of theorem 6, we have

$$\alpha_{i,j} + \hat{\alpha}_{i,j} + \breve{\alpha}_{i,j} + \beta_{i,j} + \gamma_{i,j} = 1, \quad \sum_{s=1}^{4} \hat{a}_s = 1. \tag{4.61}$$

From (4.61) and the structure of matrices $\breve{\mathcal{C}}$, $\mathcal{B}$ and $\hat{\mathcal{C}}$, given by (4.44)-(4.46) it follows that

$$\|[\breve{C}(\ell)\ B(\ell)\ \hat{C}(\ell)]\|_\infty = \max\{e^{(\lambda+r)k}, 1\} = e^{(\lambda+r)k}. \tag{4.62}$$

From the definition of $\mathcal{D}$ (4.43)), property of infinite norm of the block matrices (1.13) and (4.62), one gets

$$\|\mathcal{D}\|_\infty = \max\left\{1,\ \max_{1\leq\ell\leq N_x-1}\left\{\|[\breve{C}(\ell)\ B(\ell)\ \hat{C}(\ell)]\|_\infty\right\},\ e^{(r-q+\lambda)k}\right\} = e^{(\lambda+r)k}. \tag{4.63}$$

In order to bound the norm of the matrix $\mathcal{P}$ (4.47)-(4.50), let i_m be the row that coincides with the infinite norm of $\mathcal{P}$, therefore

$$\|\mathcal{P}\|_\infty = \frac{5h\lambda k}{24\sqrt{2\pi}\hat{\sigma}\tilde{\rho}\sigma} \sum_{\ell=0}^{N_x/5-1} \left(11g_{i_m,5\ell+1} + g_{i_m,5\ell+2} + g_{i_m,5\ell+3} + 11g_{i_m,5\ell+4}\right). \tag{4.64}$$

Since the right hand side of (4.64) represents the approximation of

$$k\lambda I_1 = \frac{k\lambda}{\sqrt{2\pi}\hat{\sigma}\tilde{\rho}\sigma} \int_a^b g(x_{i_m}, \phi)d\phi,$$

see (4.31), its value is given by

$$k\lambda I_1 = \frac{k\lambda}{2}\left(\operatorname{erf}\left(\frac{x_{i_m} - a + \mu\sigma\tilde{\rho}}{\sqrt{2}\sigma\tilde{\rho}\hat{\sigma}}\right) - \operatorname{erf}\left(\frac{x_{i_m} - b + \mu\sigma\tilde{\rho}}{\sqrt{2}\sigma\tilde{\rho}\hat{\sigma}}\right)\right). \tag{4.65}$$

Then for small enough h, we have

$$\|\mathcal{P}\|_\infty < k\lambda(I_1 + 1) = k\lambda_1, \tag{4.66}$$

and from (4.41) it follows that

$$\|\mathbf{W}^n\|_\infty \leq (\|\mathcal{D}\|_\infty + \|\mathcal{P}\|_\infty)\|\mathbf{W}^{n-1}\|_\infty, \tag{4.67}$$

and from (4.64) and (4.65), one gets

$$\begin{aligned}\frac{\|\mathbf{W}^n\|_\infty}{\|\mathbf{W}^0\|_\infty} &\leq \left(e^{(r+\lambda)k} + k\lambda_1\right)^n = e^{(r+\lambda)T}\left(1 + k\lambda_1 e^{-(r+\lambda)k}\right)^n \\ &\leq e^{(r+\lambda)T}\left(1 + k\lambda_1\right)^n \leq \exp\left((r + \lambda + \lambda_1)T\right).\end{aligned} \tag{4.68}$$

Summarizing, according to definitions 8 and 9, a conditional strong uniform stable scheme is established.

4.4 Consistency

Let us denote the local truncation error $T^n_{i,j}(w)$ as

$$T^n_{i,j}(w) = F(W^n_{i,j}) - (L(w^n_{i,j}) - I(w^n_{i,j})), \tag{4.69}$$

where w is the exact theoretical solution for the PIDE (4.9), $(w^n_{i,j} = w(x_i, y_j, \tau^n))$, $F(W^n_{i,j}) = 0$ represent the approximating finite difference equation (4.27), $L(w)$ is the differential operator of (4.9) and $I(w)$ is the integral part given by (4.13). Based on the definition of consistency of [80] and [55], a numerical scheme is consistent with a PIDE if an exact theoretical solution of the PIDE approximates well the difference scheme as the stepsizes discretization tend to zero, i.e., the proposed scheme (4.27)-(4.40) is consistent with the PIDE (4.9) if $T^n_{i,j} \to 0$ as $h \to 0$, $h_y \to 0$ and $k \to 0$.
Let w be a continuous function of x, y and τ with continuous derivatives of order four with respect to x and y and of order two with respect to τ. By using Taylor

expansion about (x_i, y_j, τ^n), we have

$$\frac{w_{i,j}^{n+1} - w_{i,j}^n}{k} = \frac{\partial w}{\partial \tau}(x_i, y_j, \tau^n) + kE_{i,j}^n(1), \tag{4.70}$$

where

$$E_{i,j}^n(1) = \frac{1}{2}\frac{\partial^2 w}{\partial \tau^2}(x_i, y_j, \chi),\ nk < \chi < (n+1)k,$$

$$\left|E_{i,j}^n(1)\right| \leq \frac{1}{2}\max\left\{\left|\frac{\partial^2 w}{\partial \tau^2}(x_i, y_j, \tau)\right|,\ \tau^n \leq \tau \leq \tau^{n+1}\right\} = \frac{1}{2}D^n(1). \tag{4.71}$$

For the second partial derivatives with respect to the spatial variables x and y, the Taylor's expansions are given by

$$\frac{w_{i+1,j}^n - 2w_{i,j}^n + w_{i-1,j}^n}{h^2} = \frac{\partial^2 w}{\partial x^2}(x_i, y_j, \tau^n) + h^2 E_{i,j}^n(2), \tag{4.72}$$

$$E_{i,j}^n(2) = \frac{1}{12}\frac{\partial^4 w}{\partial x^4}(\chi_1, y_j, \tau^n),\ x_i - h < \chi_1 < x_i + h,$$

$$\left|E_{i,j}^n(2)\right| \leq \frac{1}{12}\max\left\{\left|\frac{\partial^4 w}{\partial x^4}(x, y_j, \tau^n)\right|,\ a \leq x \leq b\right\} = \frac{1}{12}D_j^n(2), \tag{4.73}$$

and

$$\frac{w_{i,j+1}^n - 2w_{i,j}^n + w_{i,j-1}^n}{h_y^2} = \frac{\partial^2 w}{\partial y^2}(x_i, y_j, \tau^n) + h_y^2 E_{i,j}^n(3), \tag{4.74}$$

$$E_{i,j}^n(3) = \frac{1}{12}\frac{\partial^4 w}{\partial y^4}(x_i, \chi_2, \tau^n),\ y_j - h_y < \chi_2 < y_j + h_y,$$

$$\left|E_{i,j}^n(3)\right| \leq \frac{1}{12}\max\left\{\left|\frac{\partial^4 w}{\partial y^4}(x_i, y, \tau^n)\right|,\ mx_i - \nu_2 \leq y \leq mx_i - \nu_1\right\} = \frac{1}{12}D_i^n(3). \tag{4.75}$$

The expansions for the first partial derivatives with respect to x and y are given by

$$\frac{w_{i+1,j}^n - w_{i-1,j}^n}{2h} = \frac{\partial w}{\partial x}(x_i, y_j, \tau^n) + h^2 E_{i,j}^n(4), \tag{4.76}$$

$$E_{i,j}^n(4) = \frac{1}{6}\frac{\partial^3 w}{\partial x^3}(\chi_3, y_j, \tau^n),\ x_i - h < \chi_3 < x_i + h,$$

$$\left|E_{i,j}^n(4)\right| \leq \frac{1}{6}\max\left\{\left|\frac{\partial^3 w}{\partial x^3}(x, y_j, \tau^n)\right|,\ a \leq x \leq b\right\} = \frac{1}{6}D_j^n(4) \tag{4.77}$$

$$\frac{w_{i,j+1}^n - w_{i,j-1}^n}{2h_y} = \frac{\partial w}{\partial x}(x_i, y_j, \tau^n) + h_y^2 E_{i,j}^n(5), \tag{4.78}$$

$$E_{i,j}^n(5) = \frac{1}{6}\frac{\partial^3 w}{\partial y^3}(x_i, \chi_4, \tau^n),\ y_j - h_y < \chi_4 < y_j + h_y,$$
$$\left|E_{i,j}^n(5)\right| \leq \frac{1}{6}\max\left\{\left|\frac{\partial^3 w}{\partial y^3}(x_i, y, \tau^n)\right|,\ mx_i - \nu_2 \leq y \leq mx_i - \nu_1\right\} = \frac{1}{6}D_i^n(5). \tag{4.79}$$

On the other hand for the integral part, there are two error sources; the first coming from the truncation of improper integral into a bounded one (a, b) and the second coming from the numerical approximation of the finite integral using the four point open type formula. Let $\mathcal{T}_{i,j}^n(w)$ denote the total truncation error for the integral part such that

$$\begin{aligned}\mathcal{T}_{i,j}^n(w) = I(w_{i,j}^n) - \hat{\lambda}J_{i,j}^n &= (I(w_{i,j}^n) - I_{ab}(w_{i,j}^n)) + (I_{ab}(w_{i,j}^n) - \hat{\lambda}J_{i,j}^n) \\ &= \mathcal{H}_{i,j}^n(w) + \mathcal{Y}_{i,j}^n(w)\end{aligned} \tag{4.80}$$

where $I_{ab}(w) = \frac{\lambda}{\sqrt{2\pi}\hat{\sigma}\tilde{\rho}\sigma}\int_a^b g(x,\phi)w(x, y+m(\phi-x), \tau)d\phi$, the truncation error $\mathcal{H}_{i,j}^n(w) = I(w) - I_{ab}(w)$ and the error due to the numerical integration $\mathcal{Y}_{i,j}^n(w) = I_{ab}(w) - \hat{\lambda}J_{i,j}^n$. According to Briani *et. al.* [12], since the integral part contains the Gaussian function, then the absolute value of $\mathcal{H}_{i,j}^n(w)$ can be controlled using a tolerance parameter error $\varepsilon > 0$ by choosing

$$b = \sqrt{-2\hat{\sigma}^2\ln(\varepsilon\hat{\sigma}\sqrt{2\pi})},\ a = -b. \tag{4.81}$$

Furthermore, due to the symmetric property of the probability measure of Gaussian distribution, one can assume that the option price w satisfies the Lipschitz condition with respect to the spacial variables, then one has [12],

$$\left|\mathcal{H}_{i,j}^n(w)\right| < 2\hat{\sigma}^2\varepsilon. \tag{4.82}$$

Finally, from [28, p. 95],

$$\left|\mathcal{Y}_{i,j}^n(w)\right| \leq \frac{90h^4}{144}D_{i,j}^n(6), \tag{4.83}$$

where

$$D_{i,j}^n(6) = \max\left\{\left(w(\phi, y_j + m(\phi - x_i), \tau^n)\right)^{(4)},\ a \leq \phi \leq b\right\}, \tag{4.84}$$

and the fourth derivative of the function $w(\phi, y_j + m(\phi - x_i), \tau^n)$ is taken with respect to ϕ. Hence the total error for the integral part $|\mathcal{T}_{i,j}^n|$ satisfies

$$\left|\mathcal{T}_{i,j}^n\right| < 2\hat{\sigma}^2\varepsilon + \frac{90h^4}{144}D_{i,j}^n(6). \tag{4.85}$$

From (4.70), (4.72), (4.74), (4.76), (4.78), (4.80) and (4.69), the local truncation error has the following form

$$T_{i,j}^n = kE_{i,j}^n(1) - \frac{\tilde{\rho}^2\nu_{i,j}\sigma^2}{2}\left(h^2E_{i,j}^n(2) + m^2h^2E_{i,j}^n(3)\right) - \hat{\delta}_{i,j}h^2E_{i,j}^n(4)$$
$$- \tilde{\delta}_{i,j}m^2h^2E_{i,j}^n(5) - \mathcal{T}_{i,j}^n(w), \tag{4.86}$$

where $\hat{\delta}_{i,j}$ and $\tilde{\delta}_{i,j}$ correspond to expressions appearing in (4.11) when replacing ν by $\nu_{i,j}$. Finally, from (4.71), (4.73), (4.75), (4.77), (4.79), (4.85) and (4.86), we have

$$\left|T_{i,j}^n\right| \leq \frac{k}{2}D^n(1) + \left|\frac{\tilde{\rho}^2\nu_{i,j}\sigma^2}{24}\right|\left(D_j^n(2) + m^2D_i^n(3)\right)h^2 + \left(|\hat{\delta}_{i,j}|D_j^n(4) + m^2|\tilde{\delta}_{i,j}|D_i^n(5)\right)\frac{h^2}{6}$$
$$+ \frac{90h^4}{144}D_{i,j}^n(6) + 2\hat{\sigma}^2\varepsilon, \tag{4.87}$$

Therefore

$$\left|T_{i,j}^n\right| \leq \mathcal{O}(k) + \mathcal{O}(h^2) + \mathcal{O}(\varepsilon). \tag{4.88}$$

Summarizing, the consistency for the scheme is established.

4.5 Numerical solution of PIDE American option pricing under Bates model

In this section, the American option under Bates model is studied. The linear complementarity problem for this model is given

$$L(U) \geq 0,\ U \geq g_1,\ L(U)(U - g_1) = 0, \tag{4.89}$$

where

$$L(U) = \frac{\partial U}{\partial \tau} - \frac{1}{2}\nu S^2\frac{\partial^2 U}{\partial S^2} - \rho\sigma\nu S\frac{\partial^2 U}{\partial S\partial\nu} - \frac{1}{2}\nu\sigma^2\frac{\partial^2 U}{\partial\nu^2} - (r - q - \lambda\xi)S\frac{\partial U}{\partial S}$$
$$- \kappa(\theta - \nu)\frac{\partial U}{\partial\nu} + (r + \lambda)U - \lambda\int_0^\infty U(S\eta, \nu, \tau)f(\eta)d\eta = 0, \tag{4.90}$$

associated with the following boundary conditions

$$U(0, \nu, \tau) = g_1(0, \nu),\ \lim_{S\to\infty}U(S, \nu, \tau) = \lim_{S\to\infty}g_1(S, \nu),\ \lim_{\nu\to\infty}\frac{\partial U}{\partial\nu}(S, \nu, \tau) = 0. \tag{4.91}$$

By applying the transformation (4.8), we have

$$\mathcal{L}(w) = \frac{\partial w}{\partial \tau} - D(w) - I(w) \geq 0,\ w \geq g_2,\ \mathcal{L}(w)(w - g_2) = 0, \tag{4.92}$$

where,

$$D \equiv \frac{\tilde{\rho}^2 \nu \sigma^2}{2}\big(\frac{\partial^2}{\partial x^2} + \frac{\partial^2}{\partial y^2}\big) + \hat{\delta}\frac{\partial}{\partial x} + \tilde{\delta}\frac{\partial}{\partial y}, \tag{4.93}$$

$I(w)$ is given by (4.8) and

$$w(x, y) = g_2(x, y) = \max\{e^{\frac{x}{\sigma\tilde{\rho}}} - E, 0\}.$$

4.5.1 Numerical scheme construction

Here the rhomboid computational domain is discretized by a uniform mesh points (x_i, y_j) such that $x_i = a + ih,\ 0 \leq i \leq N_x$ and $y_j = y_0 + j|m|h,\ i \leq j \leq N_x + i$ where $h = (b-a)/N_x$, $y_0 = ma - \nu_2$ and $N_y = (\nu_2 - \nu_1)/|m|h$. The first and second derivatives of the spatial variables of the operator D are discretized using the central finite difference approximation as follow

$$\begin{array}{ll} \frac{\partial w}{\partial x} \approx \frac{W_{i+1,j} - W_{i-1,j}}{2h} & \frac{\partial w}{\partial y} \approx \frac{W_{i,j+1} - W_{i,j-1}}{2|m|h} \\ \frac{\partial^2 w}{\partial x^2} \approx \frac{W_{i+1,j} - 2W_{i,j} + W_{i-1,j}}{h^2} & \frac{\partial^2 w}{\partial y^2} \approx \frac{W_{i,j+1} - 2W_{i,j} + V_{i,j-1}}{m^2 h^2}. \end{array} \tag{4.94}$$

Thus the discretization of the differential operator is given by

$$D(W_{i,j}) \approx \breve{B}(i,j)W_{i-1,j} + \breve{C}(i,j)W_{i,j-1} - B(i,j)W_{i,j} + \hat{B}(i,j)W_{i+1,j} + \hat{C}(i,j)W_{i,j+1}, \tag{4.95}$$

where

$$\begin{array}{l} \breve{B}(i,j) = \left(\frac{\tilde{\rho}^2\sigma^2\nu_{i,j}}{2h^2} - \frac{\hat{\delta}_{i,j}}{2h}\right),\ B(i,j) = \frac{\sigma^2\nu_{i,j}}{m^2h^2},\ \hat{B}(i,j) = \left(\frac{\tilde{\rho}^2\sigma^2\nu_{i,j}}{2h^2} + \frac{\hat{\delta}_{i,j}}{2h}\right) \\ \breve{C}(i,j) = \left(\frac{\tilde{\rho}^2\sigma^2\nu_{i,j}}{2m^2h^2} - \frac{\tilde{\delta}_{i,j}}{2|m|h}\right),\ \hat{C}(i,j) = \left(\frac{\tilde{\rho}^2\sigma^2\nu_{i,j}}{2m^2h^2} + \frac{\tilde{\delta}_{i,j}}{2|m|h}\right), \end{array} \tag{4.96}$$

$\hat{\delta}_{ij}$ and $\tilde{\delta}_{ij}$ are obtained from (4.11) by replacing ν with $\nu_{i,j}$. It is worth mention that based on the foregoing transformation (4.8) we obtain a five point discretization stencil for the spatial differential operator D which leads to minimize the computational cost. Moreover, there is no restriction on the correlation parameter ρ.
The discretization of the integral part has been done as the same as in (4.30). The difference here is that the discretization for the time variable is not performed yet, hence we have

$$I(w) \approx \tilde{\lambda} J_{i,j}, \quad \tilde{\lambda} = \frac{5h\lambda}{24\sqrt{2\pi}\hat{\sigma}\tilde{\rho}\sigma}, \tag{4.97}$$

where $J_{i,j}$ is obtained from (4.30) by eliminating the index n.
Hence we have the following semi-discrete LCP

$$\frac{\partial \mathbf{W}}{\partial \tau} + \mathcal{A}\mathbf{W} \geq 0,\ \mathbf{W} \geq \mathbf{g_2},\ (\frac{\partial \mathbf{W}}{\partial \tau} + \mathcal{A}\mathbf{W})^T(\mathbf{W} - \mathbf{g_2}) = 0, \tag{4.98}$$

where $\mathcal{A}$ is a matrix of size $(N_x + 1)(N_y + 1) \times (N_x + 1)(N_y + 1)$ involving the differential and integral parts.
The time variable τ is discretized using nonuniform mesh points given by (4.99) and the first derivative of $\mathbf{W}$ with respect to τ is approximated using the Rannacher scheme [72]; such that the first four time levels are implemented using the implicit Euler while the rest of the time levels are obtained using Crank-Nicolson. The aim of this discretization is to avoid the oscillation of the solution, see [86].

$$\tau^n = \begin{cases} (\frac{n}{2N_\tau})^2 T, & n = 0, 1, 2, 3, \\ (\frac{n-2}{N_\tau - 2})^2 T, & n = 4, 5, \ldots, N_\tau. \end{cases} \tag{4.99}$$

Based on Rannacher scheme, we have the following LCPs

$$LCP(\tilde{\mathcal{A}}^{(n+1)}, \mathbf{W}^{(n+1)}, \tilde{\mathbf{W}}^{(n+1)}, \mathbf{g_2}), \tag{4.100}$$

where

$$\left.\begin{aligned} \tilde{\mathcal{A}}^{(n+1)} &= \begin{cases} I + k_n\mathcal{A} & n = 0, 1, 2, 3, \\ I + \frac{1}{2}k_n\mathcal{A} & n = 4, 5, \ldots, N_\tau - 1, \end{cases}, \\ \tilde{\mathbf{W}}^{(n+1)} &= \begin{cases} \mathbf{W}^{(n)} & n = 0, 1, 2, 3, \\ (I - \frac{1}{2}k_n\mathcal{A})\mathbf{W}^{(n)} & n = 4, 5, \ldots, N_\tau - 1. \end{cases} \end{aligned}\right\} \tag{4.101}$$

4.6 Numerical Examples

After removing the mixed derivative of the PIDE (4.2) for Bates model, a finite difference scheme has been constructed to obtain a numerical approximation for the option price. Furthermore, the positivity conditions are provided, also stability and consistency have been studied. In this section, several examples are provided to study the behavior of the option price obtained by the proposed scheme using Matlab.

The following example reveals the importance of the positivity conditions (4.59) and (4.60) on the stepsizes h and k.

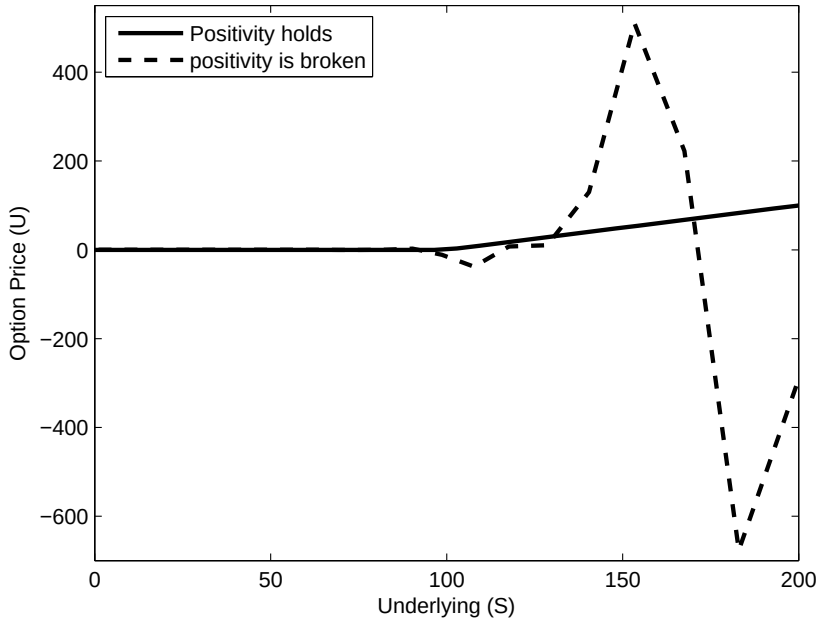

Figure 4.2: The effect of positivity conditions on the option price U

Example 4.1. Consider an European call option under Bates model with the following parameters $T = 0.5$, $E = 100$, $r = 0.05$, $q = 0$, $\theta = 0.05$, $\kappa = 2.5$, $\sigma = 0.25$, $\hat{\sigma} = 0.7$, $\mu = 0.5$, $\lambda = 0.2$, $\nu_1 = 0.1$, $\nu_2 = 1$ and $\rho = -0.5$ with a tolerance error $\varepsilon = 10^{-3}$. In Figure 4.2, the solid curve represents the option price as a function of the underlying asset S when the positivity conditions hold for $(N_x, N_y, N_\tau) = (100, 45, 150)$ corresponding to $h = 0.05$ and $k = 0.0033$, while the dashed curve represents the option price when the positivity conditions are broken for $(N_x, N_y, N_\tau) = (100, 45, 50)$ corresponding to $h = 0.05$ and $k = 0.01$.

The next example investigates the associated error for the scheme (4.27)-((4.40) when $\lambda = 0$, i.e., for European option under Heston model. Considering the strike price $E = 100$, the numerical solutions for the set of underlying assets $\mathcal{S} = \{80, 90, 100, 110, 120\}$ are obtained. In order to evaluate the error, a Matlab code for the closed form solution is used [70] obtaining the set of corresponding reference option price values $\mathcal{U} = \{0.207581, 4.889877, 10.488226, 16.503506, 22.856611\}$. The root mean square relative error (**RMSRE**) is calculated based on the equation

$$\mathbf{RMSRE} = \sqrt{\frac{1}{5}\sum_{i=1}^{5}\left(\frac{\mathcal{U}(\mathcal{S}_i, \nu_0, T) - U(\mathcal{S}_i, \nu_0, T)}{\mathcal{U}(\mathcal{S}_i, \nu_0, T)}\right)^2}, \tag{4.102}$$

N_τ	**RMSRE**	Ratio	CPU (sec)
200	1.764×10^{-3}	–	1.01
400	9.387×10^{-4}	1.88	1.05
800	4.581×10^{-4}	2.05	1.17
1600	2.371×10^{-4}	1.93	1.19
3200	1.191×10^{-4}	1.99	1.32

Table 4.1: The associated **RMSRE** for several values of N_τ.

(N_x, N_y)	**RMSRE**	Ratio	CPU (sec)
$(40, 9)$	4.166×10^{-3}	–	0.11
$(60, 14)$	2.986×10^{-3}	1.395	0.71
$(80, 18)$	9.367×10^{-4}	3.188	2.52
$(100, 23)$	3.861×10^{-4}	2.426	7.476
$(120, 27)$	9.287×10^{-5}	4.157	19.53

Table 4.2: The **RMSRE** for different values of (N_x, N_y).

where $U(\mathcal{S}_i, \nu_0, T)$ is the numerical solution at spot variance $\nu_0 = 0.4$.

Example 4.2. Here the parameters are chosen as follows $T = 0.5$, $E = 100$, $r = 0.05$, $q = 0$, $\theta = 0.05$, $\kappa = 2$, $\sigma = 0.3$, and $\rho = -0.5$. The computational domain is $[a, b] = [-0.5, 1.5]$, $\nu_1 = 0.1$ and $\nu_2 = 1$. Table 4.1 exhibits the variation of **RMSRE** for several values of N_τ while $N_x = 70$ and $N_y = 16$, the numerical order of error and CPU time in seconds.

In Table 4.2, the variation of the error due to the change of the spatial step sizes, while $N_\tau = 500$ has been studied.

The aim of the last example is to study the variation of the resultant error for European option under Bates model.

Example 4.3. The parameters are selected as follows $T = 0.5$, $E = 100$, $r = 0.05$, $q = 0$, $\theta = 0.05$, $\kappa = 2.0$, $\sigma = 0.3$, $\hat{\sigma} = 0.35$, $\mu = -0.5$, $\lambda = 0.2$ and $\rho = -0.5$ with a tolerance error $\varepsilon = 10^{-4}$. The boundary points a and b of the spatial computational domain are obtained from (4.81), while $\nu_1 = 0.1$ and $\nu_2 = 1$. Table 4.3 shows the variation of the **RMSRE** for several values of the time step sizes, for fixed $N_x = 70$ and $N_y = 35$, with respect to reference values computed at $(N_x, N_y, N_\tau) = (500, 146, 7000)$.

N_τ	**RMSRE**	Ratio	CPU (sec)
500	2.485×10^{-3}	–	6.66
1000	1.322×10^{-3}	1.88	6.94
2000	6.429×10^{-4}	2.06	7.28
4000	3.296×10^{-4}	1.95	7.69
8000	1.569×10^{-4}	2.10	7.91

Table 4.3: The **RMSRE** for several values of N_τ.

(N_x, N_y)	**RMSRE**	Ratio	CPU (sec)
$(40, 20)$	1.526×10^{-2}	–	0.32
$(60, 30)$	3.459×10^{-3}	4.412	1.83
$(80, 40)$	9.271×10^{-4}	3.371	6.95
$(100, 50)$	3.589×10^{-4}	2.583	19.64
$(120, 60)$	8.473×10^{-5}	4.236	46.72

Table 4.4: The associated **RMSRE** for different values of (N_x, N_y).

The variation of error due to the change of the spatial step sizes, while $N_\tau = 500$ has been presented in Table 4.4.

The aim of the next two examples is to obtain the value of American option under Bates model by solving (4.100) using the PSOR method with relaxation parameter $\omega = 1.5$ and also using MG.

Example 4.4. Consider an American call option under Bates model with the following parameters $T = 0.5$, $E = 100$, $r = 0.03$, $q = 0.05$, $\theta = 0.04$, $\kappa = 2$, $\sigma = 0.25$, $\hat{\sigma} = 0.4$, $\mu = -0.5$, $\lambda = 0.2$ and $\rho = -0.5$, the computational domain for $x \in [a, b]$, where a and b are obtained by (4.81) and $[\nu_1, \nu_2] = [0.1, 1]$. Table 4.5 shows the variation of the root mean square relative error (RMSRE) of the option value at $S = \{80, 90, 100, 110, 120\}$ for several values of domain discretizations (N_x, N_y, N_τ). The reference values for the prices U are given in [86].

Method	PSOR			MG		
(N_x, N_y, N_τ)	**RMSRE**	Ratio	CPU(s)	**RMSRE**	Ratio	CPU(s)
$(25, 15, 10)$	1.38×10^{-1}	–	0.024	1.23×10^{-1}	–	0.008
$(50, 28, 25)$	5.71×10^{-2}	2.41	0.185	5.21×10^{-2}	2.63	0.07
$(100, 55, 50)$	1.03×10^{-2}	5.53	5.60	9.84×10^{-3}	5.29	1.48
$(125, 69, 75)$	6.80×10^{-3}	1.51	17.08	3.09×10^{-3}	3.18	4.37
$(150, 82, 75)$	3.30×10^{-3}	2.04	51.74	9.24×10^{-4}	3.34	12.25

Table 4.5: Comparison of Scheme errors and CPU times for American option when $\rho = -0.5$.

Method		PSOR			MG	
(N_x, N_y, N_τ)	**RMSRE**	Ratio	CPU(s)	**RMSRE**	Ratio	CPU(s)
$(25, 53, 10)$	1.41×10^{-1}	–	0.24	8.74×10^{-2}	–	0.19
$(40, 85, 25)$	6.87×10^{-2}	2.05	3.56	2.68×10^{-2}	3.26	2.78
$(60, 162, 50)$	1.36×10^{-2}	5.07	57.42	4.57×10^{-3}	5.86	16.25
$(80, 216, 75)$	7.81×10^{-3}	1.74	200.73	1.06×10^{-3}	4.29	22.73
$(100, 270, 100)$	4.23×10^{-3}	1.85	415.26	2.02×10^{-4}	5.28	32.47

Table 4.6: Comparison of Scheme errors and CPU times for American option when $\rho = 0.5$.

Example 4.5. The parameters for an American call option under Bates model are selected as follow $T = 0.5$, $E = 100$, $r = 0.03$, $q = 0.05$, $\theta = 0.04$, $\kappa = 2$, $\sigma = 0.4$, $\hat{\sigma} = 0.1$, $\mu = 0$, $\lambda = 5$ and $\rho = 0.5$ with a tolerance error $\varepsilon = 10^{-4}$. The reference values are in [19], Table 4.6 reveals the associated RMSRE, ratio and CPU time for several step sizes discretization.

Results concerning to the stochastic-volatility Heston model, i.e., particular case of (4.1) with $\lambda = 0$, have been published in [22]. Results related to the Bates model developed in this chapter have been published in [37].

Conclusions

Numerical techniques for PIDEs governing option pricing under Lévy models have been proposed showing two main innovative improvements. First using suitable transformation to eliminate the reaction and convection terms. Second, by considering the whole domain of the improper integral part. It has been achieved by two different ways; one by using a double discretization approach as shown in Chapter 2 and the other by using Gauss quadrature approximation as shown in Chapter 3.

It is known that cross derivative terms involve negative coefficients in the numerical schemes that could deteriorate the quality of the solutions. In Chapter 4, numerical solution of option pricing under the two dimensional in space Bates model is studied after removing the cross derivative term from the PIDE using a suitable transformation. Also, its accuracy has been improved by discretizing the integral part using four-point open type formula.

These numerical schemes provide positive, consistent and conditionally stable solutions. Numerical simulations and comparison with other approaches in the literature show the efficiency of the proposed techniques.

Bibliography

[1] M. Abramowitz, I. A. Stegun, *Handbook of mathematical functions: with formulas, graphs, and mathematical tables*, Dover Books on Mathematics, (1961).

[2] A. Almendral, C. W. Oosterlee, Numerical valuation of options with jumps in the underlying, Applied Numerical Mathematics 53(1) (2005) 1–18.

[3] A. Almendral, C. W. Oosterlee, On American options under the Variance Gamma process, Applied Mathematical Finance 14 (2) (2007) 131—152.

[4] A. Almendral, C. W. Oosterlee, Accurate evaluation of european and american options under the CGMY process, SIAM Journal on Scientific Computing 29(1) (2007) 93–117.

[5] L. Andersen, J. Andreasen, Jump-diffusion processes: Volatility smile fitting and numerical methods for option pricing, Review of Derivatives Research 4(3) (2000) 231–262.

[6] O. E. Barndorff-Nielsen, Exponentially decreasing distributions for the logarithm of particle size, Proceeding of the Royal Society of London, A353 (1977) 401–419.

[7] O. Barndorff-Nielsen, Processes of normal inverse Gaussian type, Finance and Stochastics 2(1) (1997) 41–68.

[8] D. S. Bates, Jumps and stochastic volatility: Exchange rate processes implicit Deutsche mark options, Review Financial Studies 9 (1996) 69—107.

[9] E. Benhamou, E. Gobet, M. Miri, Smart expansion and fast calibration for jump diffusions, Finance Stoch. 13(4) (2009) 563-–589.

[10] F. Black, M. Scholes, The pricing of options and corporate liabilities, J. Political Economy. 81 (1973) 637–654.

[11] S. I. Boyarchenko, S. Z. Levendorskii, Option pricing for truncated Lévy processes, International Journal of Theoretical and Applied Finance 3(3) (2000) 549–552.

[12] M. Briani, C. La Chioma, R. Natalini, Convergence of numerical schemes for viscosity solutions to integro-differential degenerate parabolic problems arising in financial theory, Numer. Math. 98(4) (2004) 607-–646.

[13] W. L. Briggs, V. E. Henson, S. F. McCormick, *A multigrid tutorial*, SIAM, Philadelphia, PA, second ed., 2000.

[14] H. Burchard, E. Deleersnijder, A. Meister, A high-order conservative Patankar–type discretisation for stiff systems of production—destruction equations, Applied Numerical Mathematics 47 (2003) 1—30.

[15] J. Y. Campbell, A. W. Lo, A. C. MacKinlay, *The Econometrics of Financial Markets*, Princeton University Press, Princeton, NJ, USA, 1997.

[16] P. Carr, H. Geman, D. B. Madan, M.Yor, The fine structure of asset returns: an empirical investigation, Journal of Business 75(2) (2002) 305–332.

[17] M. C. Casabán, R. Company, L. Jódar, J. V. Romero, Double discretization difference schemes for partial integro-differential option pricing jump diffusion models, Abstract and Applied Analysis 2012 (2012) 1–20.

[18] B. M. Chen-Charpentier, H. V. Kojouharov, An unconditionally positivity preserving scheme for advection-diffusion reaction equations, Mathematical and Computer Modelling 57 (2013) 2177—2185.

[19] C. Chiarella, B. Kang, G. H. Mayer, A. Ziogas, The evaluation of American option prices under stochastic volatility and jump-diffusion dynamics using the method of lines. Research Paper Quantitative Finance Research Centre University of Technology, Sydney, 219 (2008) 1–43.

[20] N. Clarke and K. Parrott, Multigrid for American option pricing with stochastic volatility, Applied Mathematical Finance 6 (3) (1999) 177-–195.

[21] R. Company, L. Jódar, M. Fakharany, Positive solutions of European option pricing with CGMY process models using double discretization difference schemes, Abstract and Applied Analysis 2013 (2013) 1–11.

[22] R. Company, L. Jódar, M. Fakharany, M.-C. Casabán, Removing the correlation term in the option pricing Heston model: numerical analysis and computing, Abstract and Applied Analysis, 2013 (2013) 1–11.

[23] R. Company, L. Jódar, E. Ponsoda, C. Ballester, Numerical analysis and simulation of option pricing problems modeling illiquid markets, Computers & Mathematics with Applications 59(8) (2010) 2964–2975.

[24] R. Cont and P. Tankov, *Financial modelling with jump processes*, Chapman & Hall/CRC, Boca Raton, FL, 2004.

[25] R. Cont, E. Voltchkova, A finite difference scheme for option pricing in jump diffusion and exponential Lévy models, SIAM Journal on Numerical Analysis 43(4) (2005) 1596–1626.

[26] J. C. Cox and S. A. Ross, The valuation of options for alternative stochastic processes, J. Financial Economics, 3 (1976) 145–166.

[27] C. W. Cryer, The solution of a quadratic programming problem using systematic overrelaxation, SIAM J. Control, 9 (1971) 385–392.

[28] P. J. Davis, P. Rabinowitz, *Methods of numerical integration*, Second Edition, Academic Press, New York, USA, 1984.

[29] D. J. Duffy, *Finite Difference Methods in Financial Engineering: a Partial Differential Approach*, John Wiley & Sons Ltd, The Atrium, Southern Gate, Chichester, West Sussex PO19 8SQ, England, 2006.

[30] B. Düring, M. Fournié, High-order compact finite difference scheme for option pricing in stochastic volatility models, Journal of Computational and Applied Mathematics 236 (2012) 4462—4473.

[31] B. Düring, M. Fournié, C. Heuer, High-order compact finite difference schemes for option pricing in stochastic volatility models on non-uniform grids, Journal of Computational and Applied Mathematics 271 (2014) 247-–266.

[32] B. Düring, M. Fournié, C. Heuer, High-order compact finite difference schemes for option pricing in stochastic volatility models on non-uniform grids, Journal of Computational and Applied Mathematics 271 (2014) 247-–266.

[33] E. Eberlein, Application of generalized hyperbolic Lévy motions to finance, *Lévy Processes: Theory and Applications, O.E. Barndorff-Nielsen, T. Mikosch, and S. Resnick (eds.)*, Springer, (2001) 319–337

[34] E. Eberlein, U. Keller, K.Prause, New insights into smile, mis- pricing and Value at Risk: The hyperbolic model, Journal of Business 71 (1998) 371–405.

[35] M. Ehrhardt, R. Mickens, A fast, stable and accurate numerical method for the Black–Scholes equation of american options, International Journal of Theoretical and Applied Finance 11 (2008) 471–501.

[36] F. Fang, C. W. Oosterlee, A novel pricing method for European options based on Fourier-cosine series expansions, SIAM Journal on Scientific Computing, 31(2) (2008) 826–848.

[37] M. Fakharany, R. Company and L. Jódar. Positive finite difference schemes for a partial integro-differential option pricing model, Applied Mathematics and Computation 249 (2014) 320–332.

[38] M. Fakharany, R. Company and L. Jódar. Unconditionally positive stable numerical solution of partial integro-differential option pricing problems, Journal of Applied Mathematics 2015(960728) (2015) 1–10.

[39] P. R. Garabedian, *Partial Differential Equations*, AMS Chelsea Pubs. Co., 1998.

[40] G. H. Golub, C. F. Van Loan, *Matrix Computations,* (3rd ed.), Johns Hopkins University Press, 1996.

[41] I. S. Grandshteyn, I. M. Ryzhik, A. Jefferey (Editor), *Table of Integrals, Series and Product* (7th ed.), Academic Press, Elsevier, 2007.

[42] B. Gustafsson, H. O. Kreiss and J. Oliger, *Time dependent problems and difference methods*, John Wiley & Sons, Inc., 1995.

[43] W. Hackbusch, *Multi-grid methods and applications*, Springer, 1985.

[44] S. L. Heston, A closed-form solution for options with stochastic volatility with applications to bond and currency options, The Review of Financial Studies. 6 (1993) 327–343.

[45] F. B. Hildebrand, *Introduction to numerical analysis, second edition*, Dover Publications, INC. Mineola, New York, 1987.

[46] J. C. Hull, *Options, futures and other derivatives, 8th ed.*, Prentice Hall, New Jersey, 2012.

[47] S. Ikonen and J. Toivanen, Operator splitting methods for American option pricing, Appl. Math. Lett. 17 (2004) 809-–814.

[48] S. Ikonen, J. Toivanen, Efficient numerical methods for pricing American options under stochastic volatility, Wiley J. Numerical methods for partial differential equations, 24(1) (2008) 104–126.

[49] S. Ikonen, J. Toivanen, Operator splitting methods for pricing American options under stochastic volatility, Numer. Math. 113 (2009) 299-324.

[50] D. R. Insua, F. Ruggeri and M. P. Wiper, *Bayesian analysis of stochastic process models*, Wiley series in probability and statistics, 2012.

[51] R. Kangro, R. Nicolaides, Far field boundary conditions for Black-Scholes equations, SIAM Journal on Numerical Analysis 38(4) (2000) 1357–1368.

[52] I. Koponen, Analytic approach to the problem of convergence of truncated Lévy flights towards the Gaussian stochastic process, Physical Review E 52(1) (1995) 1197–1199.

[53] S. G. Kou, A jump diffusion model for option pricing, Management Science 48(8) (2002) 1086–1101.

[54] J. Lee, Y. Lee, Tridiagonal implicit method to evaluate European and American options under infinite activity Lévy models, Journal of Computational and Applied Mathematics 237 (2013) 234-–243.

[55] P. Linz, *Analytic and Numerical Methods for Volterra Equations*, SIAM, Philadelphia, USA, 1985.

[56] D. B. Madan, P. Carr, and E. C. Chang, The Variance Gamma process and option pricing, European Finance Review 2 (1998) 79–105.

[57] D. Madan, F. Milne, Option pricing with variance gamma martingale components, Mathematical Finance 1(4) (1991) 39–55.

[58] D. B. Madan, E. Seneta, The Variance Gamma (V.G.) model for share market returns J. Bus. 63 (1990) 511—524.

[59] D. B. Madan, M. Yor, CGMY and Meixner subordinators are absolutely continuous with respect to one sided stable subordinators, Cornell University Library arXiv: math/0601173v2, 2006.

[60] D. Madan, M. Yor, Representing the CGMY and Meixner Lévy processes as time changed Brownian motions, Journal of Computational Finance 12(1) (2008) 27-47.

[61] A.-M. Matache, P.-A. Nitsche, C. Schwab, Wavelet Galerkin pricing of American options on Lévy driven assets, Quantitative Finance 5(4) (2005) 403–424.

[62] A.-M. Matache, T. von Petersdorff, C. Schwab, Fast deterministic pricing of options on Lévy driven assets, Mathematical Modelling and Numerical Analysis 38(1) (2004) 37–71.

[63] R. C. Merton, Option pricing when underlying stock returns are discontinuous, J. Financial Economics. 3 (1976) 125–144.

[64] G. H. Meyer, J. van der Hoek, The Evaluation of American Options with the Method of Lines, Advances in Futures and Options Research 9 (1997) 265—285.

[65] M. S. Milgram, The Generalized Integro-Exponential Function, Mathematics of computation 44(170) (1985) 443–458.

[66] A. Pascucci, *PDE and martingale methods in option pricing*, volume 2 of Bocconi & Springer Series. Springer, Milan, 2011.

[67] S. Pagliarani, A. Pascucci, C. Riga, Adjoint expansions in local Lévy models, SIAM J. Financial Math. 4(1) (2013) 265—296.

[68] S. V. Patankar, *Numerical heat transfer and fluid flow*, McGraw-Hill, New York, 1980.

[69] J. Poirot, P. Tankov, Monte Carlo Option Pricing for Tempered Stable (CGMY) Processes, Asia-Pacific Finan Markets 13 (2006) 327—344.

[70] W. Poklewski-Koziell, *Stochastic Volatility Models: Calibration, Pricing and Hedging*, University of the Witwatersrand, South Africa, MSc thesis 2012.

[71] N. Rambeerich, D. Y. Tangman, M. Bhuruth, Numerical pricing of American options under infinite activity Lévy processes. The Journal of Futures Markets (2011) 31, 809–829.

[72] R. Rannacher, Finite element solution of diffusion problems with irregular data, Numer. Math. 43 (1984) 309—327.

[73] R. D. Richtmyer and K. W. Morton, *Difference methods for initial-value problems* (2nd ed.), Interscience Publishers, New York, 1967.

[74] E. W. Sachs, A. K. Strauss, Efficient solution of a partial integro-differential equation in finance, Applied Numerical Mathematics 58(11) (2008) 1687–1703.

[75] S. Salmi, J. Toivanen, An iterative method for pricing American options under jump-diffusion models, Applied Numerical Mathematics 61(7) (2011) 821–831.

[76] S. Salmi, J. Toivanen, L. Von Sydow, Iterative methods for pricing American options under the bates model, Procedia Computer Science 18 (2013) 1136–1144.

[77] W. Schoutens, J. L. Teugels, Lévy processes, polynomials and martingales, Cummun. Statist.-Stochastic Models 14(1, 2) (1998) 335-349.

[78] W. Schoutens, *Lévy processes in finance: pricing financial derivatives*, Wiley: New York, 2003.

[79] R. U. Seydel, *Tools for computational finance 4th ed.*, Springer, 2009.

[80] G. D. Smith, *Numerical solution of partial differential equations: finite difference methods* (3rd ed.), Clarendon Press, Oxford, UK, 1985.

[81] J. C. Strikwerda, *Finite difference schemes and partial differential equations*, second ed., Siam, 2004.

[82] D. Tavella, C. Randall, *Pricing Financial Instruments: The Finite Difference Method*, Wiley, New York, USA, 2000.

[83] N. M. Temme, *Special functions an introduction to the classical functions of mathematical physics*, John Wiley & Sons, Inc., 1996.

[84] J. W. Thomas, *Numerical partial differential equations finite difference methods*. Springer, 1995.

[85] J. Toivanen, Numerical valuation of European and American options under Kou's jump-diffusion model, SIAM Journal on Scientific Computing 30(4) (2008) 1949–1970.

[86] J. Toivanen, A Componentwise Splitting Method for Pricing American Options under the Bates Model, Computational Methods in Applied Sciences, Springer 15 (2010) 213—227.

[87] I. R. Wang, J. W. Wan, P. A. Forsyth, Robust Numerical Valuation of European and American Options under the CGMY process, J. Computational finance 10(4) (2007) 31–69.

[88] P. Wesseling, *An introduction to multigrid methods*, John Wiley & Sons, 1992.

[89] P. Wilmott, J. Dewynne, S. Howison, *Option Pricing: Mathematical Models and Computation*, Oxford Financial press, 1998.

[90] R. Zvan, P. A. Forsyth, K. R. Vetzal, Negative coefficients in two-factor option pricing models, Journal of Computational Finance 7 (2003) 37-73.